

*Controlling Grain Size in Cold Worked and Annealed 1100 Aluminum to Optimize Ductility in
Rocket Diaphragm Systems*

Ryan Lewis, Bryce Simmons, and Jessica Williams

Advisor: Professor Blair London

Sponsor: Aerojet Rocketdyne

Materials Engineering Department

California Polytechnic State University, San Luis Obispo

June 2016

© 2016 Ryan Lewis, Bryce Simmons, and Jessica Williams

ABSTRACT

Liquid propellant rocket diaphragms require extreme ductility. 1100 Aluminum is used for its high ductility, but the post-processing cold work and subsequent anneal result in excessively large grains. The effect of heat treatment and cold work on grain size in 1100 aluminum was explored. The samples were cold worked to 0, 5, 10, 15 and 30% using tensile elongation. The samples were then heat treated per AMS 2770 with either a "Steel Conduction" (1000 – 1150°F/min) or a "Production" (16 – 18°F/min) heating rate. The grain size of the samples were measured using the mean lineal intercept method. The grain diameter ranged from 81 – 189 μm for the Production rate and 83 – 209 μm for the Steel Conduction rate. The 15% cold worked Production rate samples were found to have significantly larger grains than those of the smaller cold work amounts as well as the 15% cold worked Steel Conduction rate samples. This indicated an interaction between the 15% cold work amount and the Production heat treatment which allowed for significant grain growth. The 30% cold worked samples were found to have grain growth in both heat treatments with the largest average grain diameters. The results indicate that the longer times at elevated temperatures during the Production heat treatment allow for significant grain growth at lower cold work amounts. In addition, grain growth is unavoidable for 30% cold work regardless of heating rate.

Key Words: Diaphragms, ductility, 1100 aluminum, grain growth, heating rate, cold work, grain size.

ACKNOWLEDGEMENTS

We would like to thank all parties involved for providing their guidance, resources, and support in completing our senior project. Professor Blair London from the Materials Engineering department for being the advisor to our senior project and always keeping us to the highest standard. Chris Shipley and Andrew Theisen from Aerojet Rocketdyne for being our technical contacts for this project ensuring we were on the right track. Dr. Jeffery Sklar from the Statistics department for statistics consulting on our senior project, which helped us manage our data. Luka Dugandzic from Dugandzic Designs for machining our specimens in a timely fashion. Finally, the California Polytechnic State University Materials Engineering department for providing resources for success.

Table of Contents

1. PROJECT OVERVIEW	1
1.1 PROBLEM STATEMENT	1
1.2 PROJECT GOALS	1
2. BACKGROUND	1
2.1 DIAPHRAGMS IN ROCKET PROPULSION SYSTEMS	1
2.1.1 Function	1
2.1.2 Ductility	2
2.1.3 Material Choice	3
2.2 PROCESSING	3
2.3 ANNEALING	4
2.3.1 Energy in Annealing	4
2.3.2 Recovery and Polygonization	6
2.3.3 Recrystallization	6
2.3.4 Grain Growth	10
2.3.5 Grain Size	11
3. EXPERIMENTAL PROCEDURE	13
3.1 SPECIMEN PREPARATION	13
3.2 COLD WORK	14
3.3 SAMPLE PREPARATION	15
3.4 HEAT TREATMENT	15
3.4.1 Production Heating Rate	15
3.4.2 Steel Conduction Heating Rate	18
3.5 METALLOGRAPHY	20
3.6 HARDNESS	21
4. RESULTS	21
5. ANALYSIS	25
5.1 INITIAL HARDNESS AND GRAIN SIZE	25
5.2 STATISTICS	28
6. CONCLUSIONS	33
REFERENCES	34
APPENDIX A	35

List of Figures

Figure 1. Diagram of a liquid propellant tank. The blue line represents the diaphragm that separates the pressurant from the propellant. Once propellant expulsion is required the pressurant is pressurized, plastically deforming the diaphragm and expelling the propellant.	2
Figure 2. The leftmost image shows the starting position of the diaphragm with a progressive increase in deformation, ending with the complete inverse of the original structure at the right [1].	2
Figure 3. Schematic of the punch draw hydroforming technique. A sheet of material (or the blank) is placed into the forming die. The top section of the die consists of a rubber pad that forms the contour of the desired shape with a fluid-filled cavity above the pad. The mating half of the die (or the punch) drives upward into the cavity and deforms the blank against the resistance provided by the fluid resulting in the formation of the workpiece [3].	3
Figure 4. Stored energy of cold work plotted with the fraction of the total work of deformation remaining as stored energy as a function of percent elongation for high purity copper [4].	4
Figure 5. Isothermal annealing curve for high purity copper. The spike in the curve corresponds to a release in energy by the sample and therefore a corresponding decrease in the power necessary to keep the sample at temperature [4].	5
Figure 6. Tensile strength and ductility as a function of annealing temperature for an annealing time of one hour in a brass alloy. The three main stages of annealing (recovery, recrystallization, and grain growth) are schematically shown [5].	6
Figure 7. Isothermal recrystallization curves for pure copper cold-rolled to 98 percent. Note the sigmoidal nature of the percent recrystallization as a function of time. Like most kinetics processes, a small increase in temperature can result in drastic shift in process times [4].	7
Figure 8. Temperature-time relationships for recrystallization of zirconium (iodide). The increase in cold work significantly decreases the time to reach recrystallization at a given temperature as a result of the lower input energy requirements (i.e., activation energy) [4].	8
Figure 9. The relationship between grain size and heating rate in 7075 aluminum (Al) and 7475 Al. This is the final step in the processing where the Al samples had been previously solution treated for three hours at 482°C, overaged eight hours at 400°C, and rolled to 90% reduction at 200°C [9].	12

Figure 10. Recrystallized grain size of 1100 aluminum after annealing at 480°C and 360°C at two separate heating rates [8]. 13

Figure 11. Furnace set-up for the Production heat treatment. The samples were placed at a minimum of one inch apart per AMS 2770 and raised to the center of the furnace using refractory bricks. 16

Figure 12. Graph of both Production heating rate (HR) tests. The blue data points represent test #1 with a heating rate of 17.99°F/min and the orange data points represent test #2 with a heating rate of 17.73°F/min. The dotted red line is the minimum temperature from AMS 2770. The data from both tests were fit with a linear model with their respective equations given in the corresponding color. The derivative of this fit was used to calculate the Production heating rate for the aluminum. 17

Figure 13. The thermal response of the 1100 aluminum throughout the hold time of two Production heating rate tests. The blue data points show that in the first test the alloy was out of specification slightly ($T_{max} = 661.5^{\circ}\text{F}$) at the maximum of its first temperature fluctuation. The orange data points show that in the second test the alloy remained in specification for the duration of the test ($T_{max} = 653^{\circ}\text{F}$). 17

Figure 14. Furnace set-up for the Steel Conduction heat treatment. A single sample was placed in between the steel plates once the plates reached 640°F. A thermocouple was placed in between the plates to record the temperature of the plates. 18

Figure 15. Graph of the time it took the 1100 aluminum to reach temperature during the three Steel Conduction heating rate (SC HR) tests. The orange data points represent the first test, green data points represent the second test, and the blue data points represent the third test. These resulted in heating rates of 1014°F/min, 1128°F/min, and 1086°F/min, respectively, calculated from the derivate of the functions displayed with the corresponding color. 19

Figure 16. The thermal response of the 1100 aluminum throughout the hold time of the three Steel Conduction heating rate tests. In all three tests, the aluminum remained well within the specification limits – given in red – throughout the duration of the test. The average steel temperature was calculated and is plotted above as a purple line. 20

Figure 17. Displayed is the gage length of the tensile specimens. The blue arrows indicate the tensile axis. The metallographic viewing plane was revealed by sectioning represented by the dotted black line. 20

Figure 18. Representative micrographs of 1100 aluminum from each sample condition. The bottom left-hand corner of the image gives the sample designation including heat treatment type, cold work amount, and replicate number. Mag 200x. Etch: NaOH solution..... 22

Figure 19. Shown are the grain size gradients in the 15% cold work samples for both heat treatments. The large grains for Steel Conduction (SC) take up a smaller area of the sample than in the Production (P) samples. In addition, the edge of the Production samples consist of only large grains whereas in the Steel Conduction samples there is a mix of both large and small grains..... 23

Figure 20. Plot of the hardness data for each heat treatment-cold work amount combination compared to the original hardness prior to heat treatment. Significant changes in hardness are seen in every cold work amount, especially 30%. 25

Figure 21. Graph of the effect of cold work on the recrystallized grain size at constant annealing temperature. There is no change until a peak in recrystallized grain size at the critical strain region and then a decline in grain size with an increase in cold work amount..... 25

Figure 22. Time vs temperature plot for 1100-H18 aluminum showing the start and completion of recrystallization [7]..... 26

Figure 23. Plot of the time and temperatures used during each of the heating rates. Production in blue reaches temperature in 35 minutes and finishes after 65 minutes. Steel Conduction in red reaches temperature in 0.5 minutes and finishes completely after 30.5 minutes..... 27

Figure 24. Average grain diameter versus the amount of cold work for the two heat treatments. In both heat treatments there appears to be grain growth. 28

Figure 25. The plots above are output by Minitab and check the two assumptions for the two-way ANOVA: normally distributed populations (*left*) and equal variance between populations (*right*). 29

Figure 26. Minitab plots of the assumptions for the two-way ANOVA of the transformed grain size measurements. The data post transformation is normally distributed (*left*) and has more equal variance between populations (*right*). 29

Figure 27. A visual representation of the Tukey pairwise comparison of the effect cold work has on grain size data. Data points that do not share the same color are significantly different..... 30

Figure 28. Activation energy (Q_r) for recrystallization as a function of cold work amount in zirconium (iodide). There is a clear inverse relationship: as one increases cold work amount, the activation energy for recrystallization decreases [4]. 31

Figure 29. A visual representation of the Tukey pairwise comparison of the effect of the interaction between cold work and heat treatment on grain size data. Data points that do not share the same color are significantly different. 32

List of Tables

Table I. Levels for the Variable of Cold Work Amount..... 14

Table II. Test Matrix and Sample Designations 15

Table III. ASTM Grain Size Number and Average Grain Diameter for Each Sample Condition 23

Table IV. Microhardness of 15% Cold Worked 1100 Aluminum Sample..... 24

Table V. Hardness of Cold Worked and Annealed Samples 24

Table VI. Statistical Significance of the Two Factors and Their Interaction on Grain Size Measurements 29

1. PROJECT OVERVIEW

1.1 PROBLEM STATEMENT

Aerojet Rocketdyne makes a wide array of liquid and solid propellant rocket engine motors that employ many different aluminum alloys in component fabrication. These rocket engine motor systems have utilized aluminum diaphragms for propellant tank applications since the 1960s. The diaphragms are typically formed by a “cold” plastic deformation process into a complex shape, which requires extreme ductility. Due to the demand for substantial ductility, commercially pure 1100 aluminum performs well in the application. In order to relieve internal stress within the material produced by the forming process, the formed diaphragm goes through an annealing heat treatment. If the annealing heat treatment is non-optimal, then the material may undergo excessive softening and grain growth, causing the material to fail ductility specifications.

1.2 PROJECT GOALS

The goal of this project is to explore the effect that heating rates have on minimizing grain size in order to increase strength and ductility. The project will take into consideration the presence of a range of cold work amounts in the diaphragm. The heating rates that will be explored will represent an industry standard heating rate and a rapid rate that is orders of magnitude faster. The conclusions will include recommendations to whether or not a change in the current annealing treatment is worth the investment.

2. BACKGROUND

2.1 DIAPHRAGMS IN ROCKET PROPULSION SYSTEMS

2.1.1 Function

Liquid propellant rocket fuel systems need a way to expel the propellant out of fuel tanks to produce thrust or to jump start more complex fuel systems like turbopumps. This requires the propellant to be expelled, but the gas pressurant and liquid propellant cannot mix; the mixture of the two could cause misfire upon ignition due to nonhomogeneous propellant. Normally, a turbopump system is put in place to provide constant propellant output to the engine. However, for multistage or horizontal flight rockets, the turbopump needs assistance. A diaphragm is put in place in the fuel tanks of these rockets in

order to separate the propellant and pressurant and to force the propellant out to aid the turbopump (Figure 1).

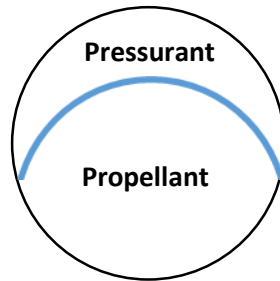


Figure 1. Diagram of a liquid propellant tank. The blue line represents the diaphragm that separates the pressurant from the propellant. Once propellant expulsion is required the pressurant is pressurized, plastically deforming the diaphragm and expelling the propellant.

Diaphragms, like the ones in propellant tanks, are usually in some form of a revolved shape (i.e., spherical). A single fuel tank can have one or two diaphragms depending on the shape and size of the tank. The amount of ductility needed for the diaphragm to operate is dependent on whether or not there are one or two diaphragms. [1]

2.1.2 Ductility

Systems with single diaphragms commonly have reversible diaphragms (Figure 2). A reversible diaphragm is a diaphragm that becomes a mirrored version of itself once deformed.

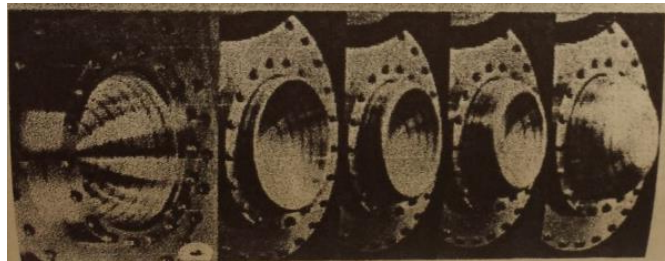


Figure 2. The leftmost image shows the starting position of the diaphragm with a progressive increase in deformation, ending with the complete inverse of the original structure at the right [1].

The amount of ductility needed for a reversible diaphragm to operate is such that the total surface area is maintained when the diaphragm is extended. For complete mirroring to occur, specialized geometries, known as convolutions, are added to the design to facilitate desired deformation. These convolutions are also added so that the diaphragm yields rather than fractures. Due to the extensive plastic deformation after engaging these diaphragms, they can only be used once. There have been attempts to refurbish used diaphragms, but it becomes too difficult to reproduce

the specific geometries needed. This is why inexpensive, ductile materials, like 1100 aluminum, are used in liquid propellant rocket diaphragms. [1]

2.1.3 Material Choice

While the need for ductility in diaphragms is evident, the underlying mechanisms behind ductility in metals are far more complex than the diaphragm application demonstrates. When a metal is considered strong, it is understood that the strength of the metal is due to the inhibited movement of dislocations. It is also understood that strength and ductility, in the case of strain hardening, are inversely related. That is, when a metal is strain hardened, the strength increases but at a loss in ductility. Ductility can be thought of as stemming from the uninhibited movement of dislocations. Metals with high dislocation densities generally have lower ductility.

Dislocation movement can be impeded by various factors. In the case of 1100 aluminum, there are relatively low amounts of impurity atoms for dislocation movement to be retarded, therefore the main barriers to dislocation movement are grain boundaries and other dislocations (i.e., dislocation pile-up). However, the dislocations in 1100 aluminum experience cross-slipping due to the face-centered cubic (FCC) crystal structure of aluminum. The FCC crystal structure has twelve different slip systems that can be utilized for dislocation movement. The increased slip distance resulting from multiple slip systems prevents dislocation pile up and therefore lowers the overall dislocation density of the material. 1100 Aluminum is corrosion resistant, lightweight, and inexpensive compared to other pure metals with similar ductility properties. [2]

2.2 PROCESSING

Diaphragms for rocket applications are typically formed using a hydroforming process (Figure 3).

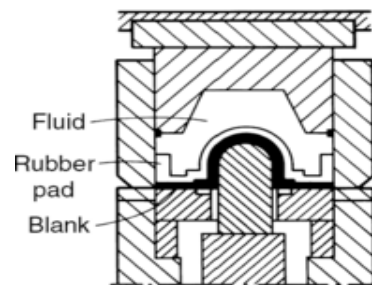


Figure 3. Schematic of the punch draw hydroforming technique. A sheet of material (or the blank) is placed into the forming die. The top section of the die consists of a rubber pad that forms the contour of the desired shape with a fluid-filled cavity above the pad. The mating half of the die (or the punch) drives upward into the cavity and deforms the blank against the resistance provided by the fluid resulting in the formation of the workpiece [3].

This process results in drawing that occurs simultaneously throughout the part. This drawing is best estimated as a tensile elongation, although in reality it is a more complex deformation process. Since the part has a complex shape, the amount of deformation varies throughout the part resulting in a gradient of cold work. This presents a problem for the annealing heat treatment of the diaphragm: the part does not have a uniform amount of cold work and thus will be affected by the input of heat differently depending on the region of the diaphragm.

2.3 ANNEALING

2.3.1 Energy in Annealing

2.3.1.1 Stored Energy

One way to store energy in a material is by a cold working process. Cold working is the process of plastically deforming a material at a temperature that is less than half of the melting temperature of the material. Most of the energy expended in this process manifests itself as heat lost to the surrounding environment. However, a finite amount of the energy put into the material by cold work is stored as strain energy associated with lattice defects that are produced by the deformation process (Figure 4).

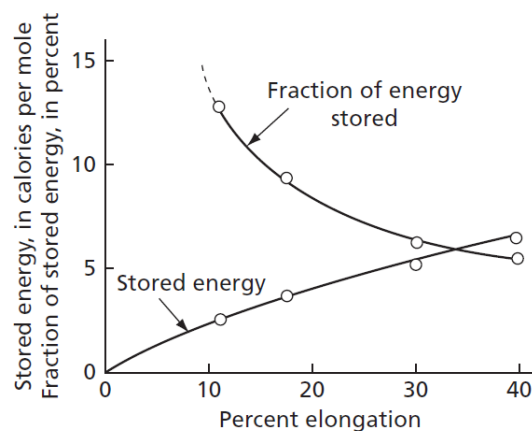


Figure 4. Stored energy of cold work plotted with the fraction of the total work of deformation remaining as stored energy as a function of percent elongation for high purity copper [4].

As the percent elongation increases, the amount of stored strain energy increases and the fraction of the total energy put into the material that becomes strain energy decreases. This means that at a certain percent elongation these two amounts will coincide, optimizing the amount of stored energy in a material with respect to input energy.

The amount of stored energy can also be greatly increased by increasing deformation, decreasing temperature of working, and by increasing the purity of the alloy. Cold working is known to increase the number of dislocations in a metal by $10^4 - 10^6$ times [4]. Since each dislocation represents a crystal defect with an associated lattice strain, increasing the dislocation density of a material increases the stored strain energy within the material.

2.3.1.2 Releasing Energy

The cold work put into a metal upsets the thermodynamic equilibrium of the metal. In order to become thermodynamically stable, the dislocations and lattice defects must align resulting in strain-free grains. This alignment requires atomic movement and therefore is dictated by kinetics. Thus, if a cold worked metal is introduced into an elevated temperature environment, the rate of atomic movement exponentially increases. This elevated temperature treatment of a cold worked metal is known as annealing.

The power necessary to maintain a cold worked metal at a given temperature can be used to determine when and how much energy is being released (Figure 5).

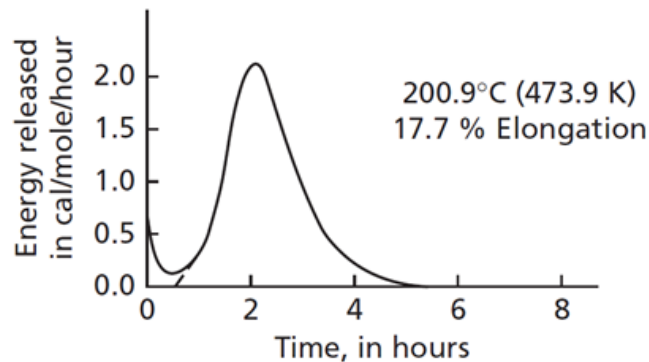


Figure 5. Isothermal annealing curve for high purity copper. The spike in the curve corresponds to a release in energy by the sample and therefore a corresponding decrease in the power necessary to keep the sample at temperature [4].

Metallographic preparation of a sample at the spike in energy displays a new set of essentially strain-free grains which grow at the expense of the originally deformed grains. This process involves the realignment of the atoms into crystals with a lower strain energy and is known as recrystallization. The recrystallization portion in Figure 5 is the portion to the right of the dashed line and represents the energy associated with recrystallization and potentially grain growth. The energy released before recrystallization is known as the recovery period.

2.3.2 Recovery and Polygonization

Cold working a metal tends to change almost all of its mechanical properties. The recovery process of annealing initiates the reversal of this process (Figure 6).

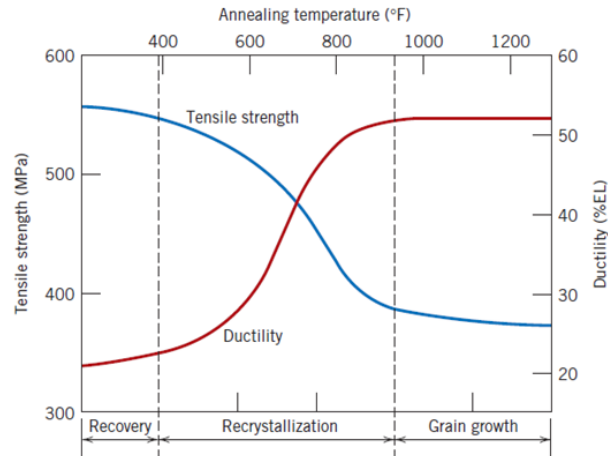


Figure 6. Tensile strength and ductility as a function of annealing temperature for an annealing time of one hour in a brass alloy. The three main stages of annealing (recovery, recrystallization, and grain growth) are schematically shown [5].

The associated tensile and compressive strain fields of the dislocations line up during the beginning of the annealing treatment. The dislocations line up in an orientation that results in the cancellation of the strain fields because the compressive region of one dislocation overlaps the tensile region of the dislocation directly below it. This results in a net loss of strain energy in the crystal, bringing the material to a lower energy state and making it more thermodynamically stable.

2.3.3 Recrystallization

The release of the energy stored by the cold working process is also the driving force for the recrystallization process. Recrystallization occurs after the recovery process and follows significantly different kinetics processes. The kinetics of recrystallization follows similar patterns to nucleation and growth and accounts for the largest energy release during the annealing process.

2.3.3.1 Effect of Time and Temperature

Recrystallization follows S-curve kinetics similar to those that a nucleation and growth process follows (Figure 7).

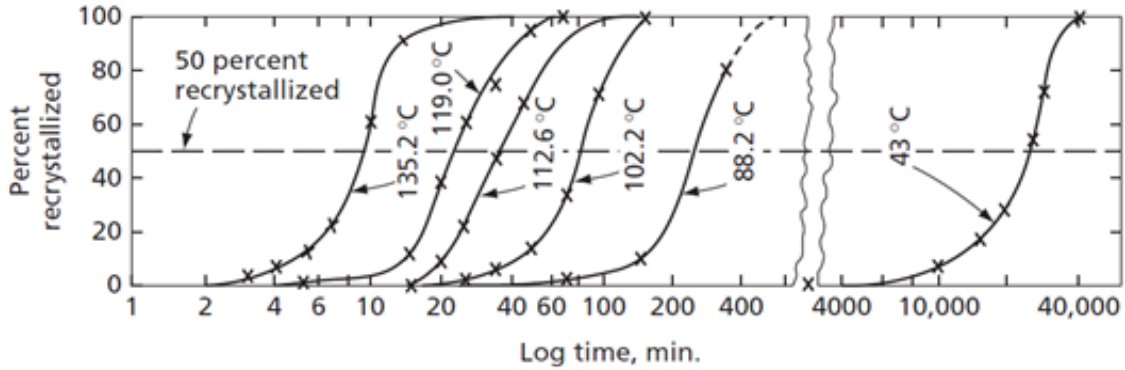


Figure 7. Isothermal recrystallization curves for pure copper cold-rolled to 98 percent. Note the sigmoidal nature of the percent recrystallization as a function of time. Like most kinetics processes, a small increase in temperature can result in drastic shift in process times [4].

The recrystallization curves show an exponential decrease in time after a relatively small linear increase in temperature. This relationship is due to the process being dictated by diffusion in which temperature has an exponentially larger effect than time. Further, the rate at which an alloy recrystallizes to any given amount ($1/\tau$) follows an Arrhenius model and is given by Equation 1:

$$\frac{1}{\tau} = Ae^{-\frac{Q_r}{RT}} \quad \text{Eq. 1}$$

where A is a constant, Q_r is the activation energy for recrystallization, T is the temperature of the treatment, and R is the ideal gas constant. The equation demonstrates the exponential effect temperature has relative to time on the recrystallization process.

The activation energy for recrystallization is still not well understood in the scientific community. Currently, the consensus is that the activation energy for recrystallization actually changes during the recrystallization process due to the depletion of cold work as new grains continue to grow [4]. Therefore, the activation energy is currently treated as an empirical constant.

2.3.3.2 Recrystallization Temperature

The recrystallization temperature is the temperature at which a specific metal with a given amount of cold work will completely recrystallize in a finite period of time. Since the recrystallization process requires large activation energies, the process appears to have a definite minimum temperature at which recrystallization appears to begin. Typically, practical engineers

will tend to regard the recrystallization temperature as a material property and ignore the time factor since moderate to low temperatures can take months to years for full recrystallization. However, recrystallization can occur at almost any temperature given a sufficient amount of time.

2.3.3.3 Effect of Strain on the Temperature Dependence of Recrystallization

The temperature dependence of recrystallization varies with the amount of cold work (Figure 8).

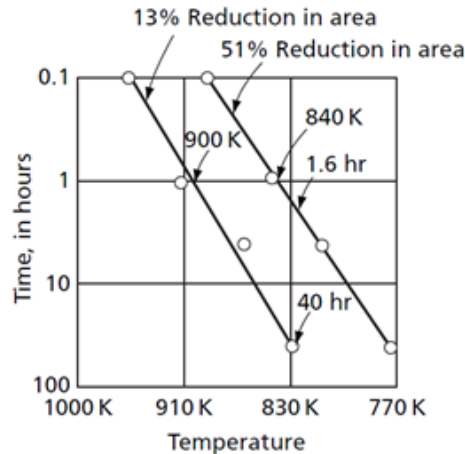


Figure 8. Temperature-time relationships for recrystallization of zirconium (iodide). The increase in cold work significantly decreases the time to reach recrystallization at a given temperature as a result of the lower input energy requirements (i.e., activation energy) [4].

This is because the activation energy for the recrystallization is a function of the amount of deformation such that activation energy decreases as cold work increases [4].

2.3.3.4 Rate of Nucleation and Rate of Growth

The rate at which a metal recrystallizes is dependent on two factors: the rate at which nuclei form, and the rate at which nuclei grow. These two rates in conjunction help determine the recrystallized grain size of an annealed metal. If the nuclei form rapidly and grow slowly, then many small crystals will form before their mutual impingement completes the recrystallization process and the resultant recrystallized grain size will be small.

2.3.3.5 Recrystallized Grain Size

The recrystallized grain size is the crystal size right after recrystallization but before grain growth occurs. This grain size relies on the amount of deformation before annealing; the grain size grows substantially with less initial deformation applied. However, if the amount of

deformation is too small then recrystallization will not have enough stored energy to occur. Thus there is a critical amount of cold work that has to be applied in order for recrystallization to occur in a reasonable amount of time.

Similar to the recrystallization temperature, the critical amount of deformation is not a material property; it can vary within a material depending on the type of deformation that occurs. Tension, torsion, compression, rolling, and forming can all have different amounts of critical deformation. The critical amount of deformation is commonly associated with large grain sizes. This is a common problem with sheet metal that is cold formed into complex shapes. If a material is cold rolled or drawn then it is easier to avoid the critical amount of deformation but if sections of the part are deformed unevenly, a gradient of cold work is formed leaving some of the part with the critical amount of deformation. [4]

If the ratio of the nucleation rate to the growth rate is low then the nucleation rate is slow compared to the growth rate and will result in a small amount of coarse grains. It can be determined from this information that the critical amount of cold work is the amount that is just enough to form the minimum number of nuclei for recrystallization resulting in large grains. It is important to note that the recrystallized grain size is independent of the recrystallization temperature, but recrystallization rate is dependent on the recrystallization temperature. [4]

2.3.3.6 Importance of Recrystallization in Pure Aluminum

For aluminum alloys, especially commercially pure alloys, the most important transformation process is recrystallization [6]. Since alloys like 1100 aluminum are not strengthened by precipitates or other microstructural features, the material's important mechanical properties are solely based on the size and distribution of grains. The main barrier to dislocation movement is grain boundaries; therefore an increase in the density of grain boundaries by high recrystallization rates increases the strength of the material.

Exceptionally pure aluminum, only 10 ppm of impurities, has demonstrated the occurrence of recrystallization at temperatures well below room temperature. The addition of finite amounts of impurities (<0.01%) strongly influences the recrystallization of such high purity aluminum. Larger amounts of impurities (around 0.1%) have a significantly smaller effect on recrystallization such that the difference between 99.6% pure aluminum and 99.5% pure

aluminum is not an appreciable amount. Since 1100 aluminum is a minimum of 99.0% pure, the concentration of impurities is high enough that recrystallization will only occur at a significantly elevated temperature. This increase in temperature is required because the presence of impurity atoms of significantly different atomic dimensions slow the growth of recrystallizing grains. Therefore, an increase in temperature is required to speed the impaired atomic movement. [2]

2.3.4 Grain Growth

2.3.4.1 Driving Force

The driving force behind grain growth is the need to decrease the grain boundary energy by decreasing the grain boundary area. Grain boundaries have a high amount of disorder compared to the grains themselves. The less grain boundaries that are present, the lower the energy state. Grain growth does not require plastic deformation, it will occur whenever the material reaches a high enough temperature. Grain growth is a complex statistical process, a process that is slower when grains are migrating into a deformed matrix. The energy reduction that occurs during grain growth is much lower than that which occurs during recrystallization. Grain growth is slow and only becomes slower as the grain size gets larger. [7]

2.3.4.2 Atomic Mechanism

The atoms that are located in the grain boundary rearrange themselves to match one of the two different crystal orientations present at the grain boundary. As the atoms in the boundaries arrange themselves to match one of the crystals, the boundary must migrate into the other grain causing the growth of one crystal at the expense of the one less preferably oriented. [7]

2.3.4.3 Grain Growth in 1100 Aluminum

Pure aluminum like other metals requires close control of the processing conditions in order to control and obtain the desired grain size. Annealing a cold worked metal is part of the processing that can be controlled. The largest amount of grain growth occurs right after the end of full recrystallization. The grain growth rate decreases the longer the material is held at temperature. [6]

2.3.5 Grain Size

The grain size that is produced after recrystallization and grain growth can be indicative of the properties that the metal will have. Larger grains are generally representative of a decrease in ductility and strength.

The final annealed grain size is a function of recrystallization and grain growth. The recrystallized grain size is heavily dependent on the amount of cold work present followed by the temperature, purity, initial grain size, and time at temperature. The final grain size after grain growth is dependent on the grain size prior to grain growth, the temperature, and how long the sample is kept in the furnace once grain growth begins.

2.3.5.1 Cold Work

One of the most important factors that influence grain size prior to grain growth is the amount of cold work that has been done on the sample. As cold work increases the recrystallized grain size decreases. The rate at which the recrystallized grain size decreases with cold work is a function of the composition, fabrication history, and the annealing conditions.

2.3.5.2 Time and Temperature

For grain growth to occur after recrystallization the sample needs to be at a high enough temperature for a sufficient amount of time. This time can vary from alloy to alloy, and a higher temperature can result in a lower time. Increasing the temperature will decrease the critical amount of deformation but it will not change the relationship between the heating rate, amount of cold work, and grain size. [8]

2.3.5.3 Heating Rates

Heating rates have been proven to affect the final grain size. Extremely slow heating rates produce coarser grain sizes (Figure 9). This is because at significantly slower heating rates only preferred nucleation sites are able to be activated and therefore recrystallize and begin to grow. These sites grow prior to other sites being activated, decreasing the amount of grains and increasing their size. This may be due to the extended time spent in the recovery stage during slower heating rates. There is a small amount of strain released during recovery which would lead to a decrease in the amount of preferred nucleation sites. Heating rates can also cause a

slight shift in the critical strain but more importantly a decrease in the maximum grain size. [8]
 [9] [10]

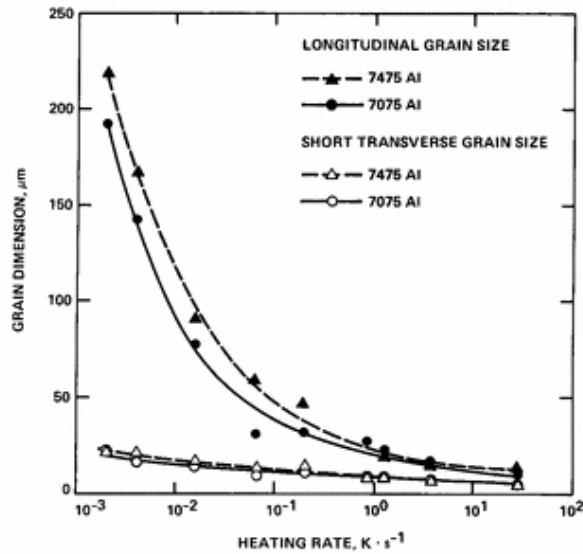


Figure 9. The relationship between grain size and heating rate in 7075 aluminum (Al) and 7475 Al. This is the final step in the processing where the Al samples had been previously solution treated for three hours at 482°C, overaged eight hours at 400°C, and rolled to 90% reduction at 200°C [9].

As the heating rate goes up logarithmically, the grain size decreases linearly. This is consistent between the longitudinal grain size and the transverse grain size; however, the change in heating rate has a negligible effect on the short transverse grain size.

2.3.5.4 Grain Size in 1100 Aluminum

In 1100 aluminum, the main factors that affect recrystallized grain size are the temperature, the heating rate, and the amount of cold work. All of these factors are important but the recrystallized grain size is most heavily reliant on the amount of cold work and the heating rate. There is an amount of cold work in which there is sufficient stored energy for recrystallization to occur (i.e., critical strain). At this strain amount, a maximum recrystallized grain size is reached followed by a decrease in grain size with increasing cold work amount. The literature has shown that an increase in heating rate can significantly decrease this peak in grain size as well as change the required critical strain (Figure 10).

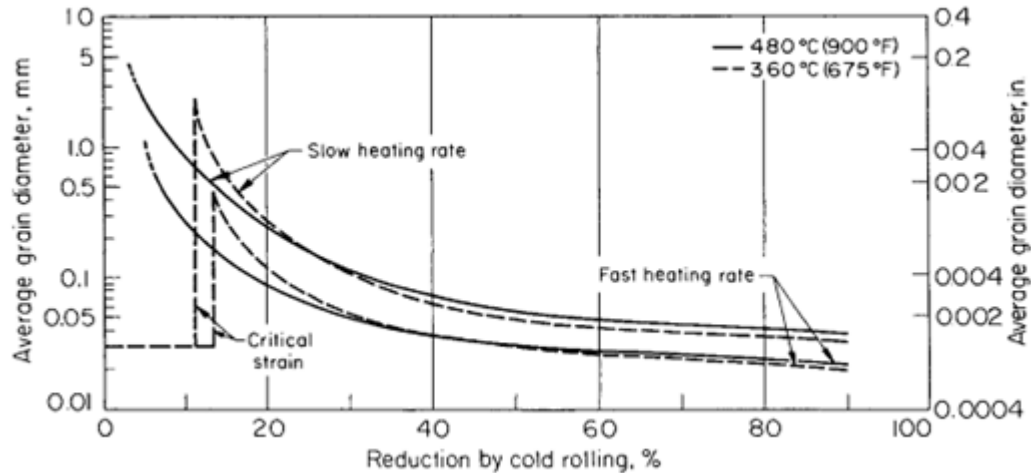


Figure 10. Recrystallized grain size of 1100 aluminum after annealing at 480°C and 360°C at two separate heating rates [8].

The effect of heating rate displayed in Figure 10 is not dependent on the amount of cold work or the annealing temperature, as a faster rate will always result in a decrease in grain size independent of those factors. The amount cold work is the factor that can lead to an increase in grain size resulting in a decrease in mechanical properties.

2.3.5.5 Grain Size Effects on Pure Aluminum Properties

Pure aluminum is used for intricate forming processes because of its high ductility and adequate yield strength. Both of these properties are improved upon a decrease in grain size. The yield strength increases with a decrease in grain size because the decreased grain size increases the number of grain boundaries in the material. The grain boundaries inhibit the motion of the dislocations present in the material, which results in an appreciable increase in the material's strength. Empirical evidence has demonstrated that a decrease in grain size can increase the ductility of the material; however, there is not a scientific consensus behind the mechanics of this relationship. In addition, hardness and toughness are improved by a reduction in grain size [6].

3. EXPERIMENTAL PROCEDURE

3.1 SPECIMEN PREPARATION

Stock material for the study was obtained in the form of 1/8 inch thick sheets of 1100 aluminum ordered from McMaster-Carr. Tensile specimens were then water-jet cut out of the sheets to specifications per ASTM E8 [11]. Water-jet cutting was employed to reduce the risk of a heat-

affected zone from the cutting operation. The rough edges of the specimens were machined to minimize fracture nucleation sites.

From preliminary tensile tests of the specimens, it was determined that there was some residual cold work from the prior processing of the alloy. Therefore, a standardization anneal was conducted on all of the specimens, before experimental cold work was applied, to remove residual cold work and produce a uniform microstructure within the specimens. The standardization anneal consisted of four tensile specimens placed in a furnace at a minimum of one inch apart from each other. The treatment was at 343°C (650°F) and the specimens were left in the furnace for an hour.

3.2 *COLD WORK*

Tensile elongation was used to represent the deformation process that an alloy sheet would undergo during hydroforming. A range of cold work was chosen to incorporate multiple amounts believed to lie within the critical strain region for 1100 aluminum, 5-15%, as well as the potential extremes 0% and 30% (Table I).

Table I. Levels for the Variable of Cold Work Amount

Cold Work Amount				
0%	5%	10%	15%	30%

After the standardization anneal the specimens were placed in the Instron Universal Testing Machine to apply tensile elongation to the specimens. An effective gage length of 2.6 inches was diamond scribed onto the tensile specimens. The 5%, 10%, and 15% specimens were elongated by the Instron programmed to stop at the respective elongation value based on the reading from an Epsilon extensometer. The 30% cold work amount was out of the range of the extensometer. Therefore, the extensometer measured the first 15% strain and the final strain to 30% was calculated by the crosshead displacement. The 0% cold worked specimens were not elongated before sectioning. There were three replicate conditions of each of the specimens for each cold work amount giving ten total specimens (eight of which were elongated). All percent elongation values were checked by hand calculations, based on the marked effective gage length.

3.3 SAMPLE PREPARATION

Following elongation, samples were taken from the effective gage length of the cold worked tensile specimens. The sample length was set for all samples at 0.750 ± 0.025 inches. However, the exact thickness and width of the samples varied based upon amount of cold work during the elongation process. Three samples were cut from the effective gage length of each of the specimens using an abrasive saw. The samples were randomized so that there was no bias in determining which sample came from which tensile specimen. After randomization each sample was given a specific designation (Table II) for organizational purposes.

Table II. Test Matrix and Sample Designations

Heating Rate Method	Cold Work Amount				
	0	5	10	15	30
Production (16-18°F/min)	P-0-1	P-5-1	P-10-1	P-15-1	P-30-1
	P-0-2	P-5-2	P-10-2	P-15-2	P-30-2
	P-0-3	P-5-3	P-10-3	P-15-3	P-30-3
Steel Conduction (1000-1150°F/min)	SC-0-1	SC-5-1	SC-10-1	SC-15-1	SC-30-1
	SC-0-2	SC-5-2	SC-10-2	SC-15-2	SC-30-2
	SC-0-3	SC-5-3	SC-10-3	SC-15-3	SC-30-3

3.4 HEAT TREATMENT

The annealing heat treatment factors were constrained by AMS 2770 such that the treatment must be conducted at a temperature within the 630-660°F range and must incorporate a 30-minute hold time once the material reaches that temperature range [12]. The freedom within the specification is the heating rate, the rate at which the alloy reaches the minimum specification temperature. Prior research indicated that increasing the heating rate would decrease the recrystallized grain size of the material. Therefore, two different annealing treatments, one with a slow heating rate and one with a significantly faster heating rate were developed. A 3 kW SentroTech Programmable Furnace was used for both annealing heat treatments.

3.4.1 Production Heating Rate

For the slower heating rate, the furnace was programmed to reach the annealing temperature (650°F) in 35 minutes giving an approximate heating rate of 16°F/min. This rate was meant to represent the heating rates of typical large-scale production furnaces and was denoted the

"Production" heating rate. For this treatment, three samples were heat treated at a time (Figure 11).



Figure 11. Furnace set-up for the Production heat treatment. The samples were placed at a minimum of one inch apart per AMS 2770 and raised to the center of the furnace using refractory bricks.

Multiple furnace surveys were performed in order to test that the heating rate programmed was indeed the heating rate the samples were experiencing. In these tests, the set up of the furnace was the same as the heat treatment with the addition of two thermocouples. A thermocouple was placed in the back of the furnace to measure the temperature of the furnace due to some issues with the furnace's internal thermal couple. The front sample was replaced with a test coupon of similar geometry with a thermocouple press-fit into a hole drilled into its center. Two additional test coupons without thermocouples were added to the back and middle of the furnace to simulate the thermal mass in the actual heat treatment. Data was taken at 15-second intervals from the thermocouples using an Omega data logger. Two furnace surveys were run for the Production heat treatment (Figure 12).

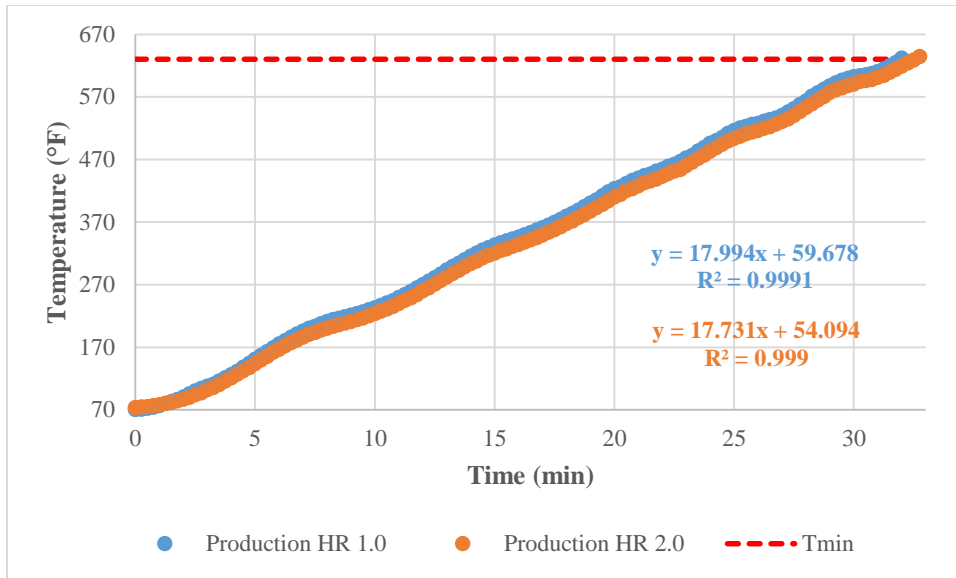


Figure 12. Graph of both Production heating rate (HR) tests. The blue data points represent test #1 with a heating rate of 17.99°F/min and the orange data points represent test #2 with a heating rate of 17.73°F/min. The dotted red line is the minimum temperature from AMS 2770. The data from both tests were fit with a linear model with their respective equations given in the corresponding color. The derivative of this fit was used to calculate the Production heating rate for the aluminum.

Data was also analyzed for the duration of the hold time for the surveys to ensure the samples would remain within specification for the entire heat treatment (Figure 13).

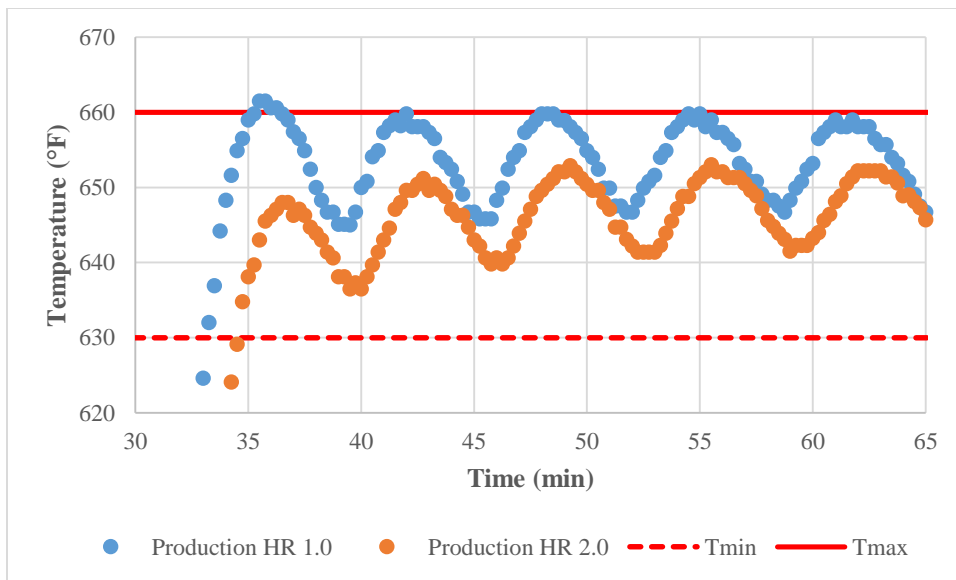


Figure 13. The thermal response of the 1100 aluminum throughout the hold time of two Production heating rate tests. The blue data points show that in the first test the alloy was out of specification slightly ($T_{\max} = 661.5^{\circ}\text{F}$) at the maximum of its first temperature fluctuation. The orange data points show that in the second test the alloy remained in specification for the duration of the test ($T_{\max} = 653^{\circ}\text{F}$).

For the first Production furnace survey the aluminum went slightly out of specification. In order to remedy this, the programmed temperature was lowered by 3°C and resulted in no significant difference in heating rate yet a steady fluctuation in temperature about 645°F. The program for the second furnace survey was employed for all of the Production heat treatments.

3.4.2 Steel Conduction Heating Rate

The SentroTech programmable furnace is limited to a maximum heating rate of 18°F/min and could not produce a heating rate faster than the Production heat treatment. In order to achieve a significantly faster heating rate, the samples were subjected to heating via conduction in a heat treatment method denoted "Steel Conduction". For this method, two 3.3" x 5" x 0.5" steel plates were put into the SentroTech furnace with a thermocouple placed in between the plates to measure the temperature of the steel. The steel was then heated to a temperature within the AMS specification range by programming the furnace to reach 650°F. Once the steel plates were within the temperature range (at least 640°F), the furnace door was opened and the aluminum sample was placed in between the two steel plates – taking proper safety precautions and ensuring planar contact between the surfaces of the sample and the surfaces of the steel plates (Figure 14).

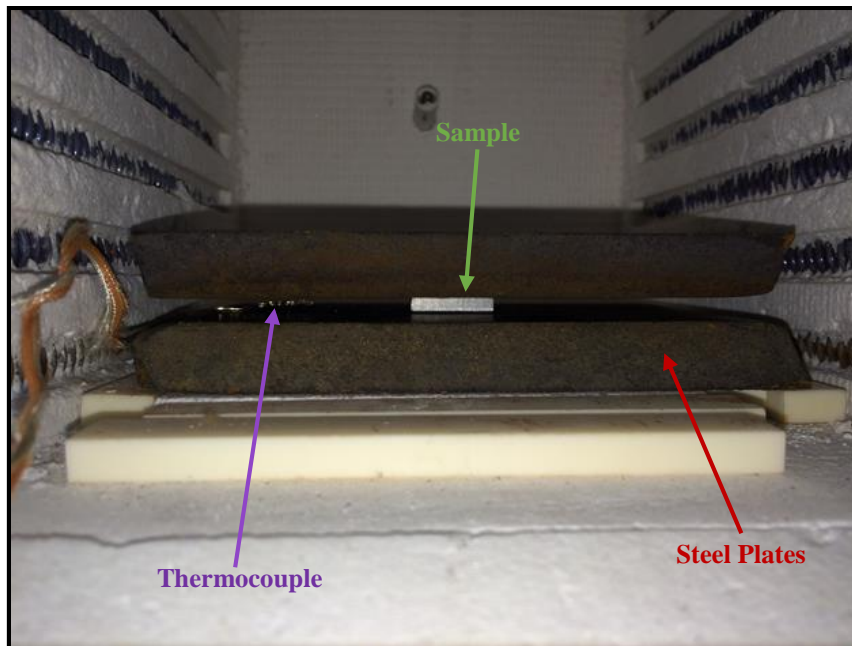


Figure 14. Furnace set-up for the Steel Conduction heat treatment. A single sample was placed in between the steel plates once the plates reached 640°F. A thermocouple was placed in between the plates to record the temperature of the plates.

Similar to the Production heat treatment, multiple furnace surveys were executed in order to determine the heating rate the samples experienced during the heat treatment. In these tests, the set-up was the same as in Figure 14 with the sample in the middle of the plates being replaced with the test coupon from the Production heating rate furnace surveys. Only one sample was tested at a time for this method. Data was taken at 5-second intervals from the thermocouples using an Omega data logger. Three furnace surveys were performed for the Steel Conduction heat treatment (Figure 15).

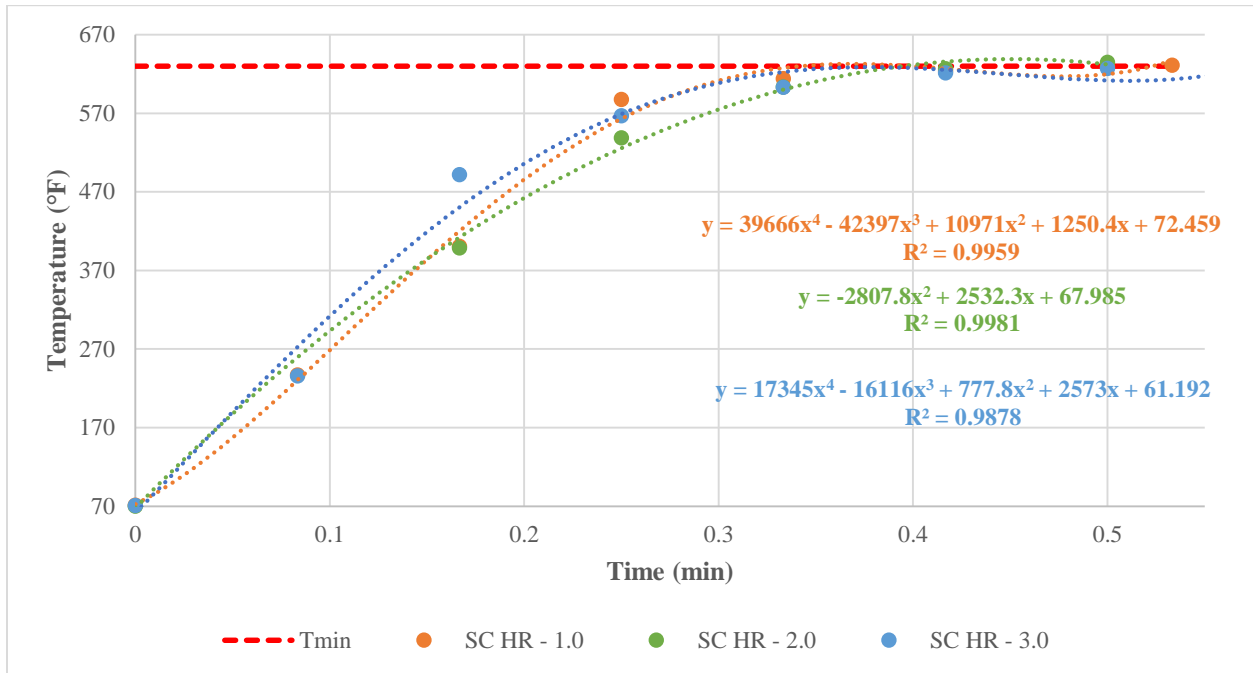


Figure 15. Graph of the time it took the 1100 aluminum to reach temperature during the three Steel Conduction heating rate (SC HR) tests. The orange data points represent the first test, green data points represent the second test, and the blue data points represent the third test. These resulted in heating rates of 1014°F/min, 1128°F/min, and 1086°F/min, respectively, calculated from the derivate of the functions displayed with the corresponding color.

Data was also analyzed for the duration of the hold time for the surveys to ensure the samples would remain within specification for the entire heat treatment (Figure 16).

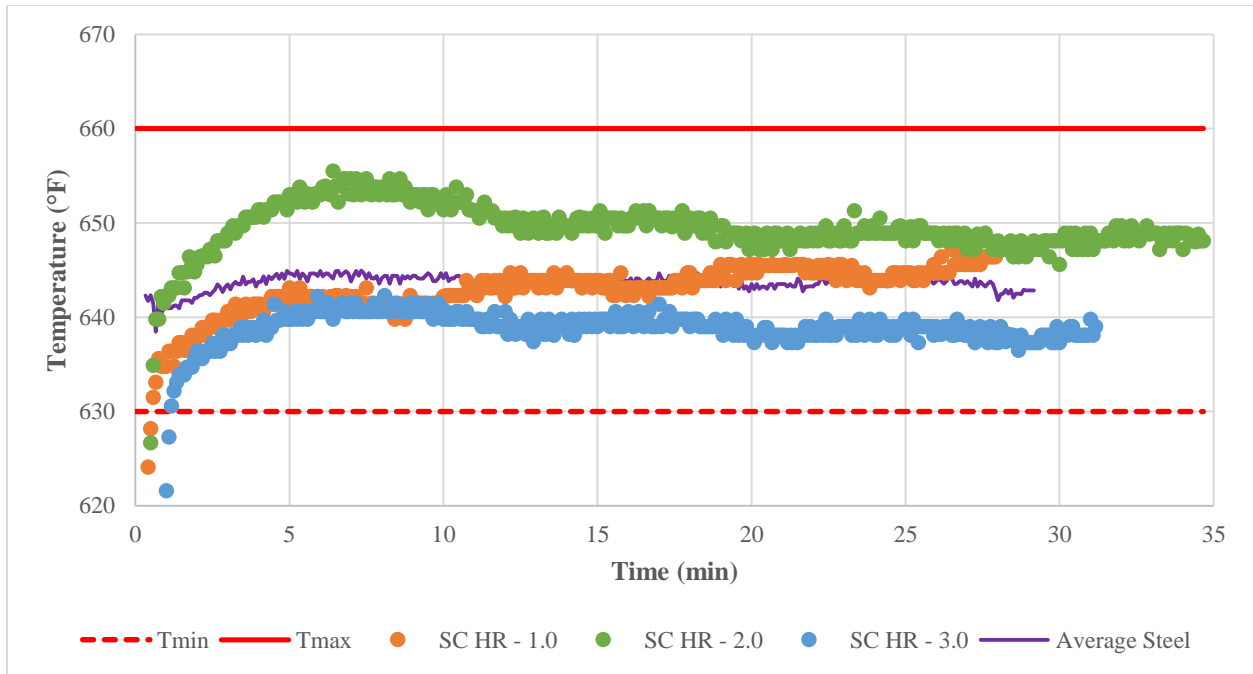


Figure 16. The thermal response of the 1100 aluminum throughout the hold time of the three Steel Conduction heating rate tests. In all three tests, the aluminum remained well within the specification limits – given in red – throughout the duration of the test. The average steel temperature was calculated and is plotted above as a purple line.

The aluminum test coupon did not exceed the AMS temperature range in any of the furnace surveys. Figure 16 displays the average steel temperature for the duration of the three tests. From this data, the heat treatments for this method were standardized such that the sample was not placed in between the steel plates until a minimum temperature of 640°F was reached. With the furnace surveys conducted, the heat treatments were fully verified and reproducible.

3.5 METALLOGRAPHY

Following the heat treatments, the samples were mounted in acrylic to observe the face perpendicular to the tensile axis (Figure 17).

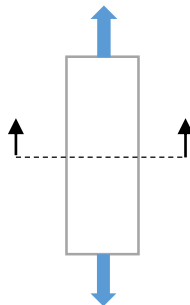


Figure 17. Displayed is the gage length of the tensile specimens. The blue arrows indicate the tensile axis. The metallographic viewing plane was revealed by sectioning represented by the dotted black line.

Along with the cold worked and heat treated samples, three samples were mounted and imaged to obtain initial grain size. These samples only underwent the standardization anneal in order to characterize the grain size prior to any processing. Standard metallographic procedures were followed to rough polish the samples using 240, 360, 400, 600, 800, and 1200 grit emery paper. For final polish, 6 μ m, 3 μ m, 1 μ m monocrystalline diamond suspensions, and a 0.05 μ m colloidal silica/alumina solution were used on the appropriate polishing pads for eight minutes, four minutes, four minutes, and eight minutes, respectively. The samples were then etched using an alkaline solution consisting of 20 grams of NaOH in 20 mL of distilled water [13]. The samples were submerged in the solution for a duration of 20 minutes. Three micrographs were taken on each sample in order to calculate average grain size using the mean lineal intercept method from ASTM E112 [14]. Details of this procedure can be found in Appendix A.

3.6 HARDNESS

After examining the micrograph data, it was determined that supplemental hardness data was required for further analysis. To obtain hardness data on the post-cold work, pre-heat treatment condition, the remaining gage length from each of the original tensile specimens (ten specimens) was tested on a Wilson Rockwell Hardness Tester using the HRH scale. After microscopy was complete, a sample representing each cold work/heat treatment condition (ten samples) was broken out of its respective acrylic mold and hardness tested using the HRH scale. In addition, a portion of the gage length of the 15% cold work tensile specimen was cut and mounted in order to be tested using the Buehler Micromet Microhardness Tester to determine if a gradient of cold work existed in the 15% cold work samples.

4. RESULTS

The results collected consisted of micrographs, grain size measurements, and hardness data. The primary results were the micrographs and their corresponding grain size measurements. Figure 18 displays representative micrographs, one from each heating rate and cold work amount.

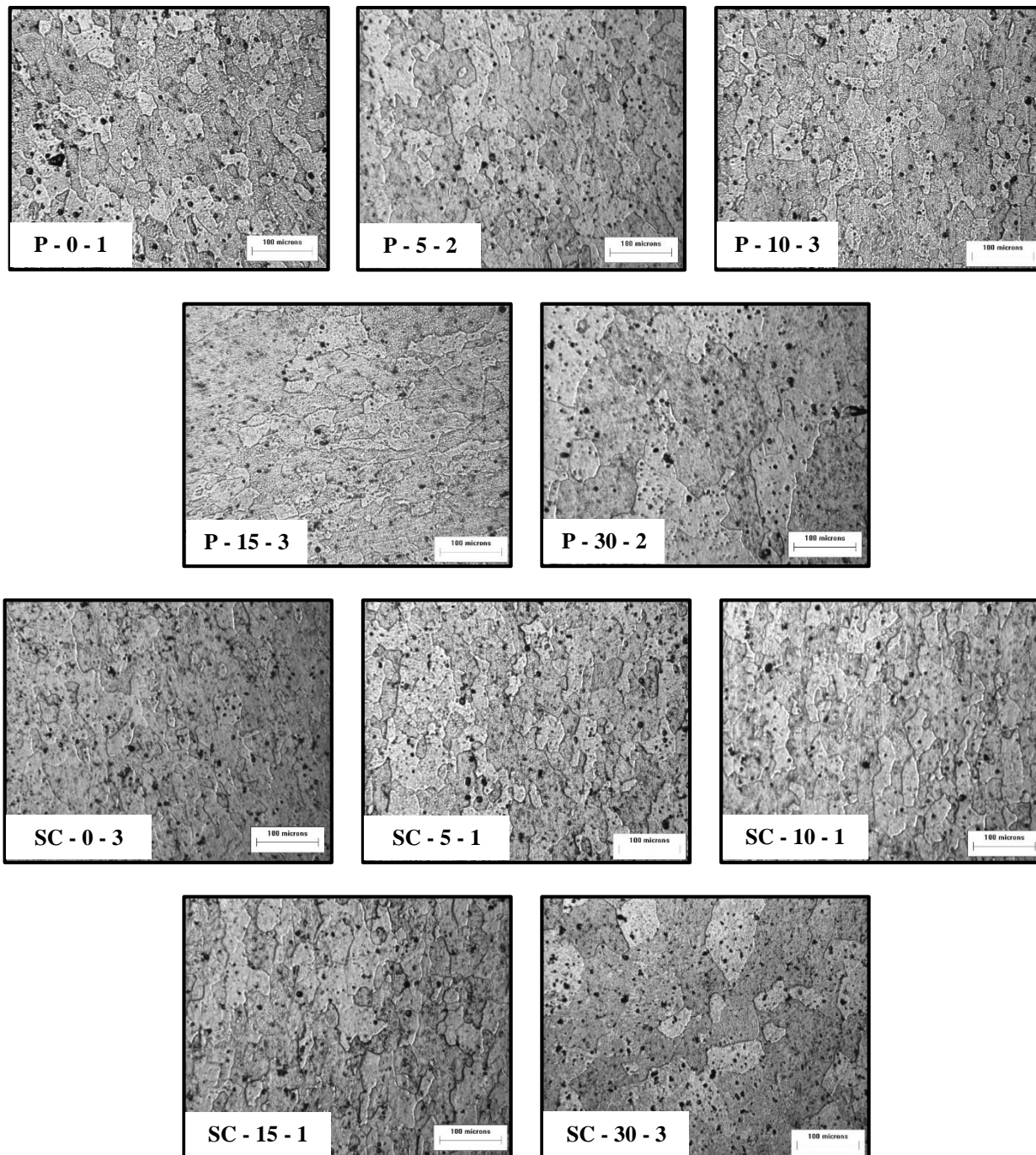


Figure 18. Representative micrographs of 1100 aluminum from each sample condition. The bottom left-hand corner of the image gives the sample designation including heat treatment type, cold work amount, and replicate number. Mag 200x. Etch: NaOH solution.

Micrographs from each sample can be found in Appendix A. The grain size data can be represented by ASTM grain size number (n) or by average grain diameter. Table III gives the grain size data according to the cold work-heat treatment combination.

Table III. ASTM Grain Size Number and Average Grain Diameter for Each Sample Condition

CW (%)	ASTM n		Avg. Grain Diameter (µm)	
	Production	Steel Conduction	Production	Steel Conduction
0	4.27	3.73	82.02	99.08
5	4.29	3.58	81.41	104.11
10	4.21	4.06	83.73	88.05
15	2.95	4.23	129.32	83.31
30	1.86	1.57	188.92	209.05
IGS	4.22		83.72	

When observing the data for the Production heat treatment there appeared to be similar grain diameters for 0, 5 and 10% cold work, which closely matches the initial grain size (IGS). At 15% there was an increase in grain diameter followed by another increase at 30%. Looking at the Steel Conduction heat treatment the 0% cold work and 5% cold work grain sizes were larger than the IGS. However, the grain size decreased when the cold work was at 10% and 15% cold work. Both these cold work amounts for Steel Conduction were also comparable to the IGS. Similar to the Production heat treatment at 30% cold work there was a spike in average grain diameter for the Steel Conduction heat treatment.

The grain size data for the 15% cold work had a caveat; there was a grain size gradient: larger grains on the edges and smaller grains in the center. Since the measurements were only taken at the center of the samples it was possible that the grain size measurements would not produce a representative average grain diameter of the samples. It should be noted that this gradient was only seen in the 15% cold work samples and occurred regardless of the annealing treatment. However, the edge grains represented a greater area of the sample in the Production heat treated samples than in the Steel Conduction heat treated samples (Figure 19).

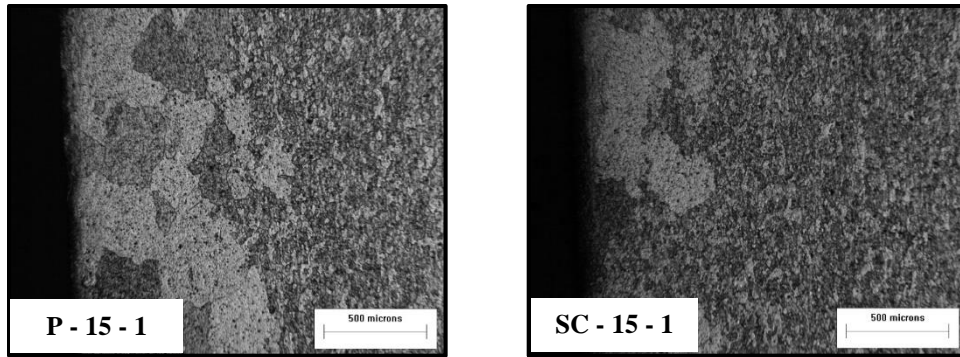
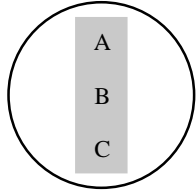


Figure 19. Shown are the grain size gradients in the 15% cold work samples for both heat treatments. The large grains for Steel Conduction (SC) take up a smaller area of the sample than in the Production (P) samples. In addition, the edge of the Production samples consist of only large grains whereas in the Steel Conduction samples there is a mix of both large and small grains.

Microhardness testing was used to determine if there was a gradient in cold work for the 15% cold worked samples correlating to the gradient in grain size; if so the center grains would be sufficient to produce a representative average grain diameter. Table IV shows the microhardness data across the sample along with a corresponding visual representation of a mounted sample.

Table IV. Microhardness of 15% Cold Worked 1100 Aluminum Sample

	Hardness Vickers (HV)			
	Section A	Section B		Section C
Edge	35.4	22.7	25.3	33
Center	36.8	38	37.7	38.9



1080 Aluminum, an alloy of similar composition to 1100 aluminum, has a Vickers hardness value of 20 HV and 40 HV for an annealed and fully hard condition, respectively [15]. Table IV shows that the edge of the 15% cold worked sample prior to heat treatment displays a gradient of cold work from a value indicative of an annealed state (22.7 – 25.3 HV) to a value representative of the presence of cold work (33 – 35.4 HV). The center of the sample remains consistent however with a value that is expected for a cold worked sample prior to annealing. Therefore, all measurements taken on the 15% cold worked samples were taken at the center of the samples, avoiding the significantly larger edge grains because the cold work across the edge of the sample was not continuous.

Table V presents the HRH data of all sample conditions. The hardness of pre-annealed samples is also included to observe the effects the annealing treatments had on hardness.

Table V. Hardness of Cold Worked and Annealed Samples

CW %	Pre-Heat Treatment		Post-Heat Treatment	
	Cold Worked (HRH)	Production (HRH)	Steel Conduction (HRH)	
0	25.0	26.2	27.7	
5	53.4	39.1	45.4	
10	61.3	52.1	52.2	
15	65.8	39.9	51.2	
30	72.7	23.4	21.2	

5. ANALYSIS

5.1 INITIAL HARDNESS AND GRAIN SIZE

The hardness data (Figure 20) shows a significant drop between the as-cold worked pre-heat treatment specimens and the post-heat treatment samples for both the Steel Conduction and Production heat treatments.

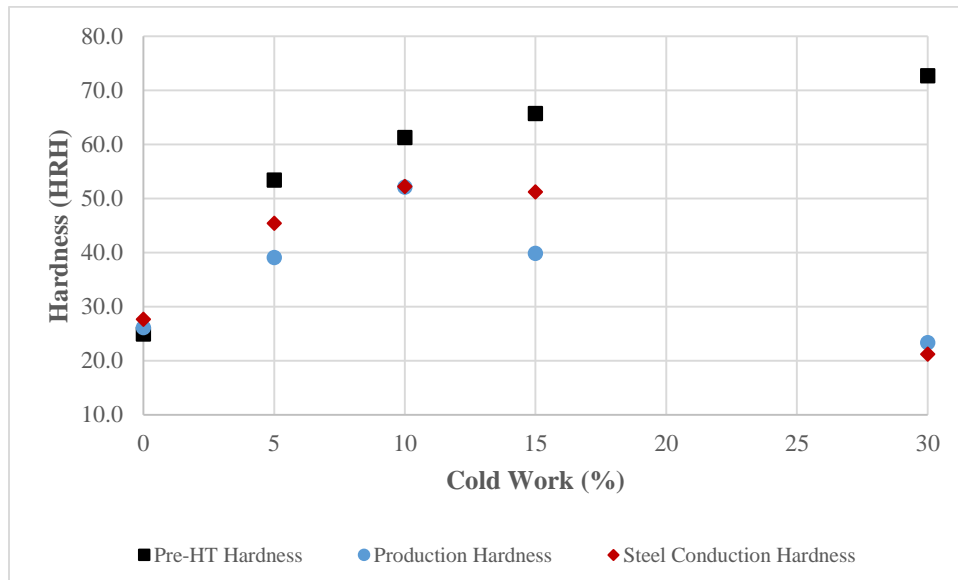


Figure 20. Plot of the hardness data for each heat treatment-cold work amount combination compared to the original hardness prior to heat treatment. Significant changes in hardness are seen in every cold work amount, especially 30%.

This drop in hardness is large enough to indicate that the samples at every cold work percentage experienced some recrystallization. This means that all samples are going to be past the critical strain region (Figure 21).

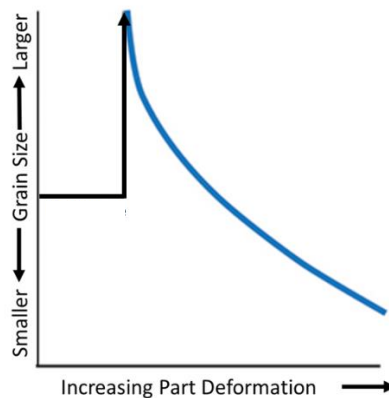


Figure 21. Graph of the effect of cold work on the recrystallized grain size at constant annealing temperature. There is no change until a peak in recrystallized grain size at the critical strain region and then a decline in grain size with an increase in cold work amount.

The critical strain region must be below 5% for these samples in order for there to be recrystallization in the 5% cold worked sample for both heat treatments. Furthermore, the drop in grain size after the peak should be significant enough such that 0% cold work and 5, 10 and 15% cold work would have similar recrystallized grain sizes.

The driving force for recrystallization is the amount of strain energy present in the alloy. However, recrystallization is a diffusion-based process and therefore time and temperature dictate recrystallization. A treatment at a lower temperature would require significantly longer times than a treatment at higher temperatures to achieve the same amount of recrystallization. The energy input at a higher temperature is substantially greater than that of the lower temperature and results in an expedited recrystallization process (Figure 22).

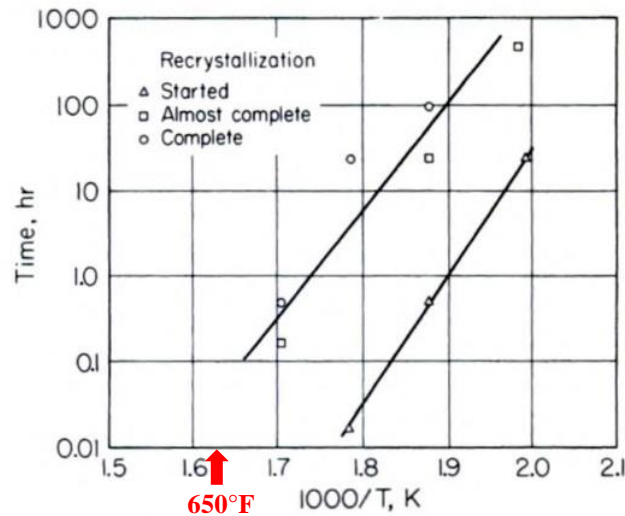


Figure 22. Time vs temperature plot for 1100-H18 aluminum showing the start and completion of recrystallization [7].

This plot shows in the fully hardened state, at temperatures lower than the AMS specification temperature of 650°F (1.62 on the scale in Figure 22 above), recrystallization will complete in less than 30 minutes with the rest of energy input going to grain growth. For this experiment both heat treatments had a hold time of 30 minutes in order to be in compliance with specification AMS 2770. This 30-minute hold time alone is more than enough time for recrystallization to occur. However, there is also a ramp up time associated with each heating rate, for the Steel Conduction heat treatment it is about 30 seconds and will likely not contribute to much recrystallization for samples lower than 30% cold work. However, for the Production heat treatment the time to temperature is 35 minutes (Figure 23). Though the sample is not at 650°F

until the end of the 35 minutes, it slowly passes through all the lower temperature ranges, which allows for some recrystallization to occur. In addition, the samples spend five minutes from 550-650°F in which recrystallization may finish in all samples with sufficient cold work shortly after beginning the 30-minute hold.

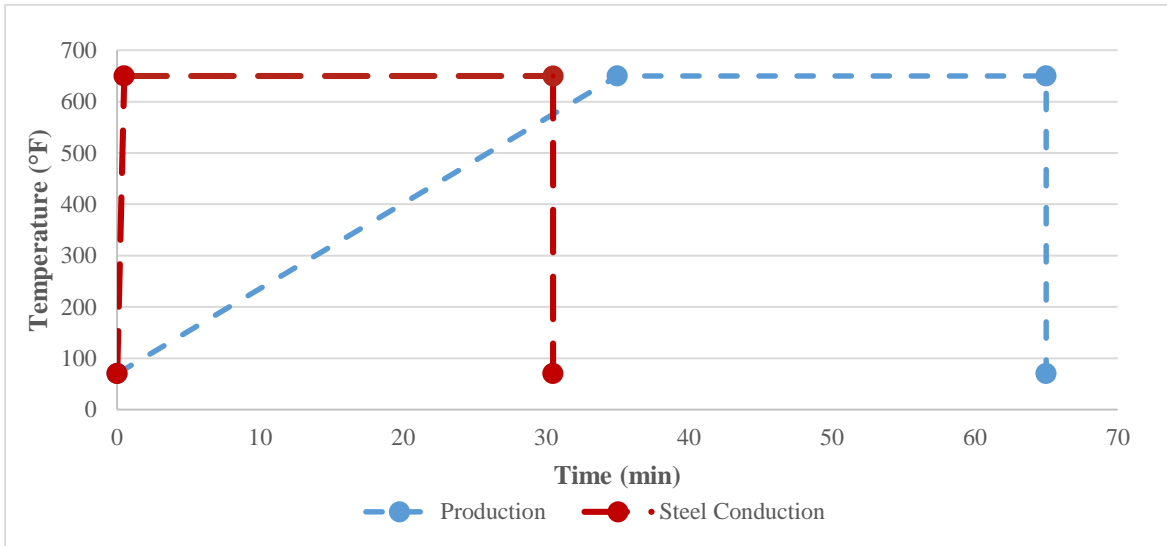


Figure 23. Plot of the time and temperatures used during each of the heating rates. Production in blue reaches temperature in 35 minutes and finishes after 65 minutes. Steel Conduction in red reaches temperature in 0.5 minutes and finishes completely after 30.5 minutes.

Figures 22 and 23 demonstrate that in both heat treatments there was sufficient time at elevated temperature to allow for recrystallization to occur in all the cold work amounts. The time appears to be sufficient enough such that there may be grain growth occurring in all of the samples for both heating rates. Though there is enough time for grain growth to occur at this temperature, the amount of stored energy present must also be taken into consideration. Samples lacking a high enough amount of cold work may only allow initial recrystallization, but not grain growth.

Figure 24 shows the grain size data as it varies for different cold work amounts for the two different heat treatments. Implementing the hardness results, the grain size data that was collected was analyzed as grain size after recrystallization with any increase in size treated as potential grain growth.

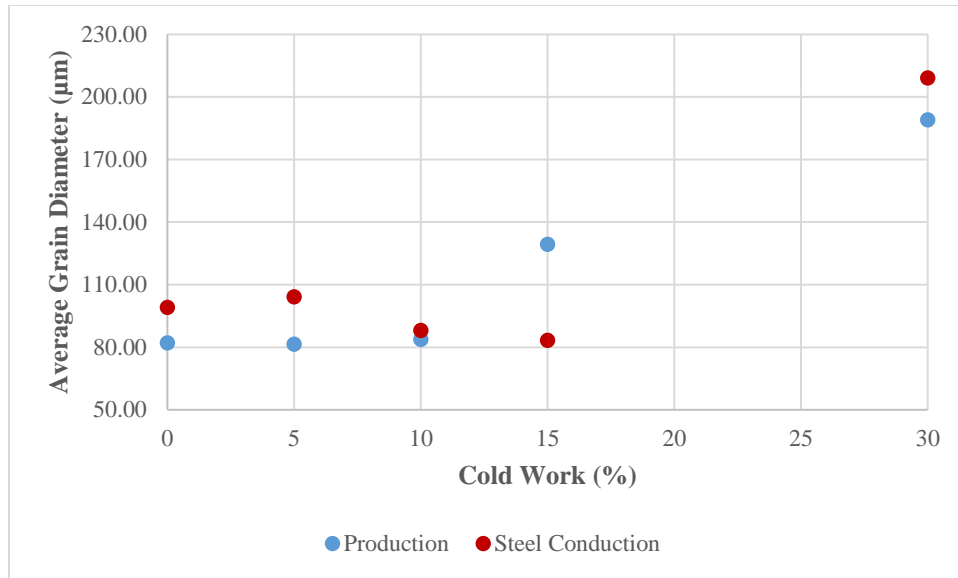


Figure 24. Average grain diameter versus the amount of cold work for the two heat treatments. In both heat treatments there appears to be grain growth.

The grain growth of the aluminum appears to be substantial for both heat treatments at 30% cold work indicating a possible affect of cold work on grain growth. For the Production heat treatment, the growth begins at lower cold work amounts than the Steel Conduction heat treatment potentially indicating an effect of heat treatment type.

5.2 STATISTICS

In order to support these assertions, statistical analysis was run on the mean lineal intercept (grain size measurement) data to determine whether or not there was a significant difference in grain size. This would determine whether or not grain growth had occurred in any of the samples. A two-way analysis of variance (ANOVA) was used to determine whether or not there was a significant difference in the means of the grain size data with respect to the two factors: cold work amount and heat treatment type. In addition to assessing the effect of the two individual factors, the interaction between the two factors was also tested to determine whether or not the two factors had any combined effects on the grain size of the samples.

A general linear model was used to conduct the two-way ANOVA. The two major assumptions associated with the two-way ANOVA are that the populations of data are normally distributed and that there is equal variance between the populations. Along with the results from the ANOVA, the statistical software output two plots to check these assumptions (Figure 25).

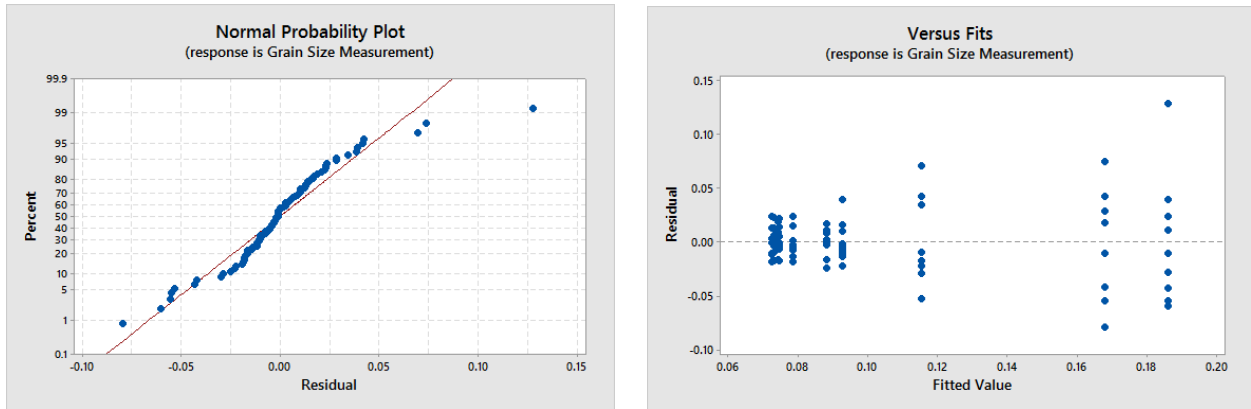


Figure 25. The plots above are output by Minitab and check the two assumptions for the two-way ANOVA: normally distributed populations (*left*) and equal variance between populations (*right*).

The distribution of the data did not appear to be normally distributed and displayed a "fanning" out, from left to right, of the variance in grain size measurements. This spread of data was an indication that the constant error variation (i.e., equal variances) assumption may be null. In order to remedy this, a logarithmic transformation of the data was performed. The natural log was taken of each of the mean lineal intercept values and these data points were used for the two-way ANOVA. The logarithmic transformation improved both the normality and equal variance of the populations (Figure 26).

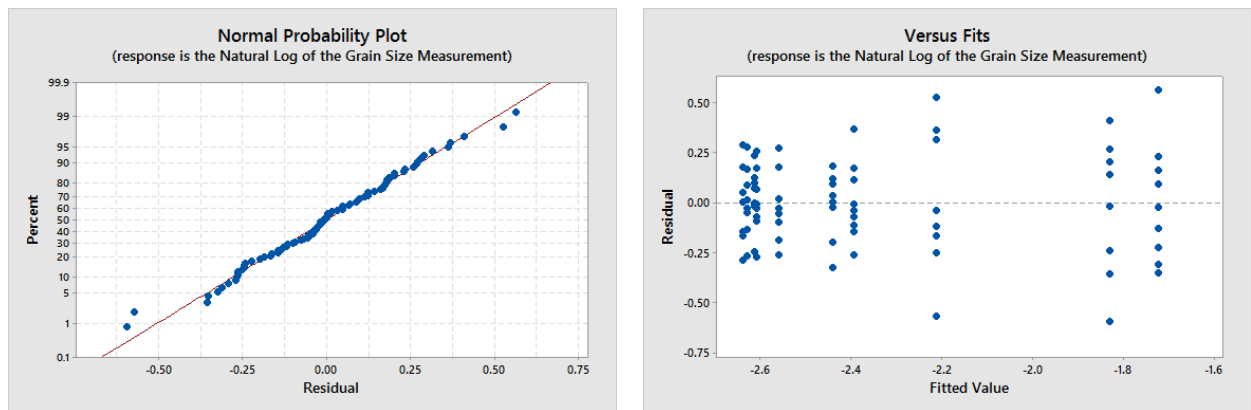


Figure 26. Minitab plots of the assumptions for the two-way ANOVA of the transformed grain size measurements. The data post transformation is normally distributed (*left*) and has more equal variance between populations (*right*).

Since the assumptions of the model were correct, the results from the two-way ANOVA could be analyzed. Table VI displays the p-values from the two-way ANOVA.

Table VI. Statistical Significance of the Two Factors and Their Interaction on Grain Size Measurements

Experimental Factor	P-Value
Heat Treatment	0.432
Cold Work Amount	0.000
Interaction Between Cold Work and Heat Treatment	0.000

The p-values from the two-way ANOVA indicated that there was no statistically significant effect on grain size from the two heat treatments. However, there was a statistically significant effect on grain size due to the amount of cold work and the combination of cold work and heat treatment.

After the two-way ANOVA was conducted, post hoc analysis in the form of Tukey pairwise comparisons were run to assess which populations were statistically similar enough to be grouped together. First, the effect of cold work amount on the grain size of the samples was grouped through a Tukey pairwise comparison (Figure 27).

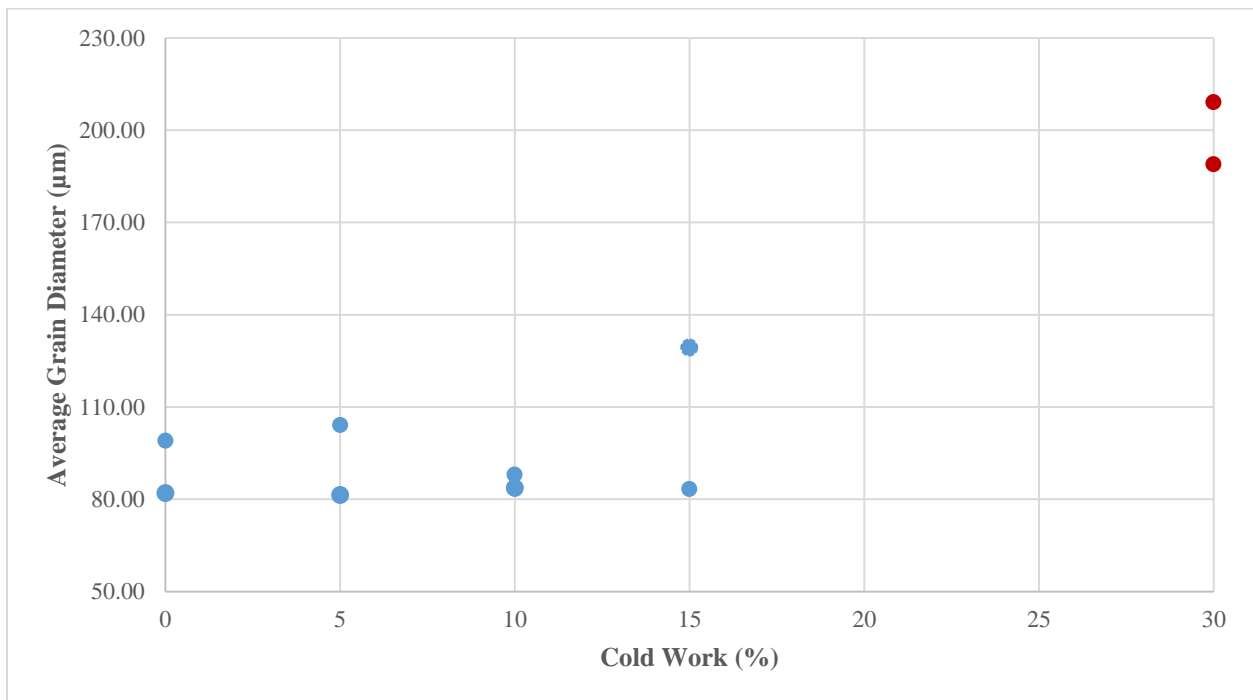


Figure 27. A visual representation of the Tukey pairwise comparison of the effect cold work has on grain size data. Data points that do not share the same color are significantly different.

Since the samples were at an elevated temperature for a sufficient amount of time it was concluded that the samples experienced varying amounts of grain growth. The Tukey pairwise comparisons demonstrated that there was a significant difference in the grain size of the 30% cold worked samples relative to the samples with all other cold work amounts. Therefore, the 30% cold worked samples experienced the most grain growth. This can be attributed to the fact that the amount of cold work in the alloy decreases the energy required for the recrystallization to occur (Figure 28).

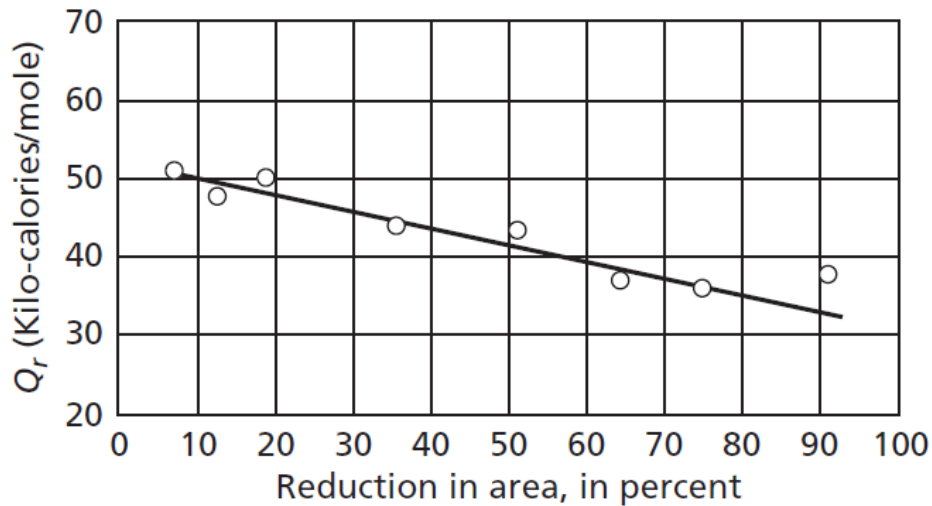


Figure 28. Activation energy (Q_r) for recrystallization as a function of cold work amount in zirconium (iodide). There is a clear inverse relationship: as one increases cold work amount, the activation energy for recrystallization decreases [4].

The presence of such a high degree of cold work (30%) allowed for recrystallization to happen at a significantly faster rate than that of the other cold work amounts given the same elevated temperature. Since the 30% cold worked samples recrystallized first, the energy absorbed for the rest of the time at the elevated temperature was put into grain growth. Since the most significant grain growth occurs directly after recrystallization ends there was no significant difference in the grain size of the 30% cold work samples between the two heat treatments. In addition, the grain growth process is a diffusion process. Therefore, the effect of temperature on grain growth is exponentially larger than the effect of time. Thus, the extra 30 minutes at temperature - which likely was after the bulk of grain growth occurred - did not produce significantly larger grains for the Production sample at 30% cold work since the same sample for Steel Conduction heat treatment had the same heat treatment temperature.

The second post hoc Tukey pairwise analysis grouped samples together based on the effect the combination of cold work amount and heat treatment type had on the grain size of the samples (Figure 29).

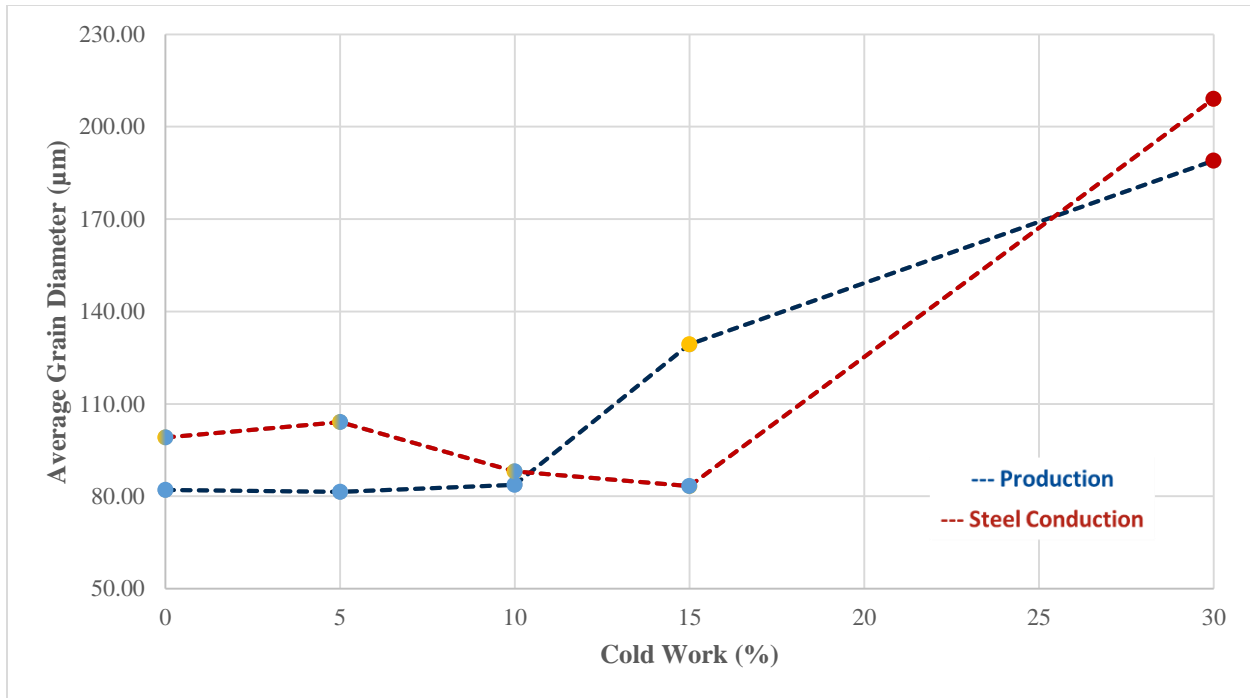


Figure 29. A visual representation of the Tukey pairwise comparison of the effect of the interaction between cold work and heat treatment on grain size data. Data points that do not share the same color are significantly different.

The Tukey pairwise comparison for the interaction between experimental factors shows no significant change in grain size within a heat treatment group until 15 and 30% cold work. For the Production heat treatment there was a significant difference in grain size in the 15% cold work samples. Therefore, the interaction between cold work and heat treatment type produced grain growth in the 15% cold worked samples for the Production heat treatment while grain growth did not occur for the Steel Conduction samples until 30% cold work. The Steel Conduction heat treatment reaches temperature magnitudes faster than the Production heat treatment. During the heat up period for both heat treatments, the 30% cold worked samples had sufficient energy stored to recrystallize at a significantly lower activation energy. This allowed for early recrystallization and time for sufficient grain growth in both heat treatments. However, the samples reach peak temperature within a minute during the magnitudes faster heat treatment. At the peak temperature, all cold work amounts would have had enough energy to recrystallize, thus all samples would begin recrystallizing. During the slow heat treatment, however, the samples slowly increased in temperature, staying at all temperatures up to 660°F for longer times. At the lower temperatures, recrystallization favors the higher cold worked samples such that they begin to grow before the other cold work amounts begin to recrystallize. Therefore, the

combination of longer times at lower temperatures and the sufficient stored energy of 15% cold work allowed for grain growth at 15% cold work for the Production heat treatment.

6. CONCLUSIONS

1. Grain growth is unavoidable for 30% cold work regardless of heating rate for the rates investigated for a maximum temperature of 660°F.
2. The longer times at elevated temperatures during the Production heat treatment allowed for significant grain growth at lower cold work amounts.

REFERENCES

- [1] G.-P. Sutton, *History of Liquid Propellant Rocket Engines*, Reston: American Institute of Aeronautics and Astronautics, 2006.
- [2] P. Cotterill and P. R. Mould, *Recrystallization and Grain Growth in Metals*, New York: Wiley, 1976.
- [3] "Rubber-Pad Foming and Hydroforming, Metalworking: Sheet Forming," in *ASM Handbook*, vol. 14B, ASM International, 2006, pp. 375-385.
- [4] R. Abbaschian, L. Abbaschian and R. E. Reed-Hill, *Physical Metallurgy Principles*, Cengage Learning, 2009, pp. 216 - 243 .
- [5] C. R. Brooks, *Heat Treatment, Structure and Properties of Nonferrous Alloys*, American Society for Metals, 1982.
- [6] H. R. R. Ashtiani and P. Karami, "Prediction of the Microstructural Variations of Cold-Worked Pure Aluminum during Annealing Process," *Modeling and Numerical Simulation of Material Science*, vol. 5, pp. 1-14, 2015.
- [7] J. E. Hatch, *Aluminum: Properties and Physical Metallurgy*, American Society for Metals, 1984, pp. 105-125.
- [8] C. C. Bampton, J. A. Wert and M. W. Mahoney, "Heating Rate Effects on Recrystallized Grain Size in Two Al-Zn-Mg-Cu Alloys," *Metallurgical and Materials Transactions*, vol. 13, no. 2, pp. 193-198, 1982.
- [9] W. D. Callister and D. G. Rethwisch, *Fundamentals of Materials Science and Engineering: An Integrated Approach*, 3 ed., John Wiley and Son Inc, 2008, pp. 242-270.
- [10] "Grain Size," in *Heat Treating Aluminum Alloys*, Louisville, Reynolds Metals, 1946, p. 77.
- [11] *ASTM E8-15a Standard Test Methods for Tension Testing of Metallic Materials*, West Conshohocken, PA: ASTM International, 2015.
- [12] *AMS 2770N Heat Treatment of Wrought Aluminum Alloy Parts*, SAE International, 2015.
- [13] A. Theisen, Interviewee, *Winter Conference Call #3: 1100 Aluminum Etchant*. [Interview]. 4 February 2016.
- [14] *ASTM E112-13 Standard Test Methods for Determining Average Grain Size*, West Conshohocken, PA: ASTM International, 2013.
- [15] *CES Edupack Software*, Granta Design, 2015.

APPENDIX A

Methods and Microstructures Used for Calculating ASTM Grain Size Number

The ASTM E112 line intercept method was used to calculate the ASTM grain size number of the 1100 aluminum. The method consists of counting the number of grain boundaries intersected by lines drawn on a micrograph of a sample and then using these counts to calculate a grain size number. To begin, three lines are drawn on a sample and the grain boundary intersections are counted.

After counting the intersections, the effective length of the superimposed lines are determined. For this experiment, this was determined by using the measurement tool on the imaging software used for microscopy. Three lines were drawn across the image with the measurement tool displaying the actual length of the lines. The effective length (l_{eff}) of the three lines was calculated by:

$$l_{eff} = (l_1 + l_2 + l_3) \times \frac{M}{100} \quad (\text{Eq. 1})$$

where l_1 is the length of the first line, l_2 is the length of the second line, l_3 is the length of the third line, and M is the magnification of the image. With the number of counts and the effective length of the lines across the sample, the ASTM grain size number (n) can be calculated:

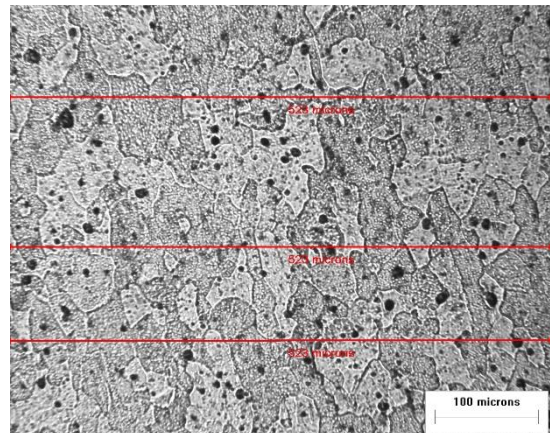
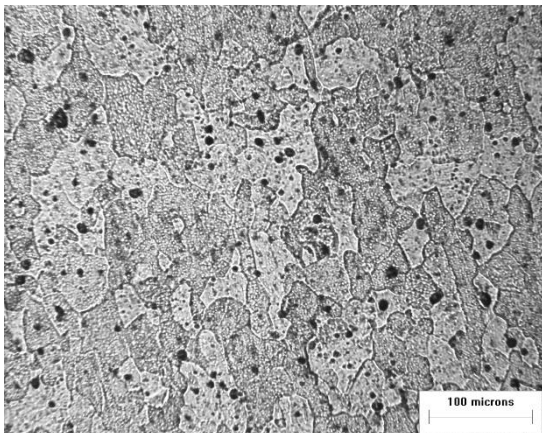
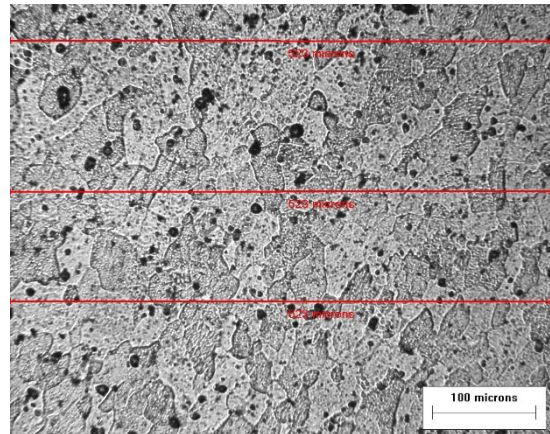
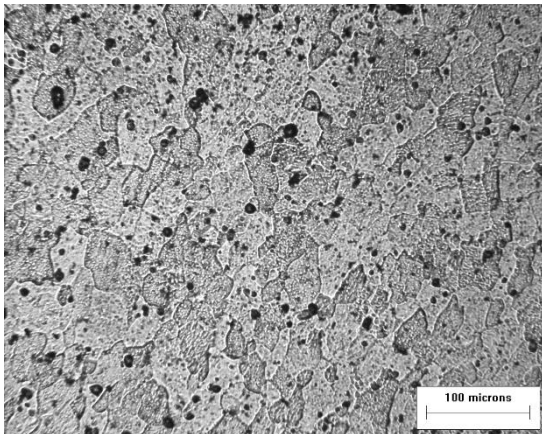
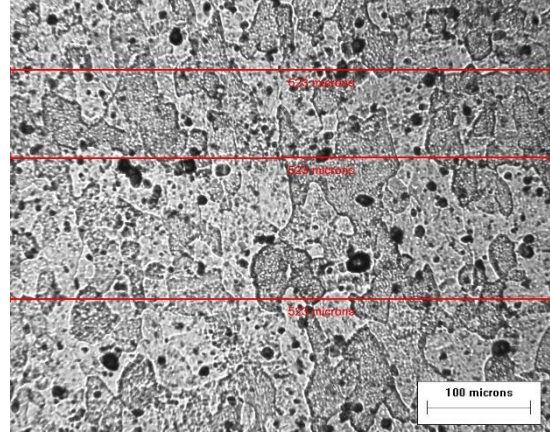
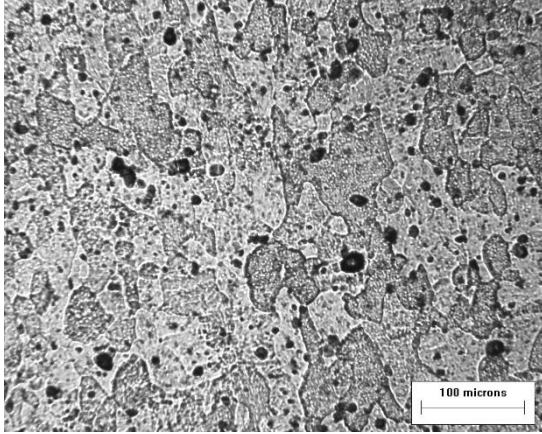
$$n = \left[-6.644 \times \log \left(\frac{l_{eff}}{N} \right) \right] - 3.288 \quad (\text{Eq. 2})$$

where N is the total number of grain boundary intersections and l_{eff} is the effective length in millimeters.

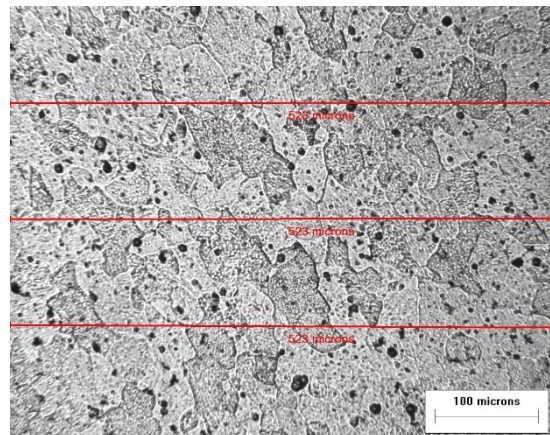
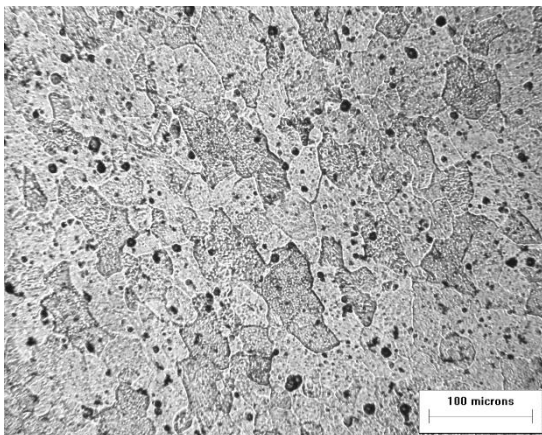
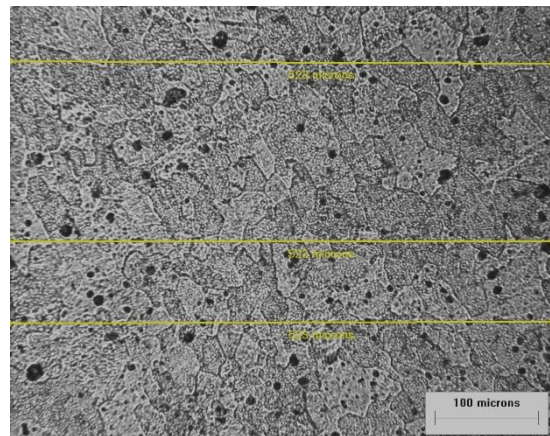
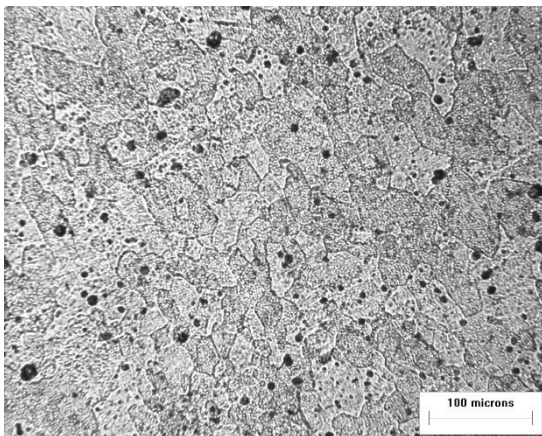
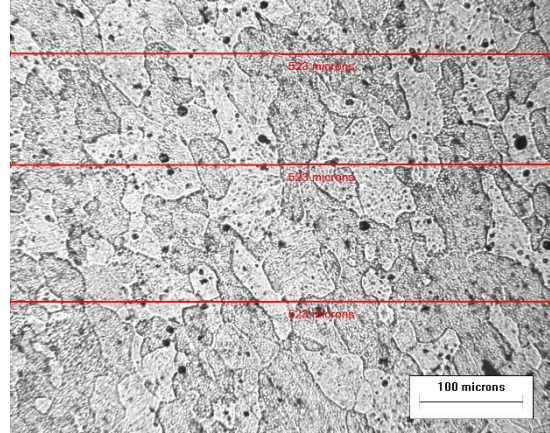
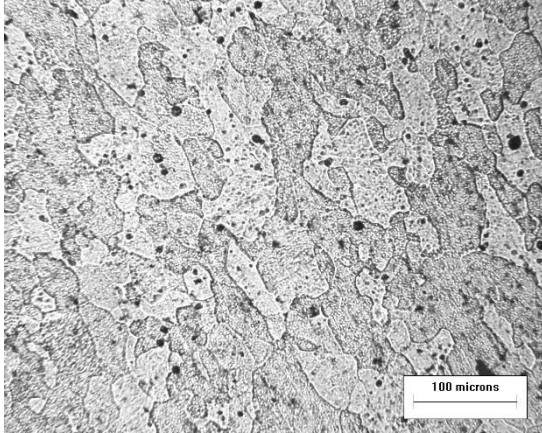
In order to ensure that the calculations are representative of the entire sample, the grain size measurements are taken from a minimum of three different locations on each sample.

Below are the microstructures of each condition and their respective replicates for the study. The left figures display the micrograph and the right figures display the lines drawn on each of the images for the grain boundary intersections.

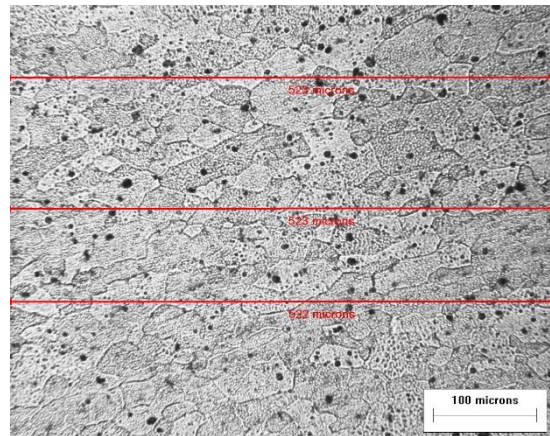
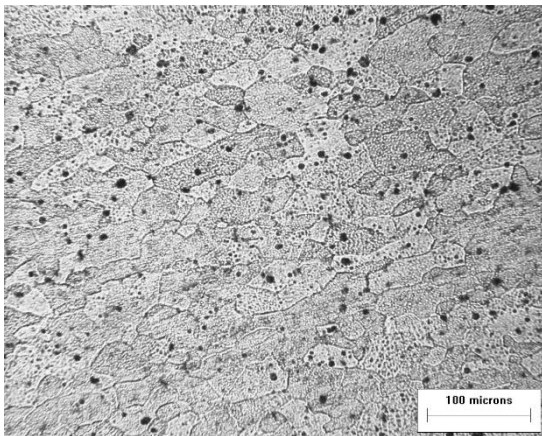
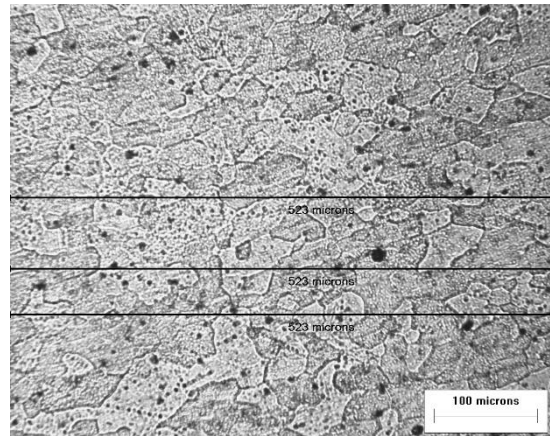
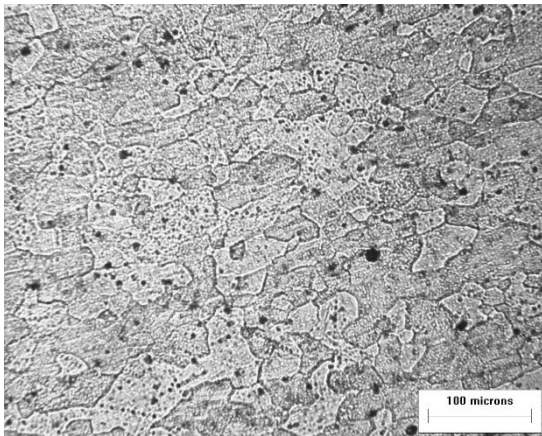
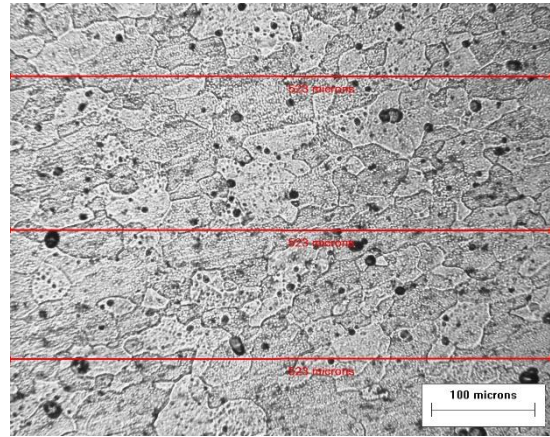
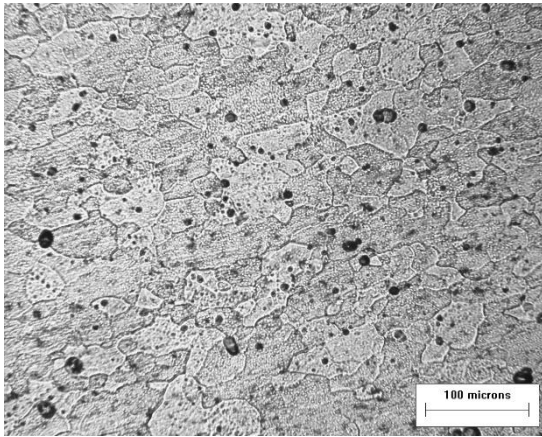
Initial Grain Size (IGS) – 1



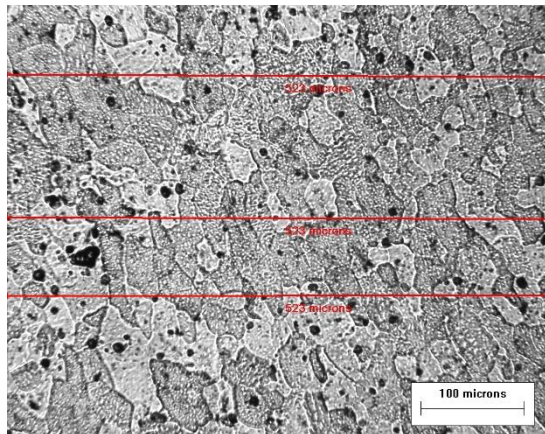
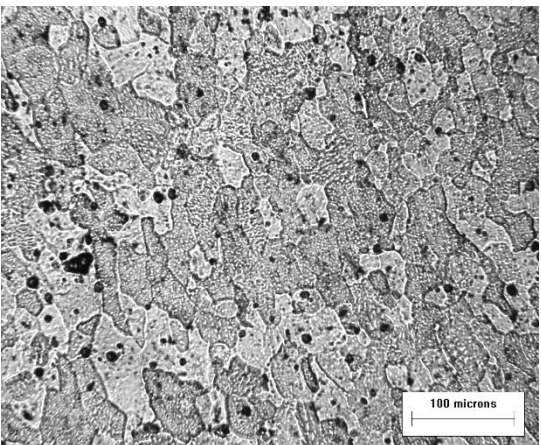
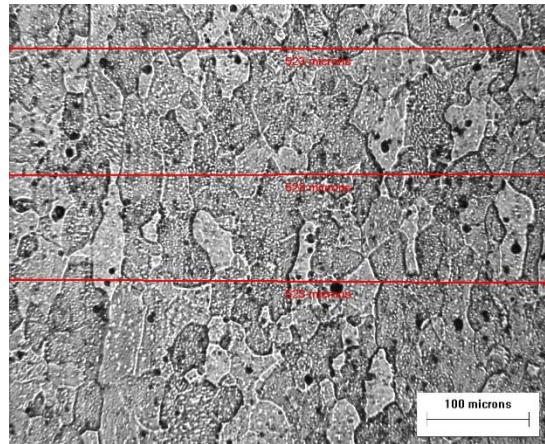
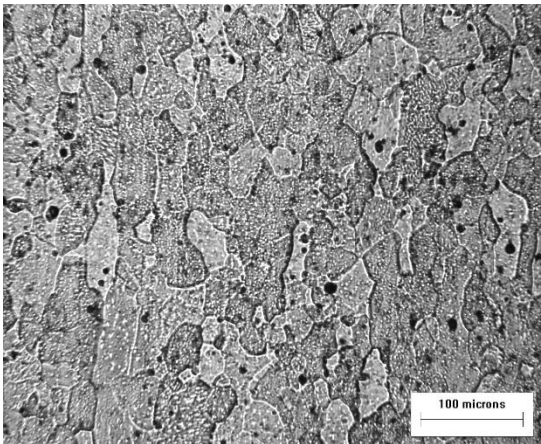
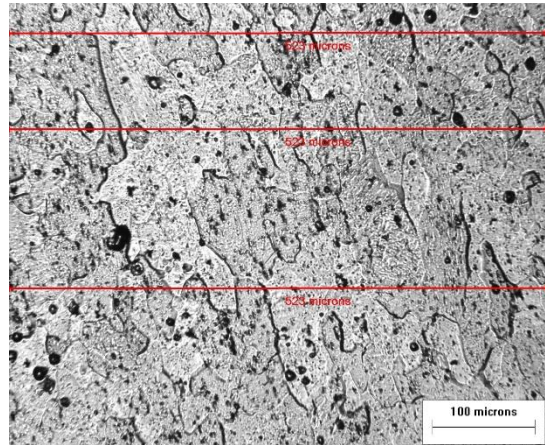
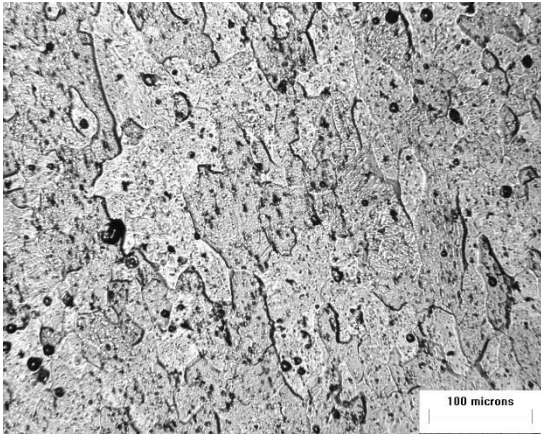
Initial Grain Size (IGS) – 2



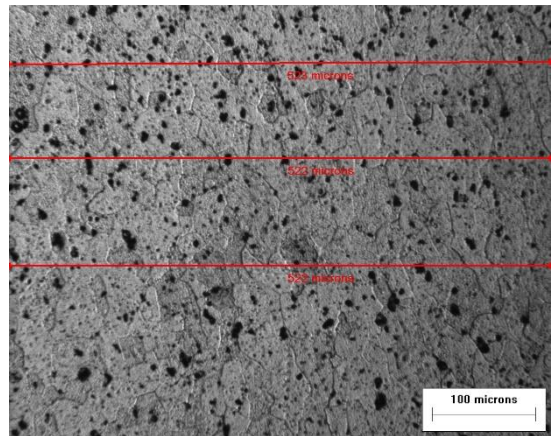
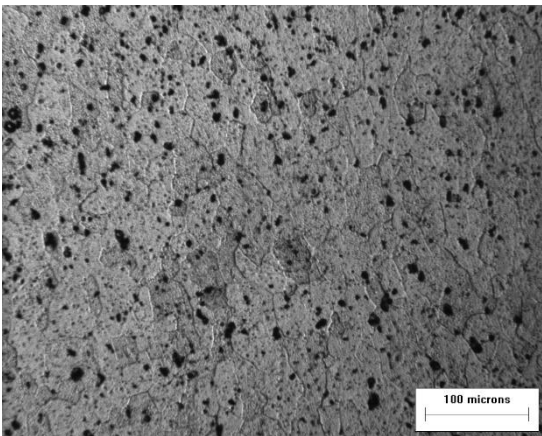
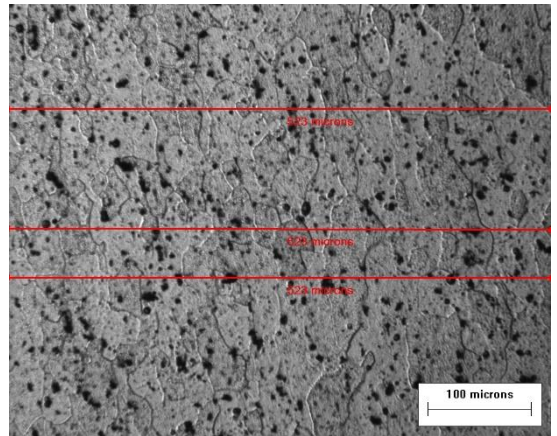
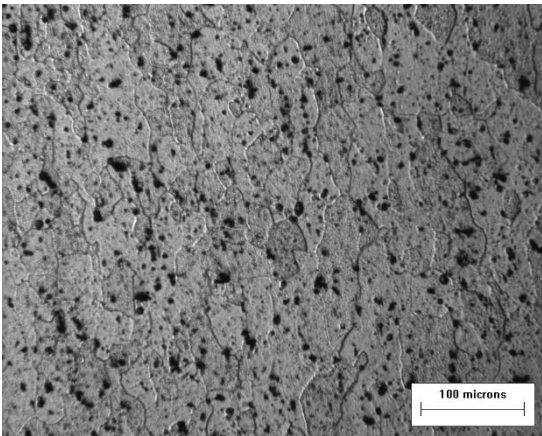
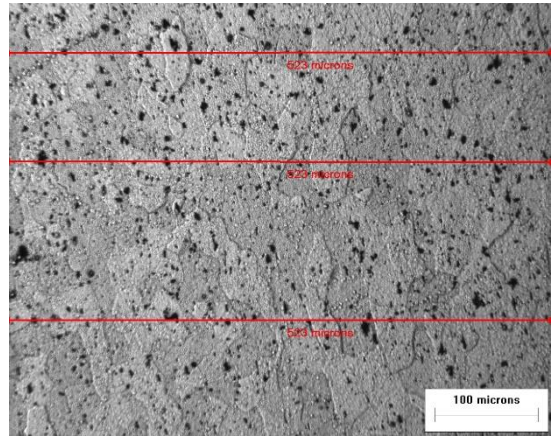
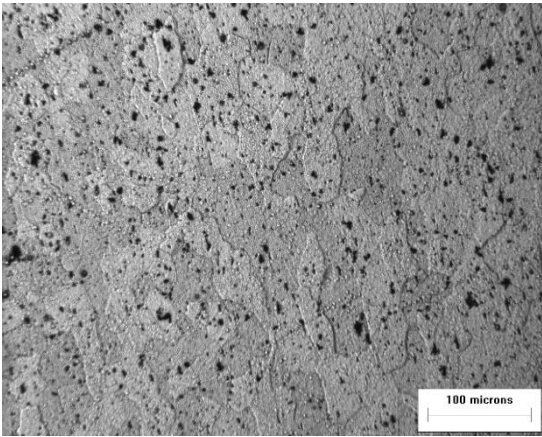
Initial Grain Size (IGS) – 3



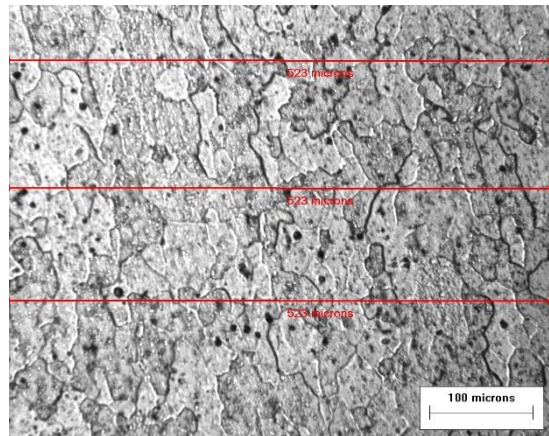
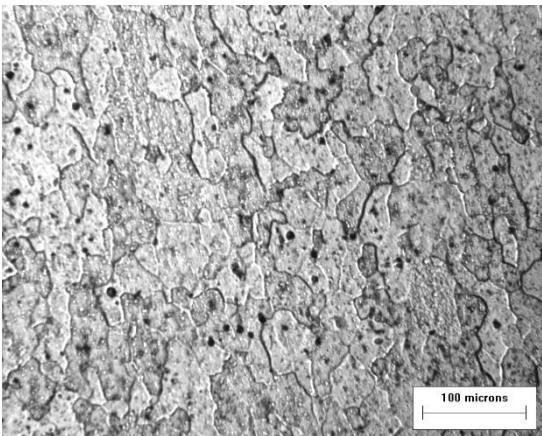
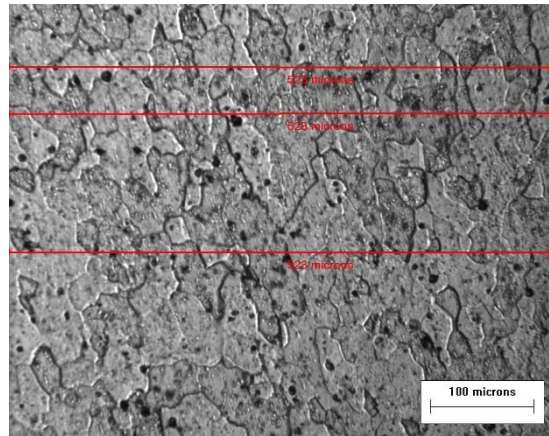
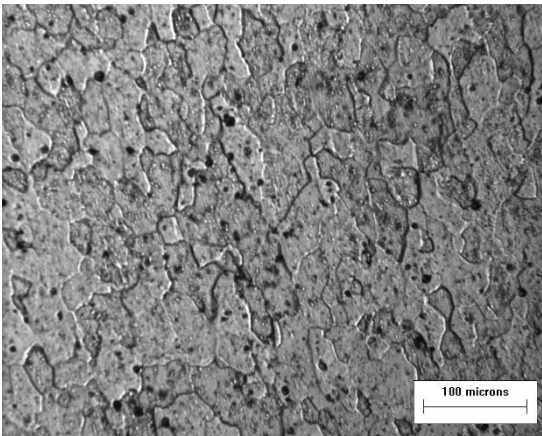
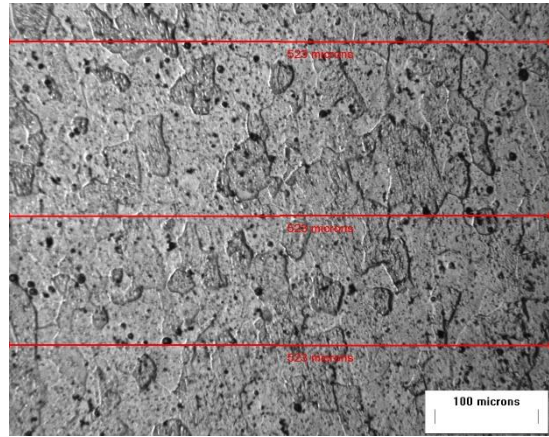
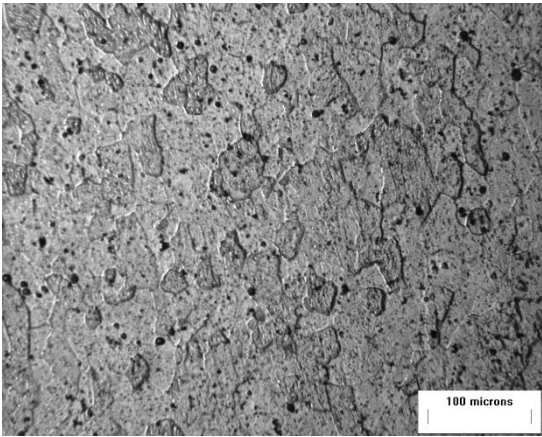
P-0-1



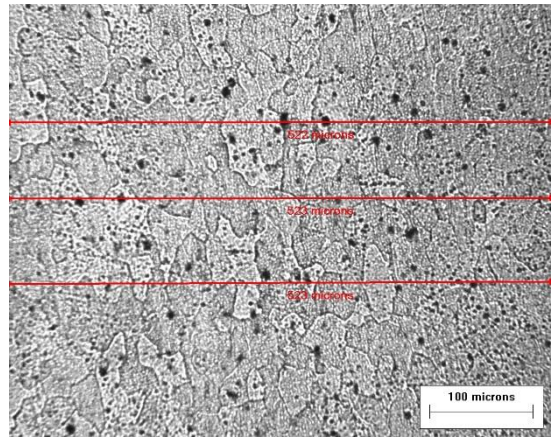
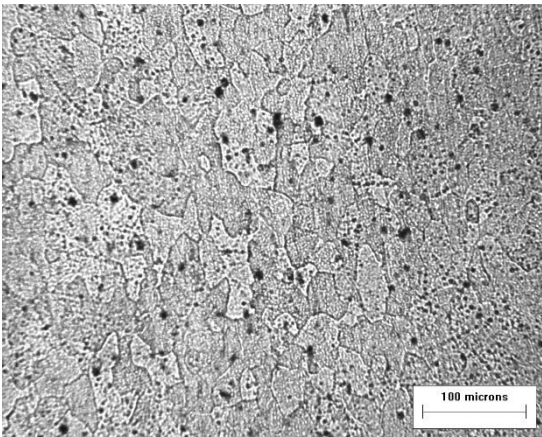
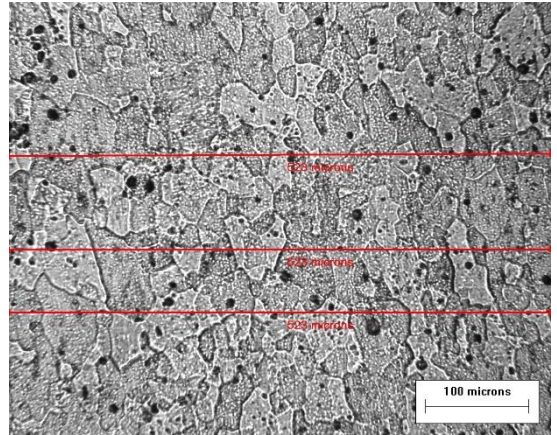
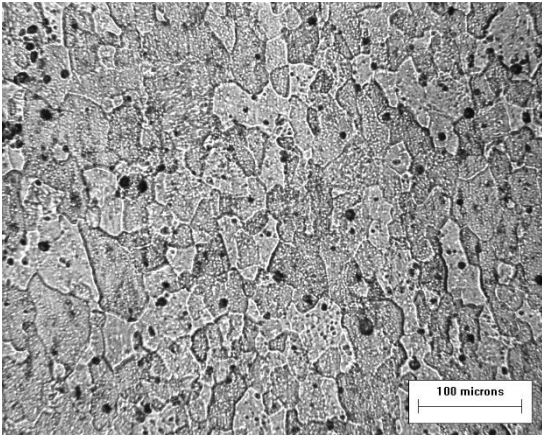
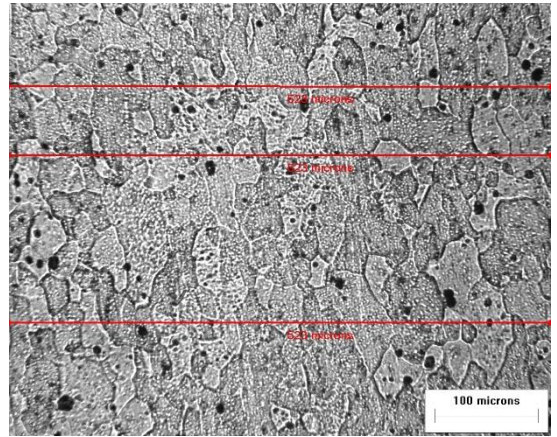
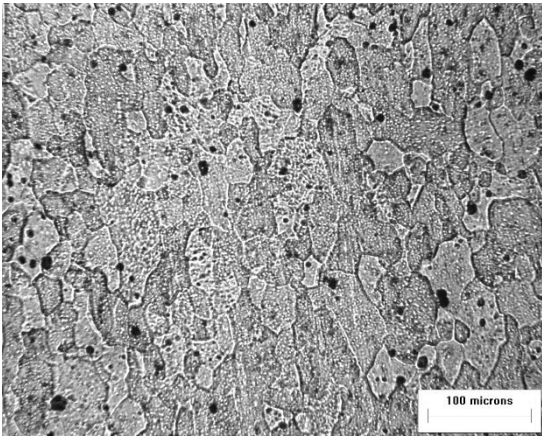
P-0-2



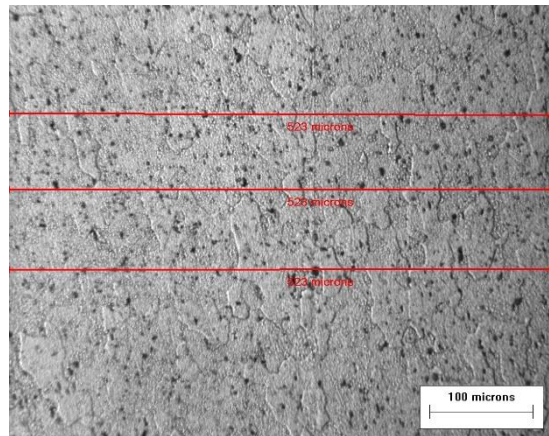
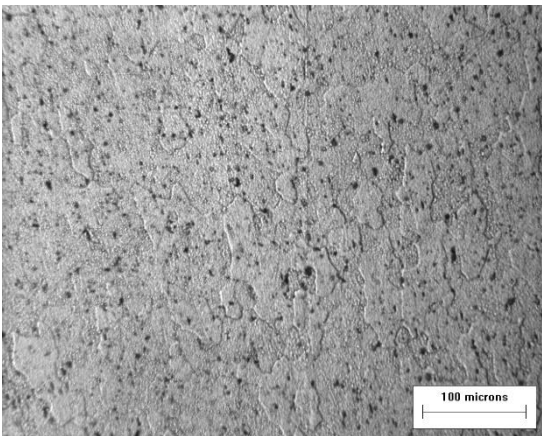
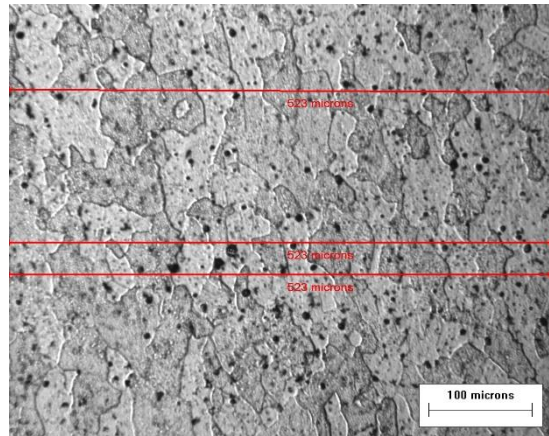
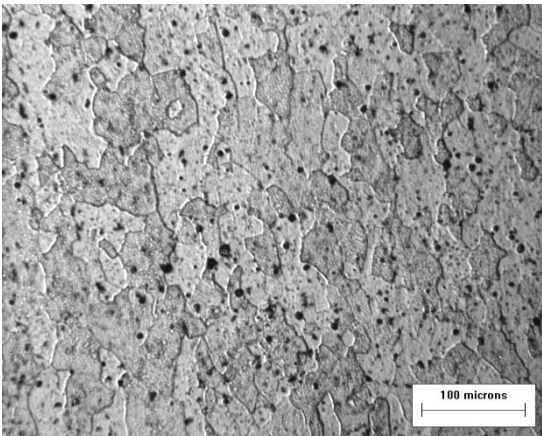
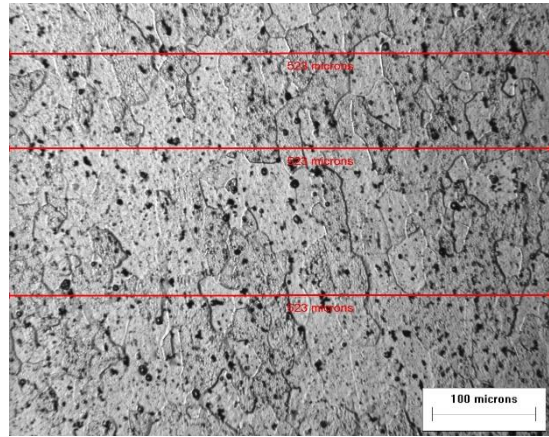
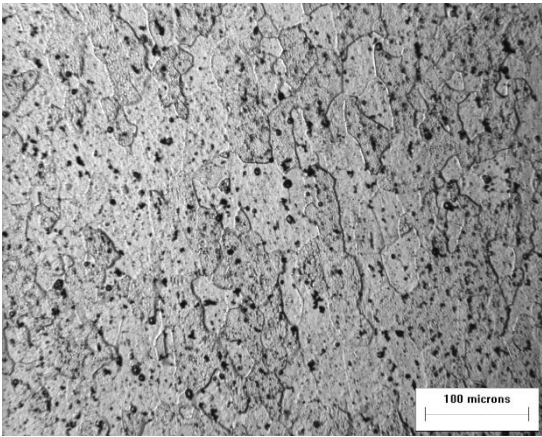
P-0-3



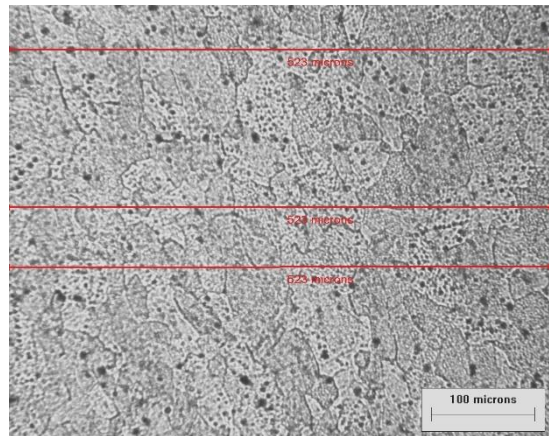
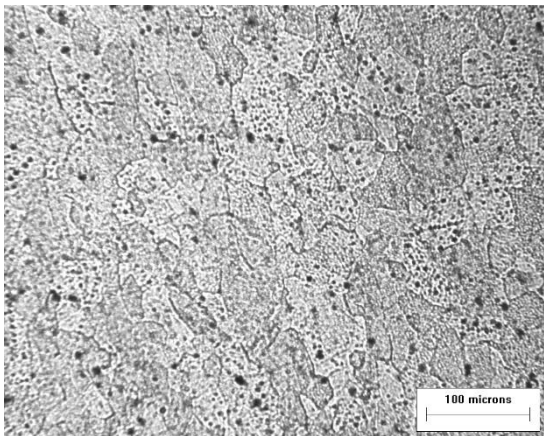
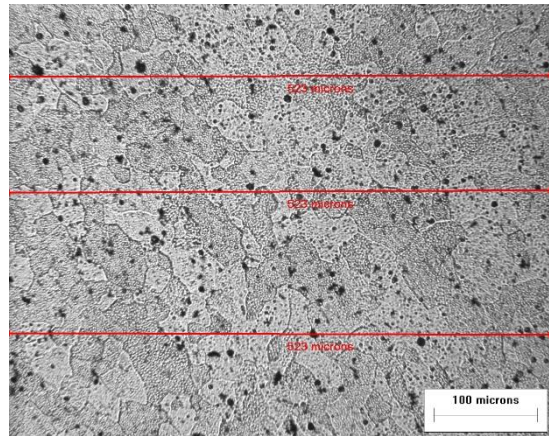
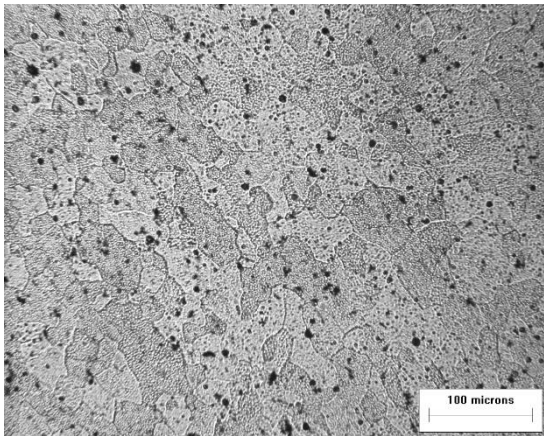
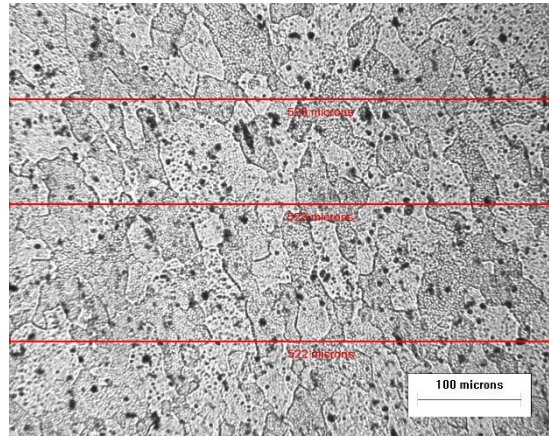
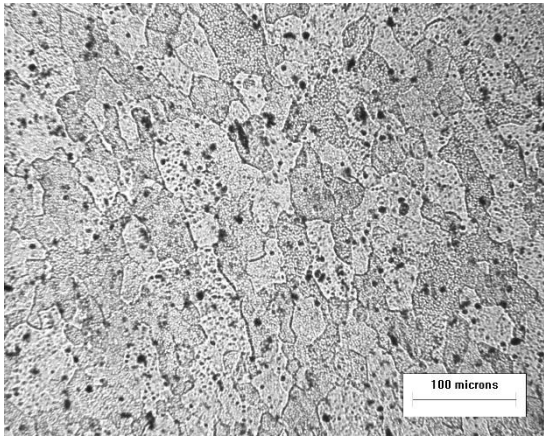
P-5-1



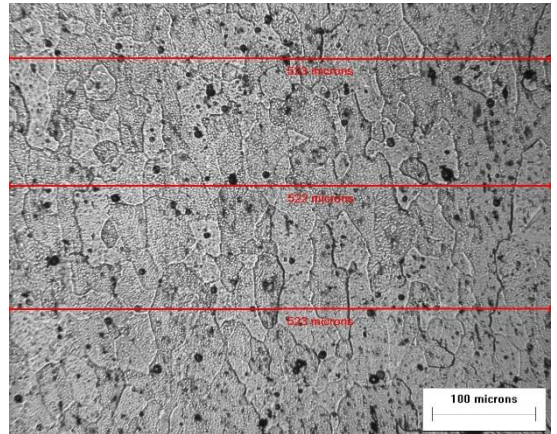
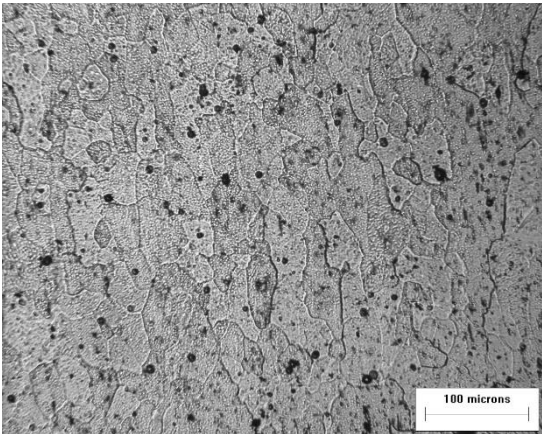
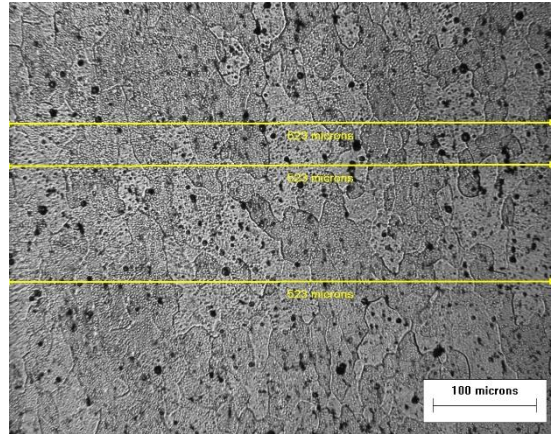
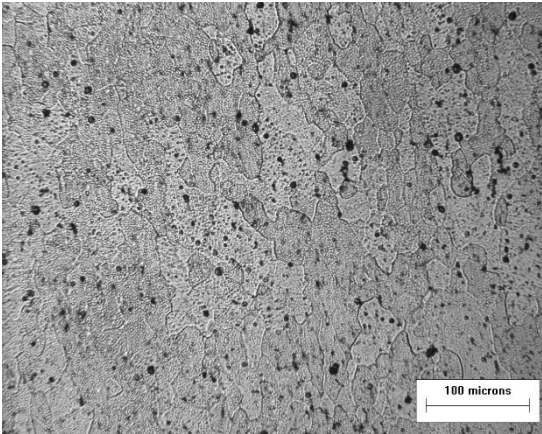
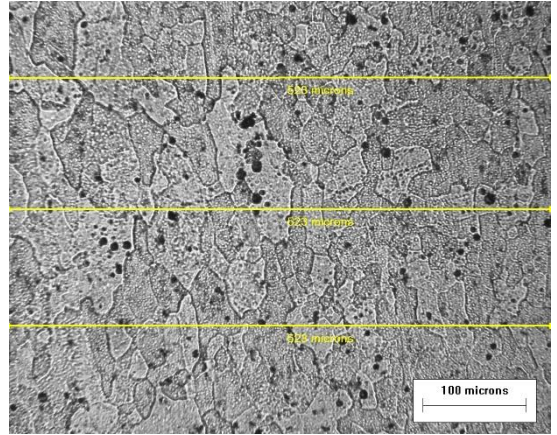
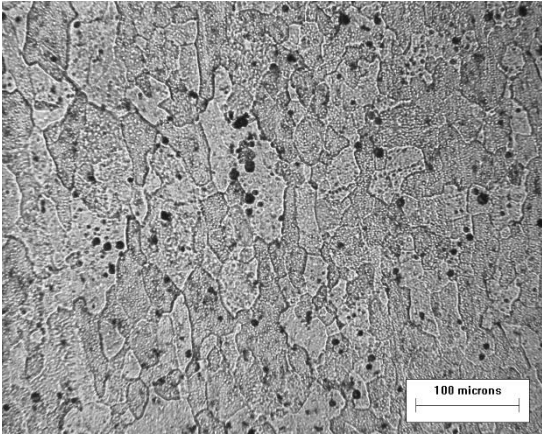
P-5-2



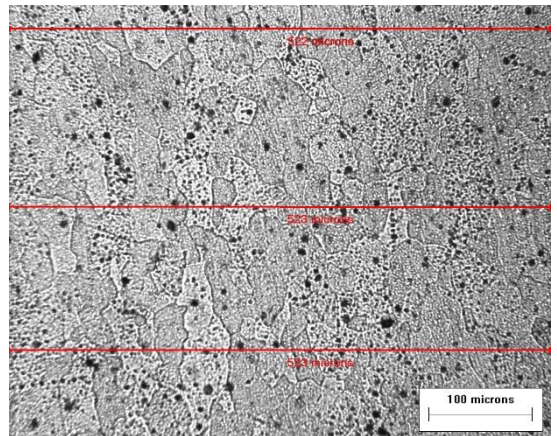
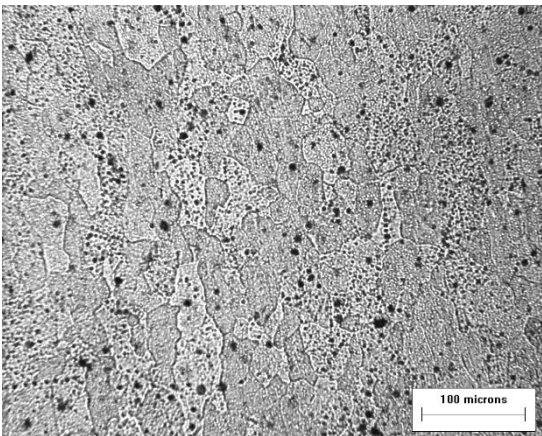
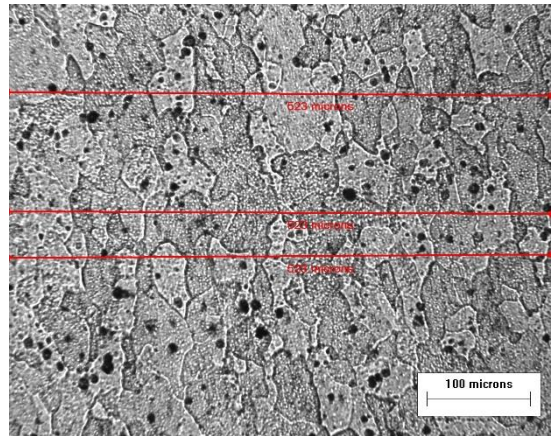
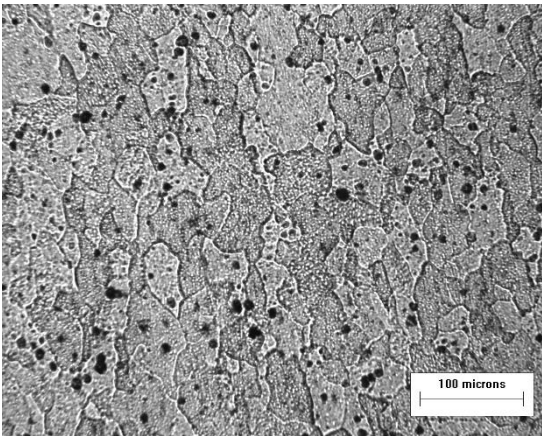
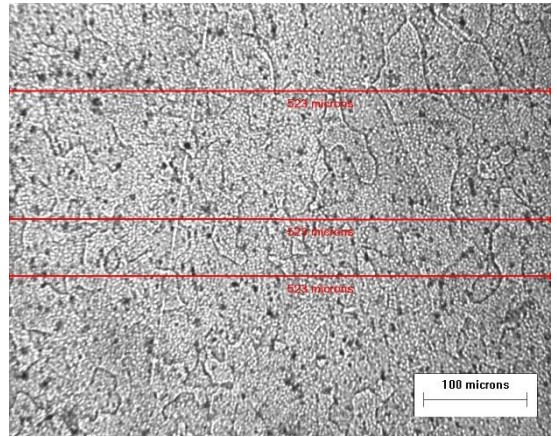
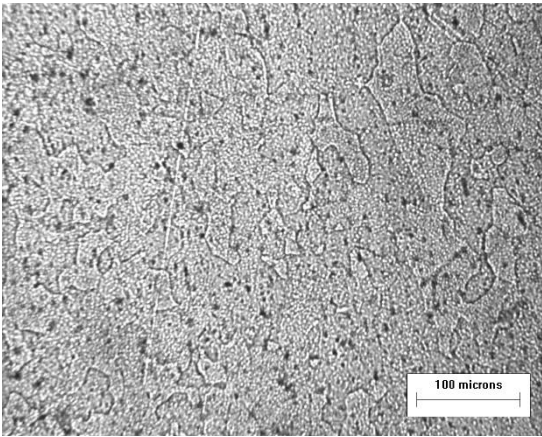
P-5-3



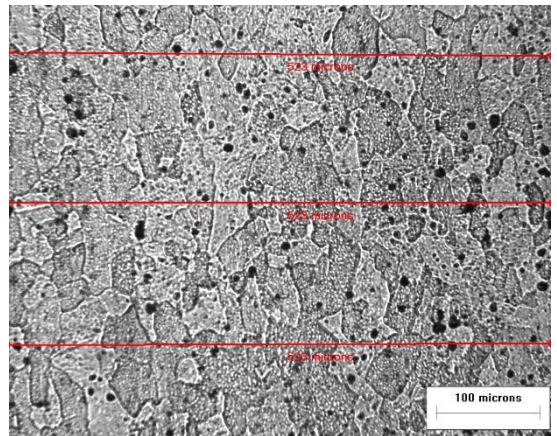
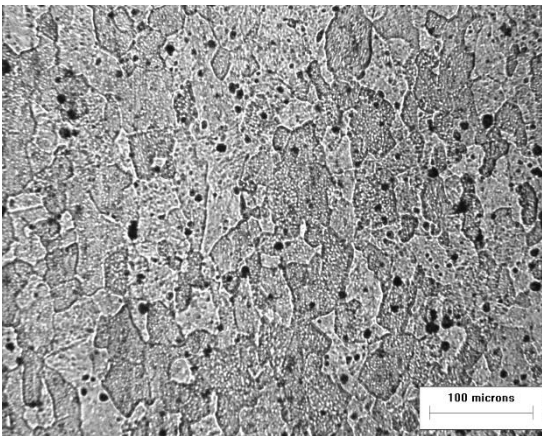
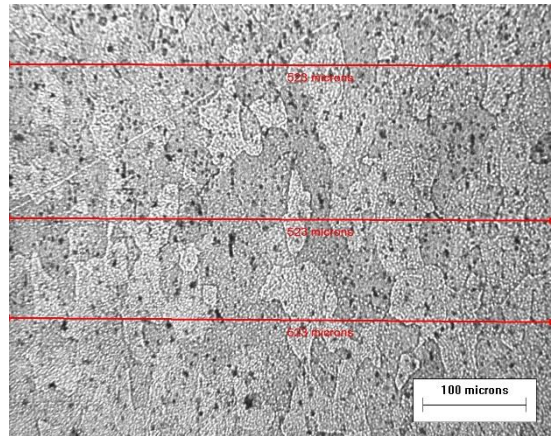
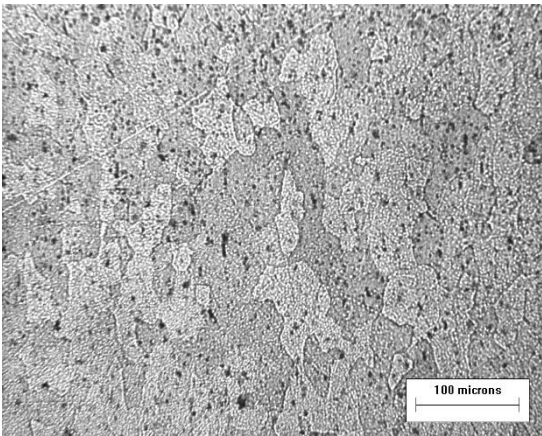
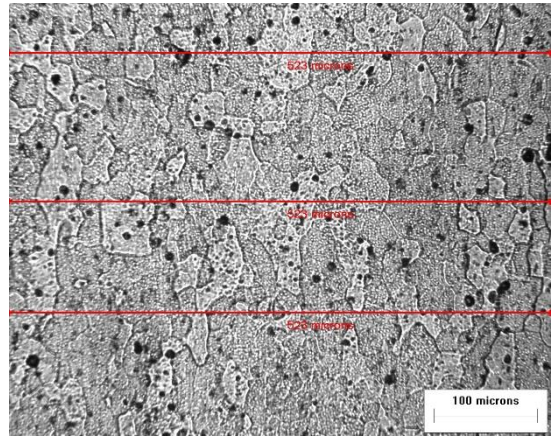
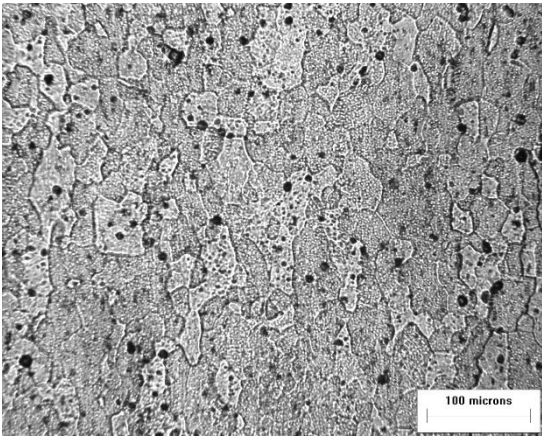
P - 10 - 1



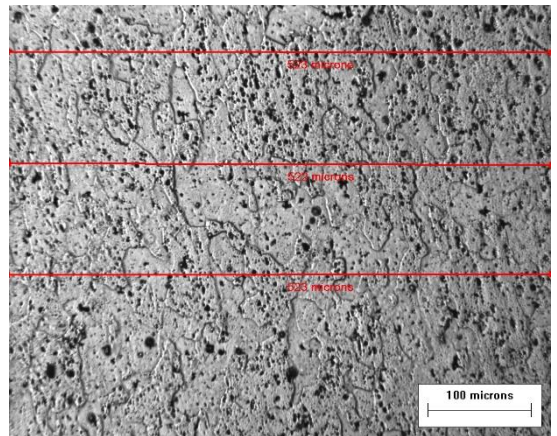
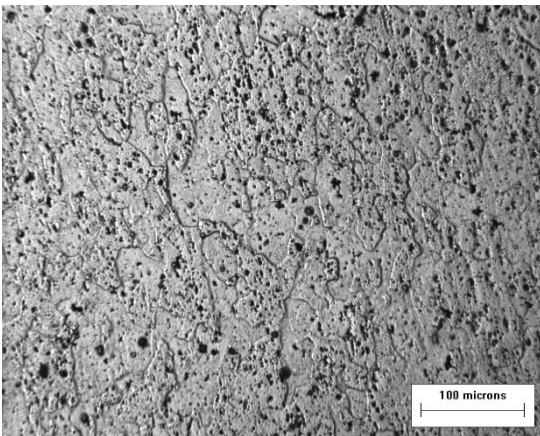
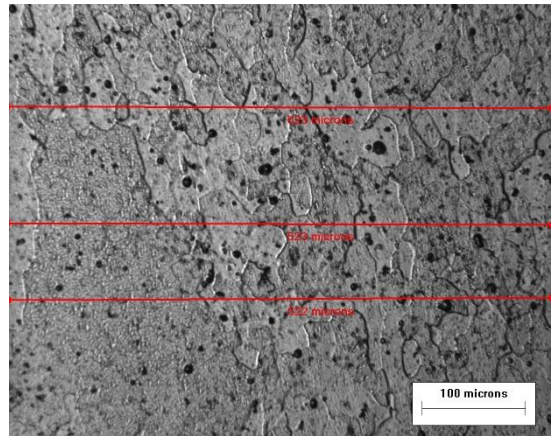
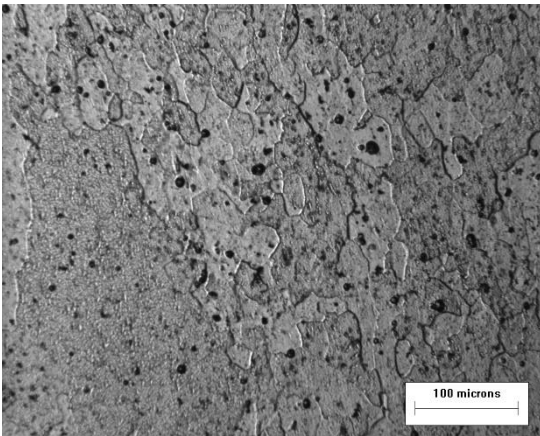
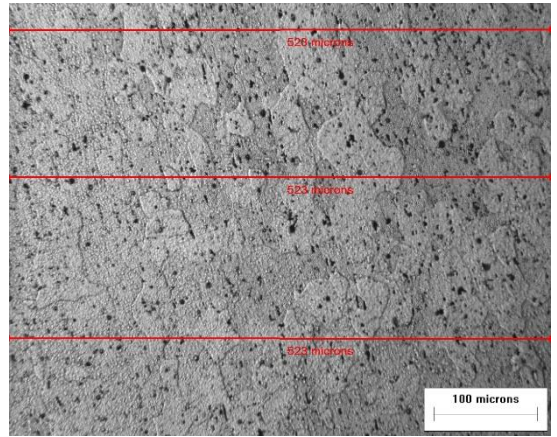
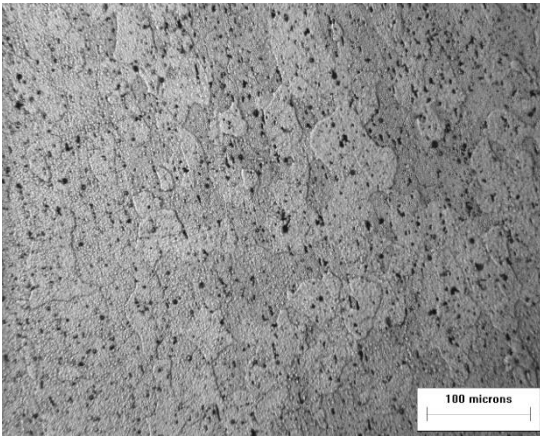
P - 10 - 2



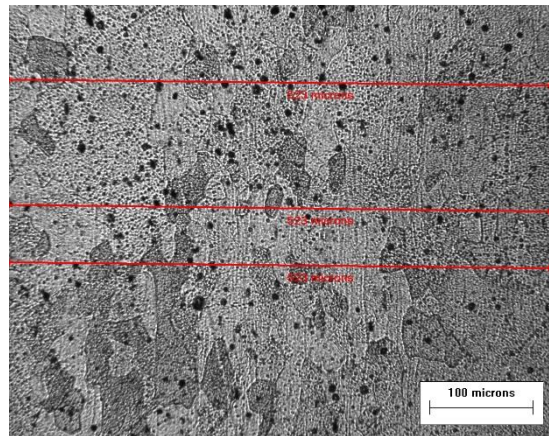
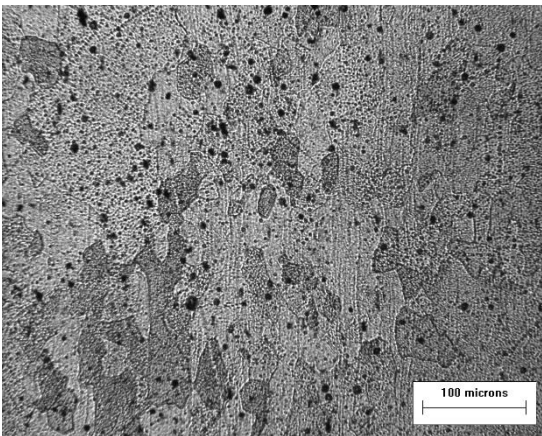
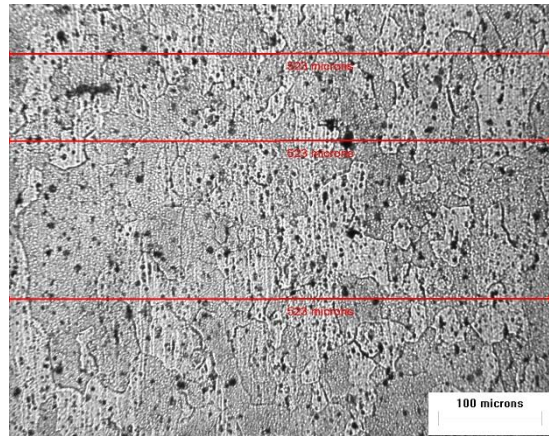
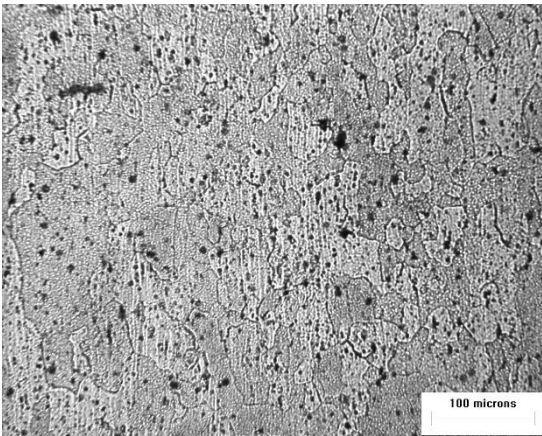
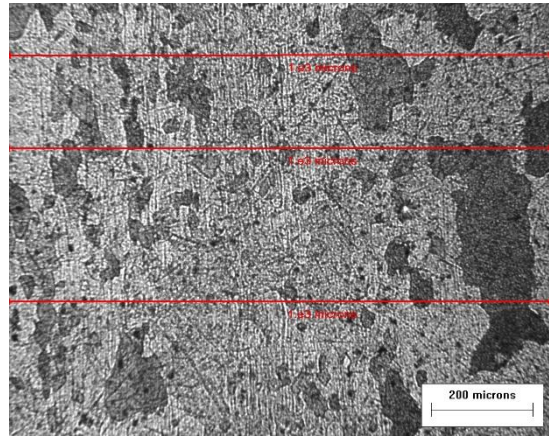
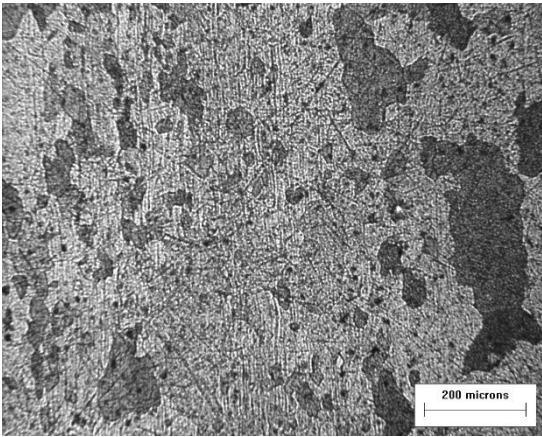
P - 10 - 3



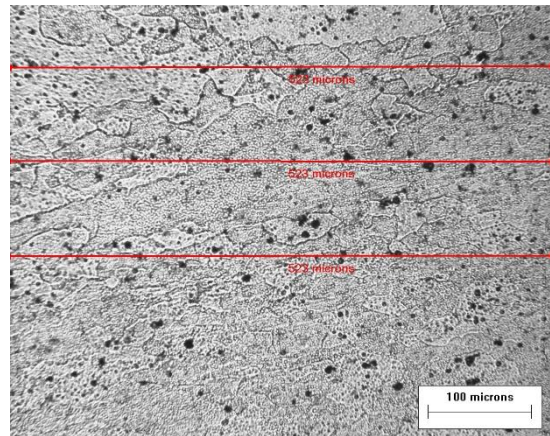
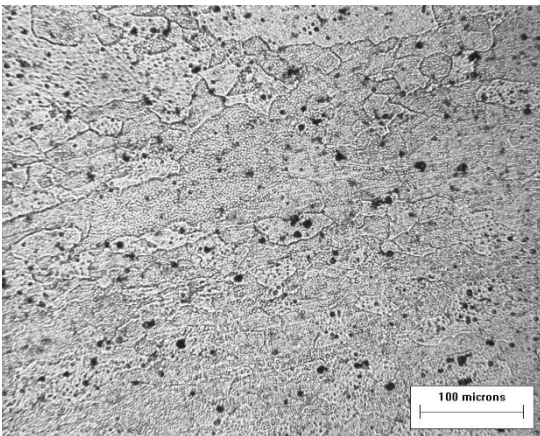
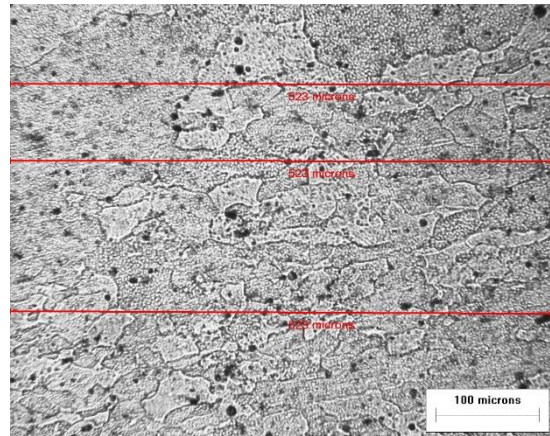
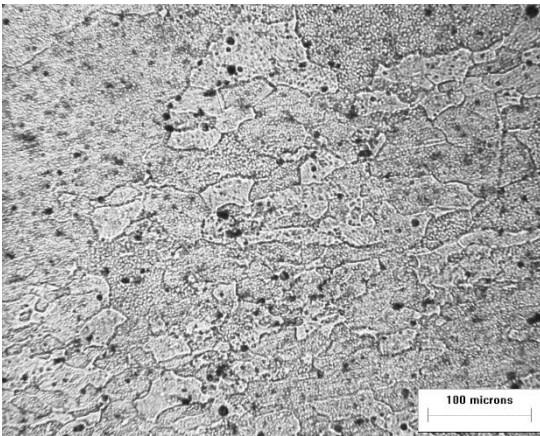
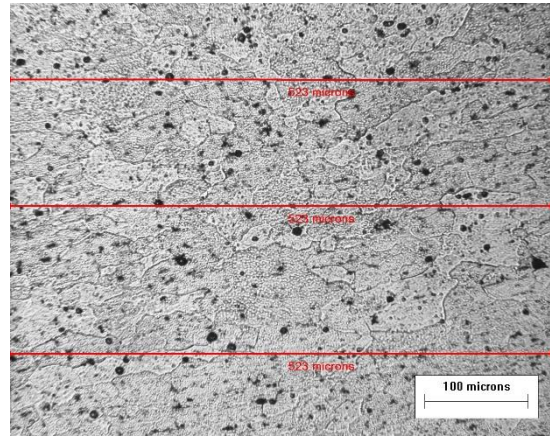
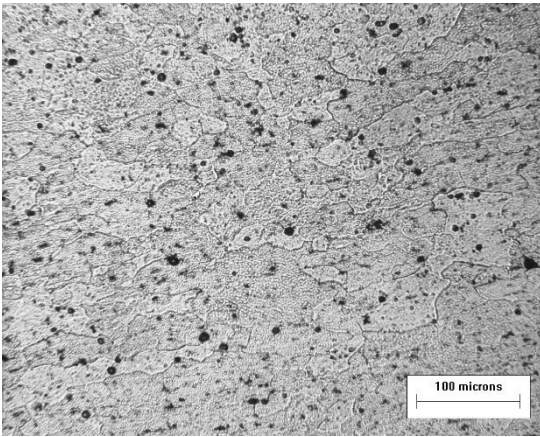
P - 15 - 1



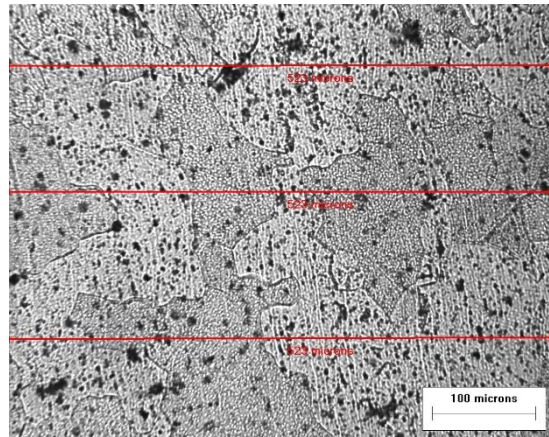
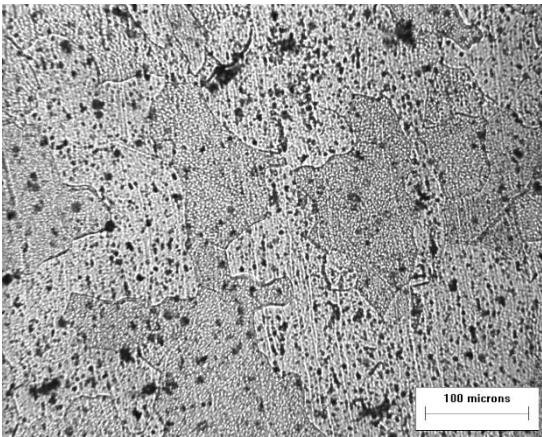
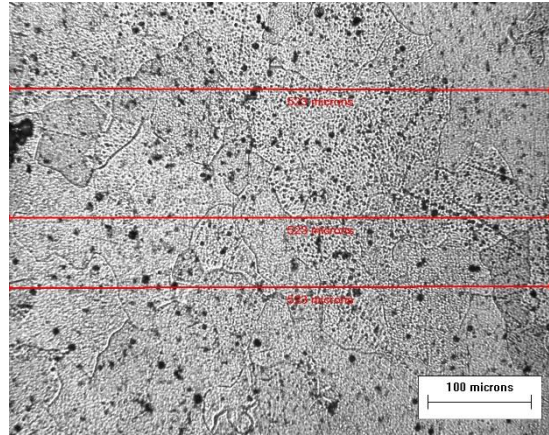
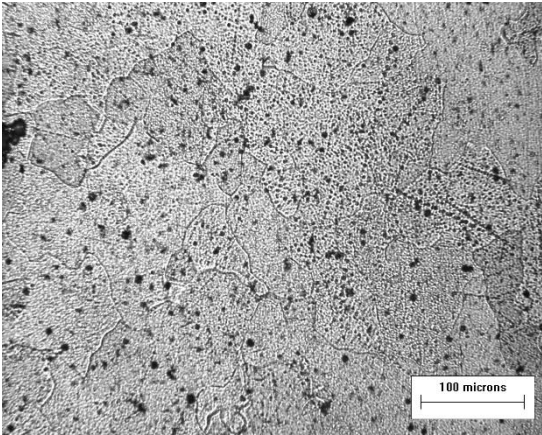
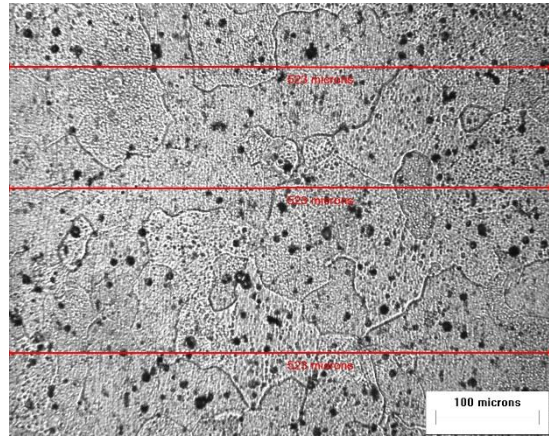
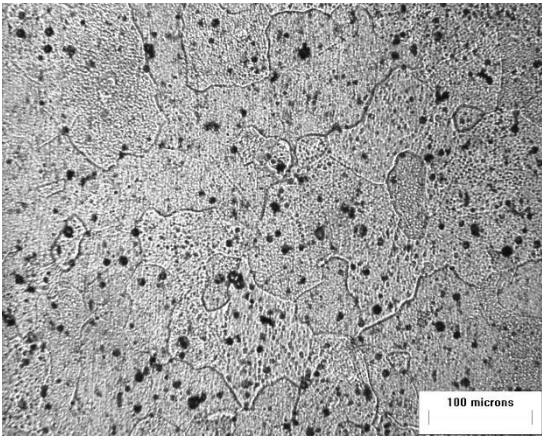
P - 15 - 2



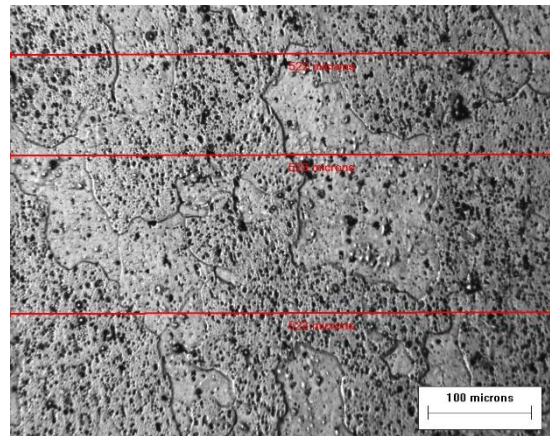
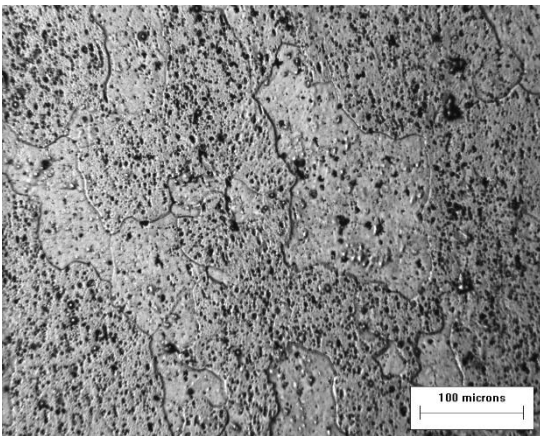
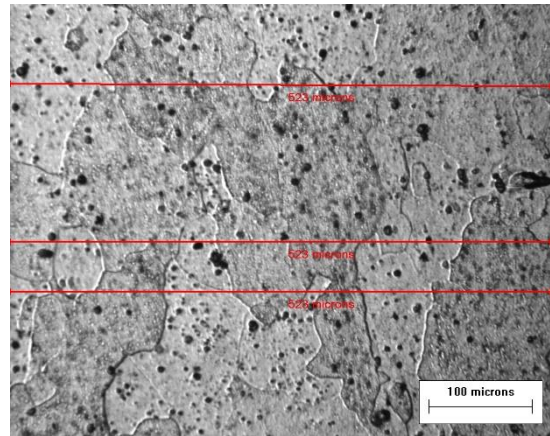
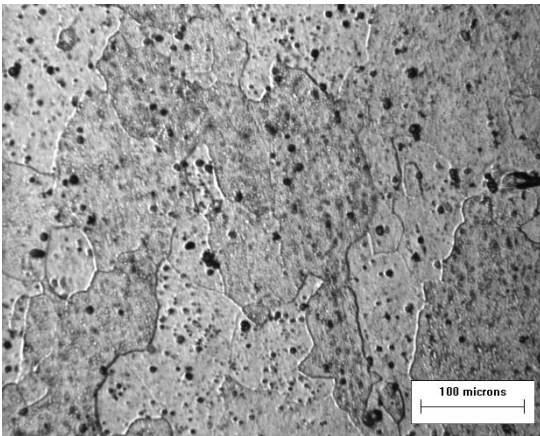
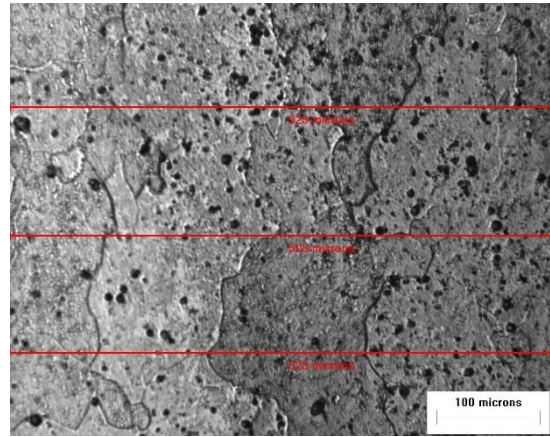
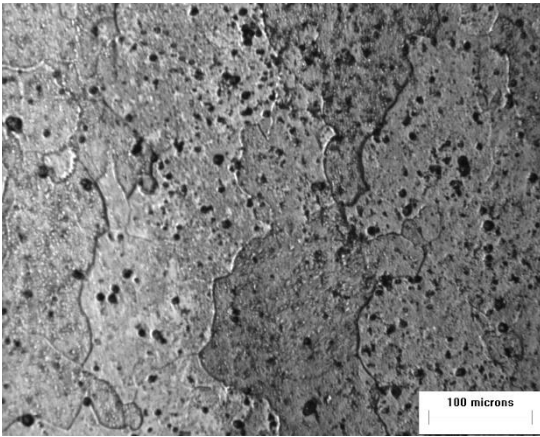
P - 15 - 3



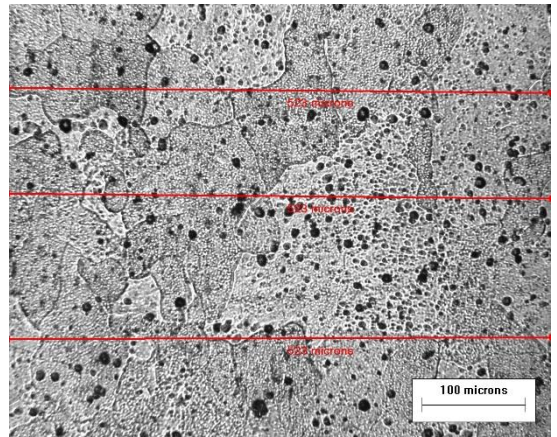
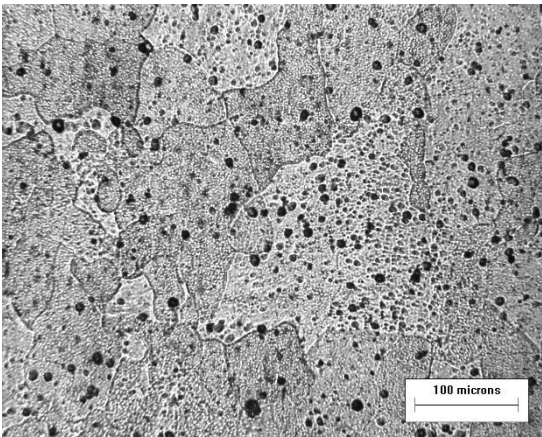
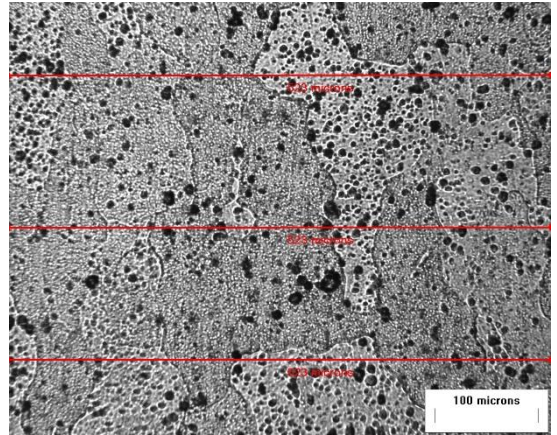
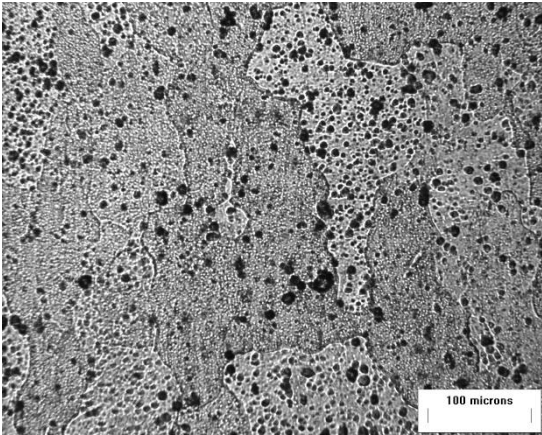
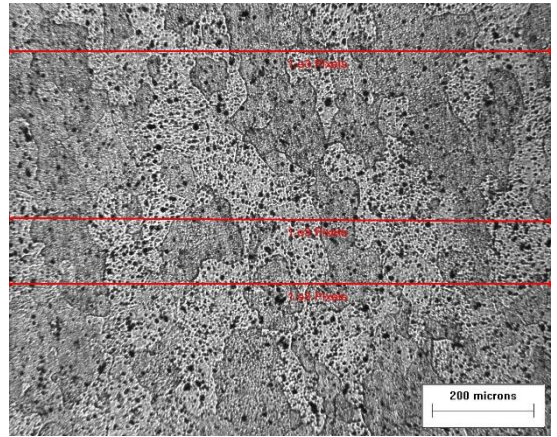
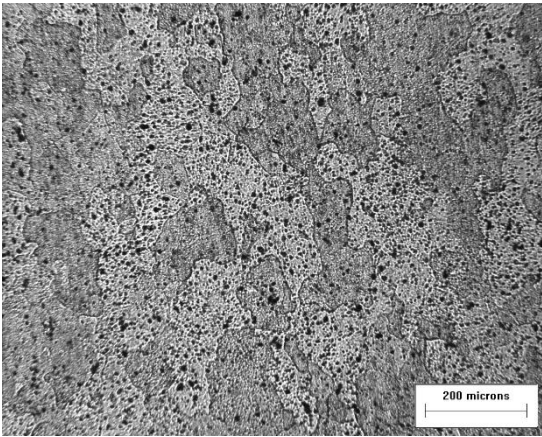
P - 30 - 1



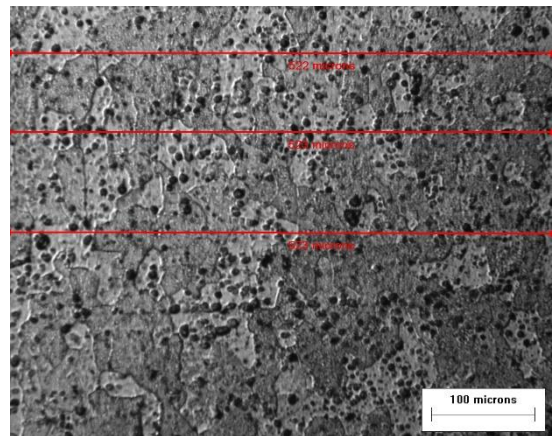
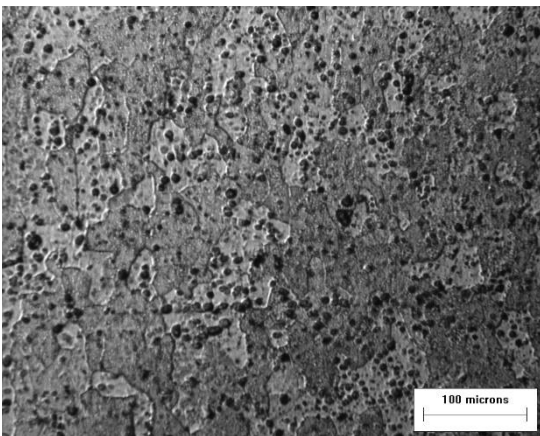
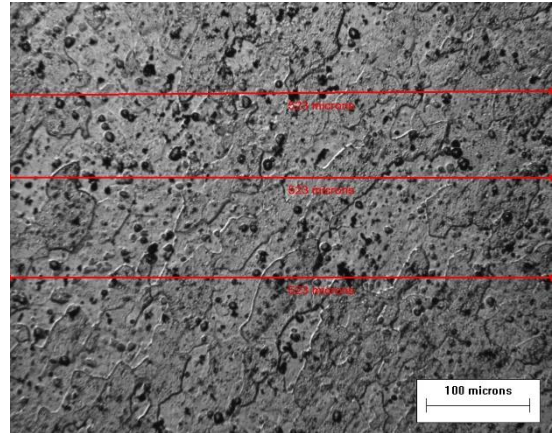
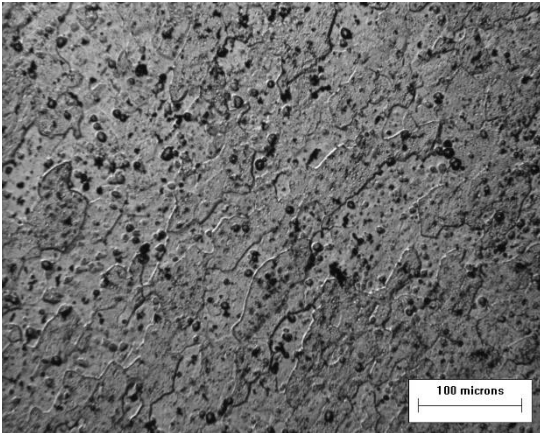
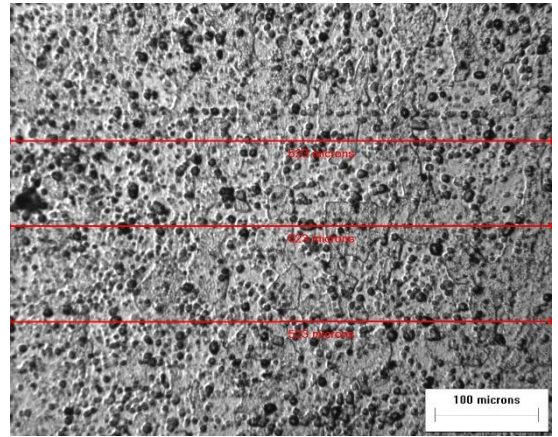
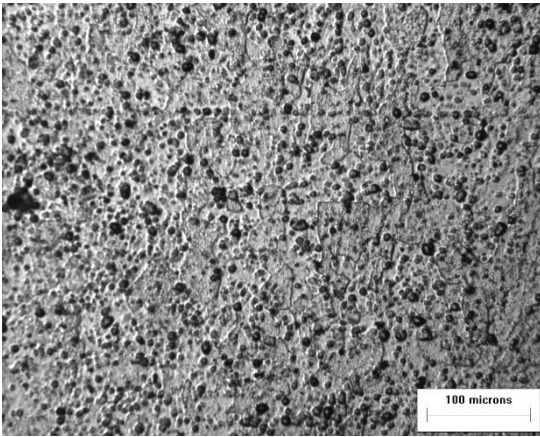
P - 30 - 2



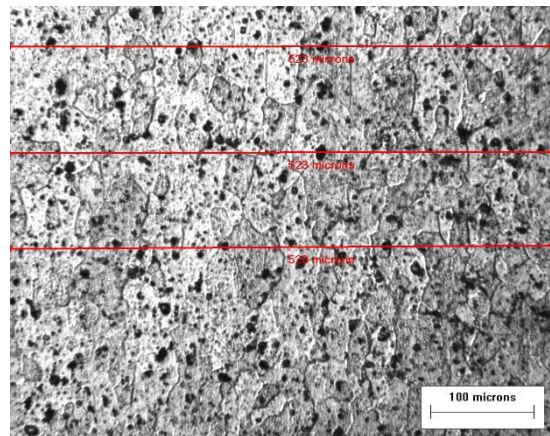
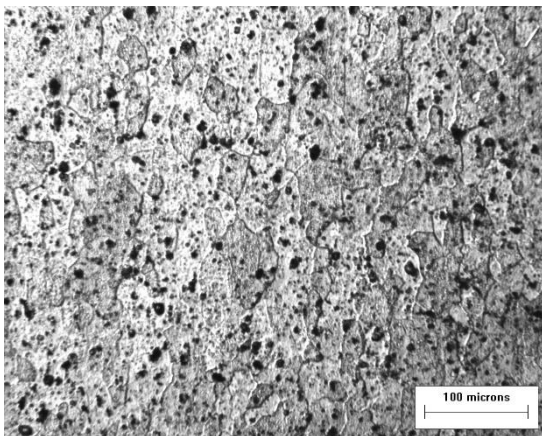
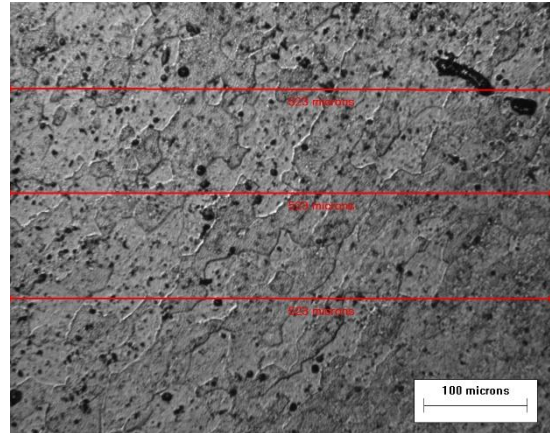
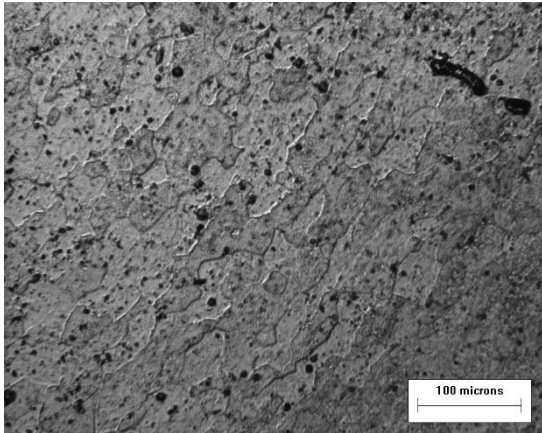
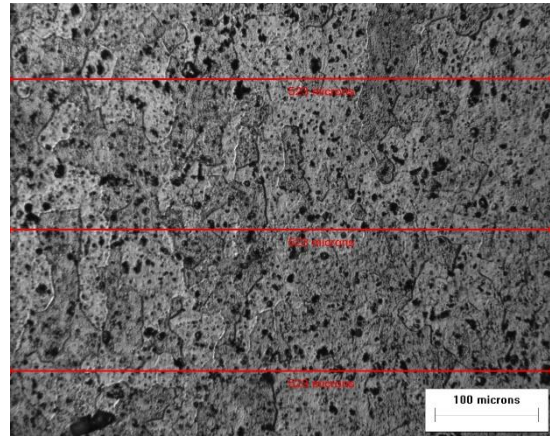
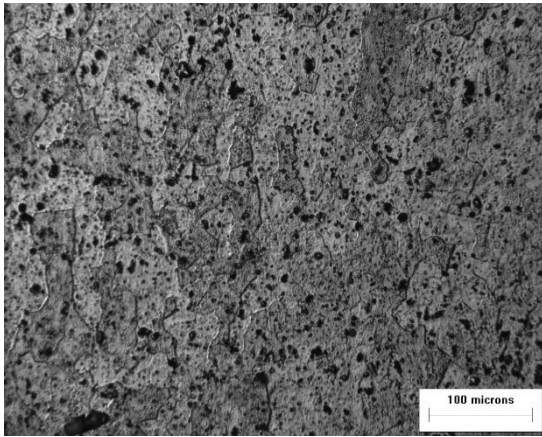
P - 30 - 3



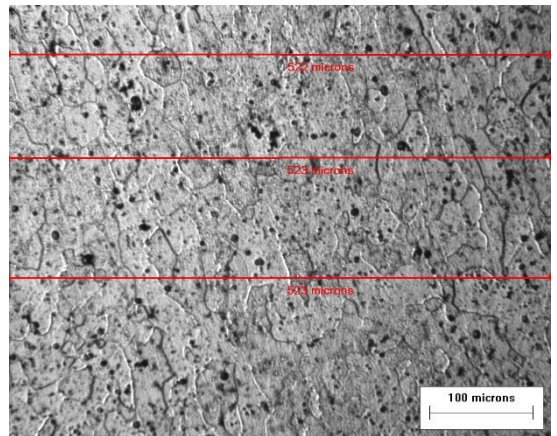
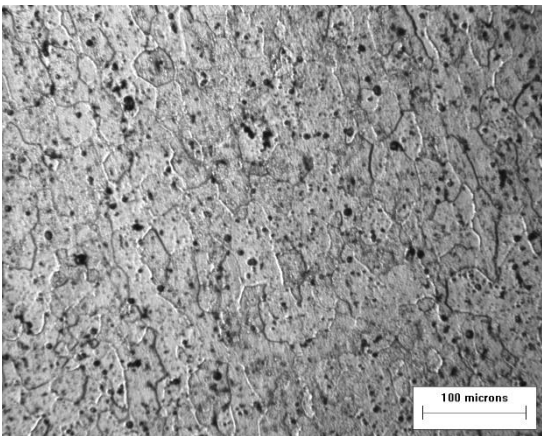
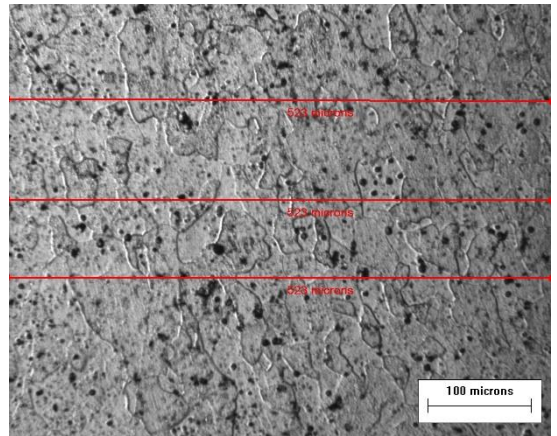
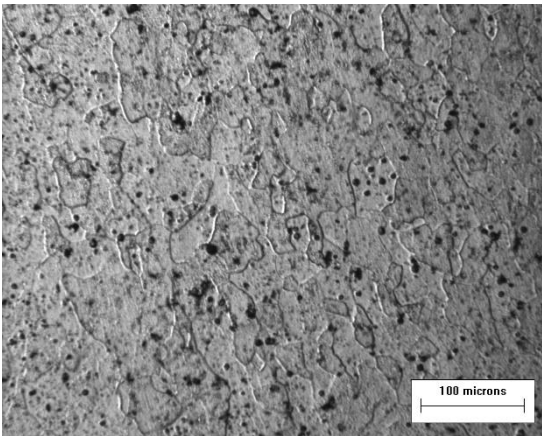
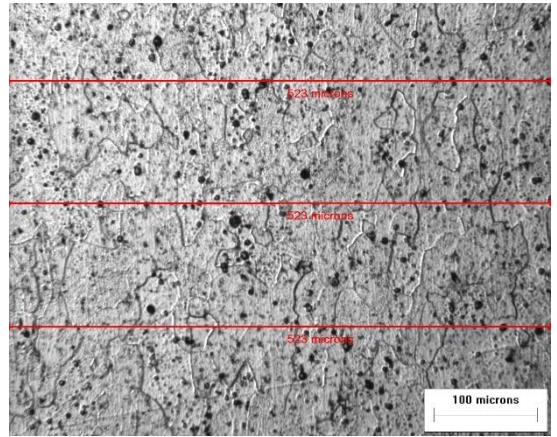
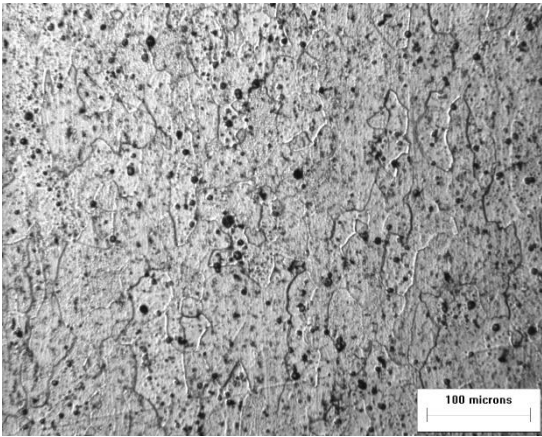
SC - 0 - 1



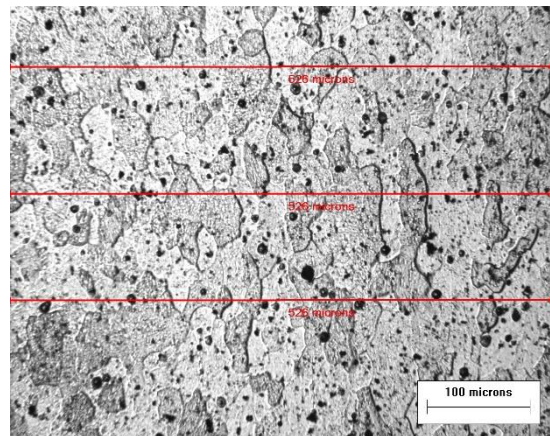
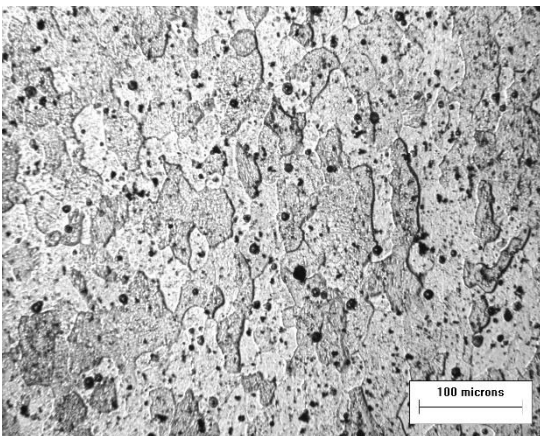
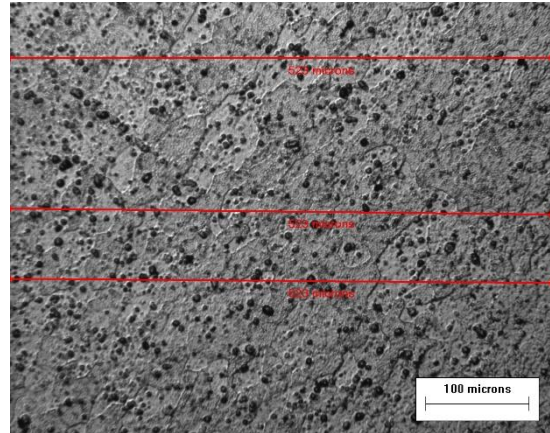
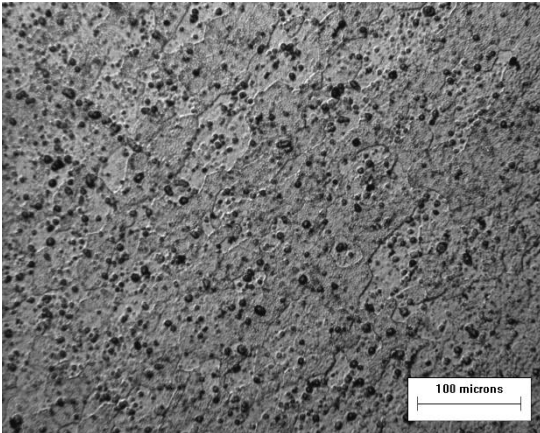
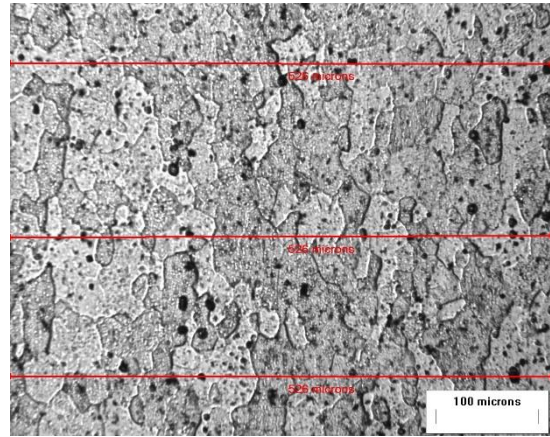
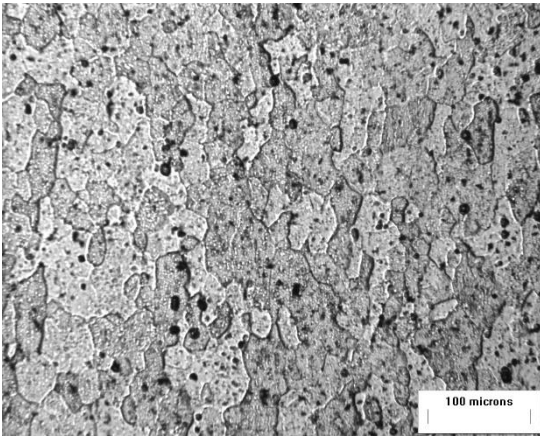
SC - 0 - 2



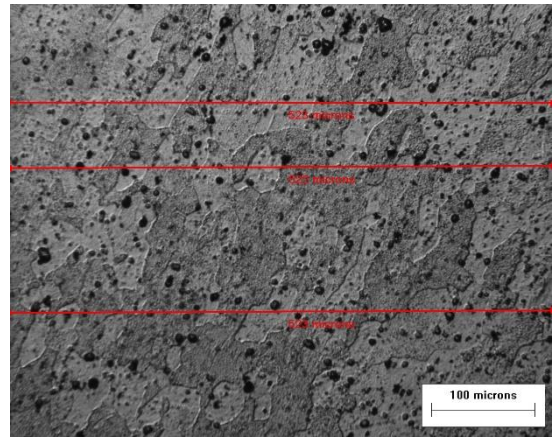
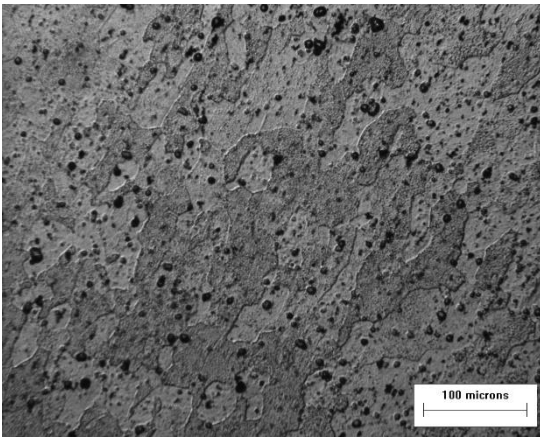
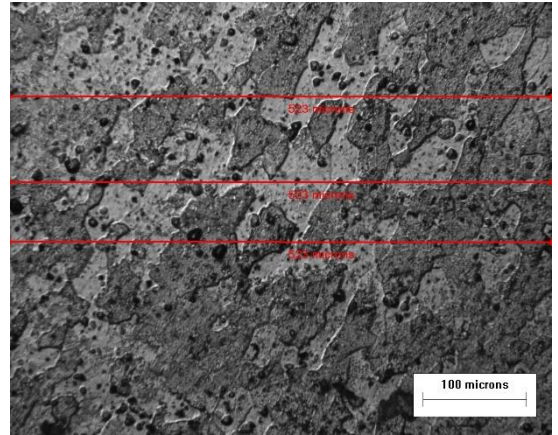
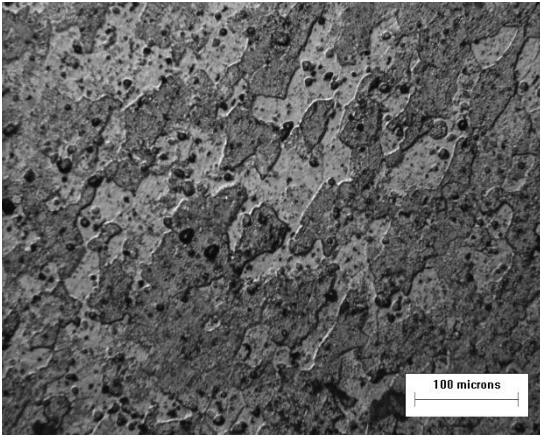
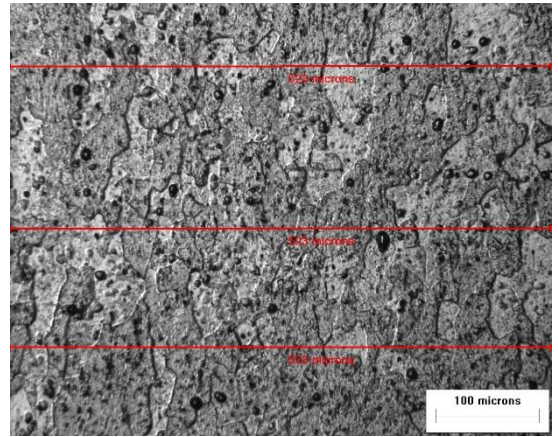
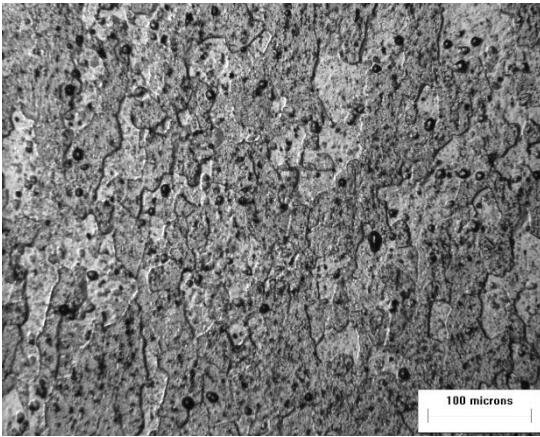
SC - 0 - 3



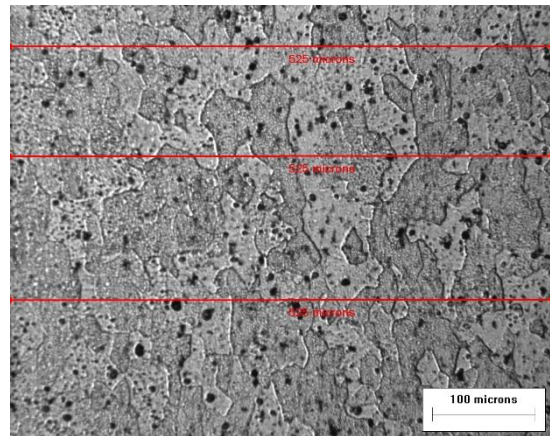
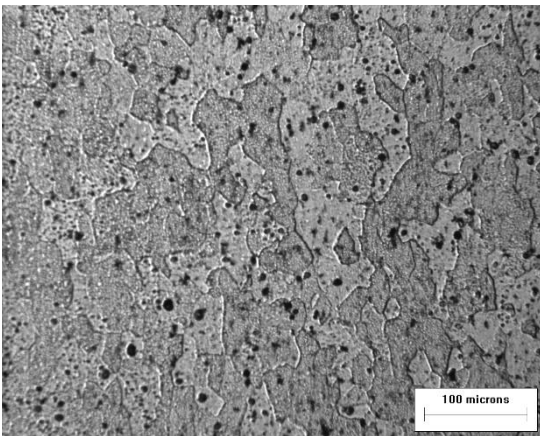
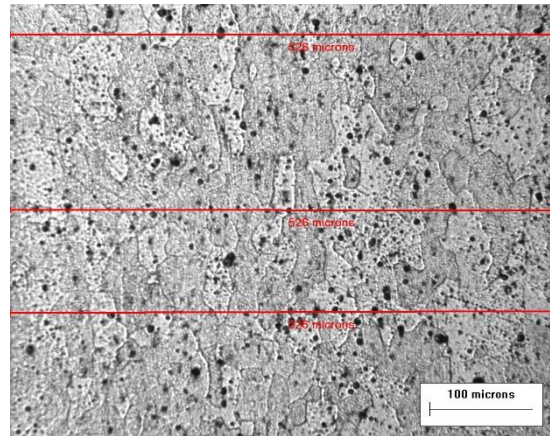
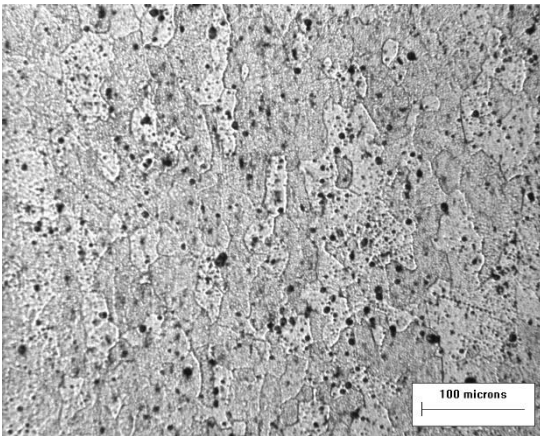
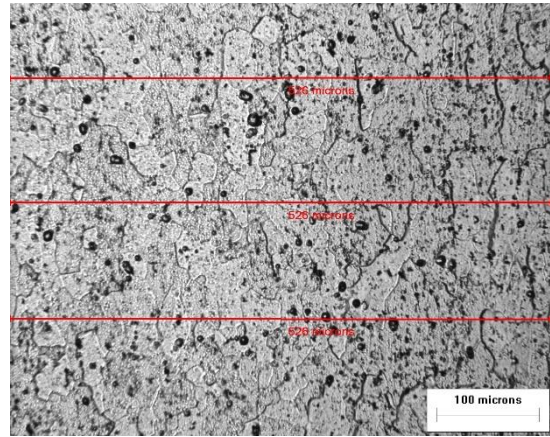
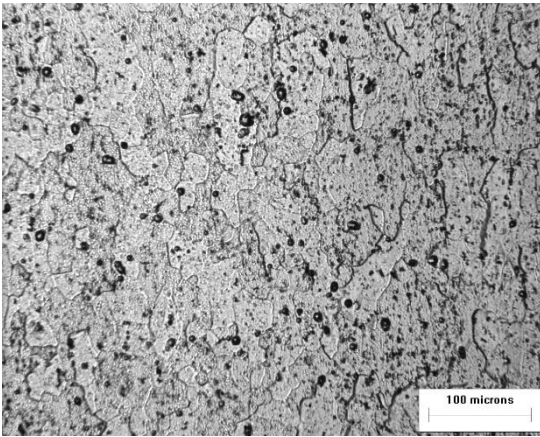
SC - 5 - 1



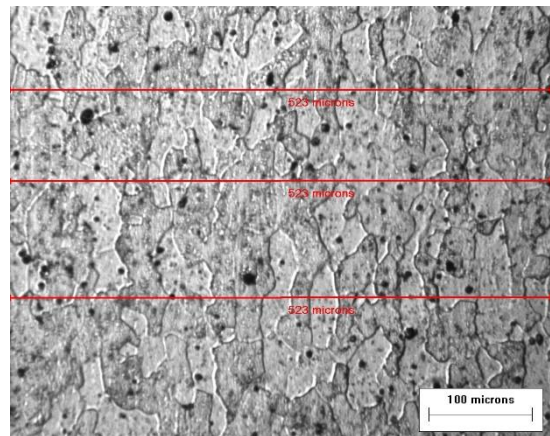
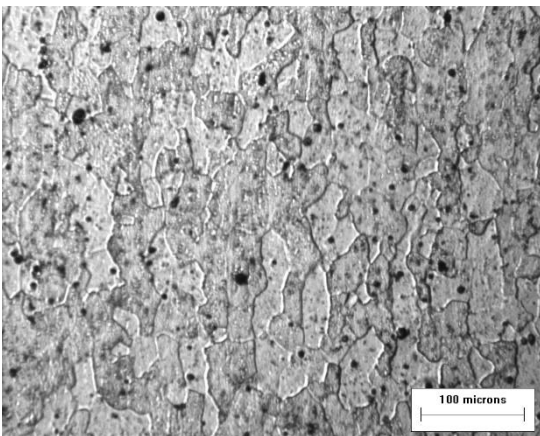
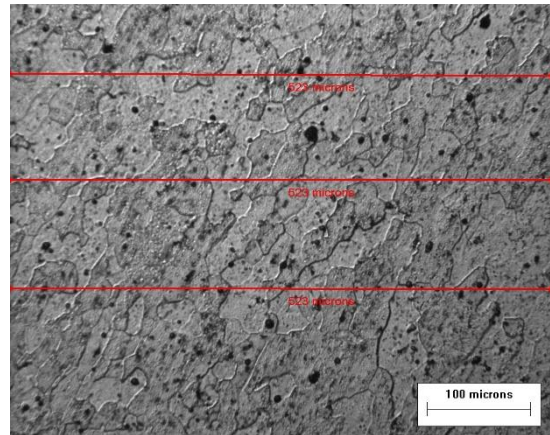
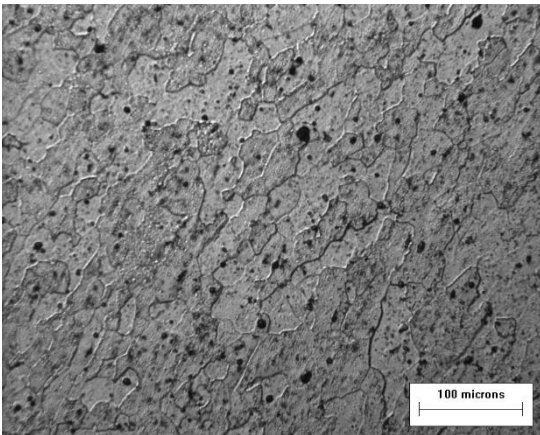
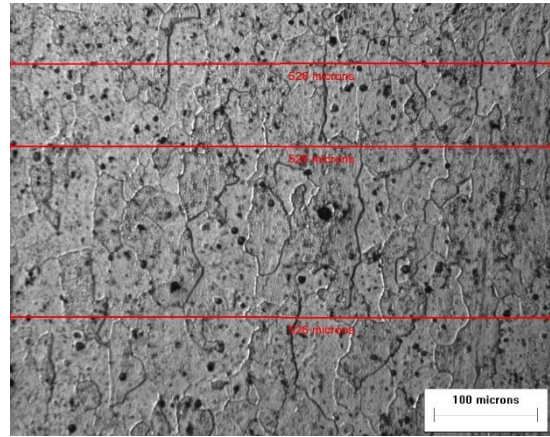
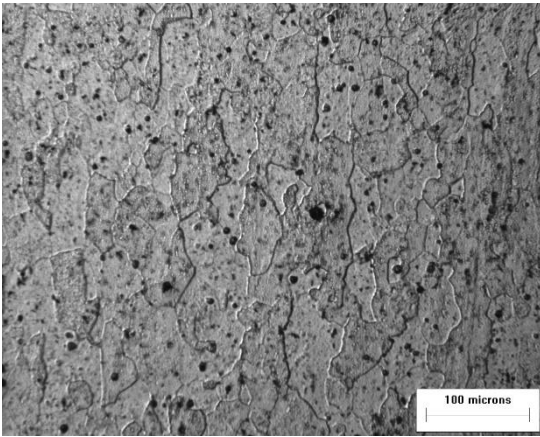
SC - 5 - 2



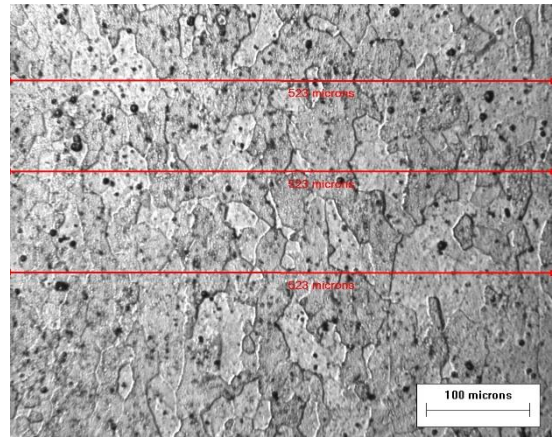
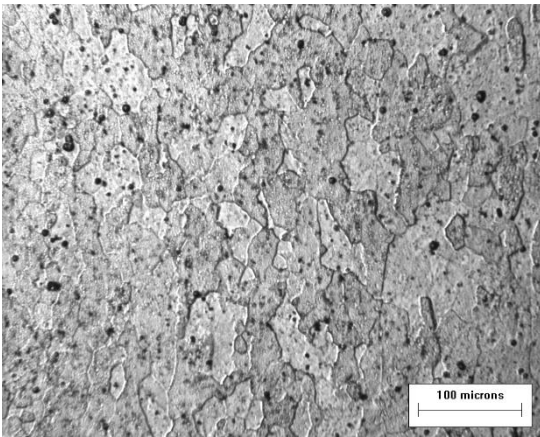
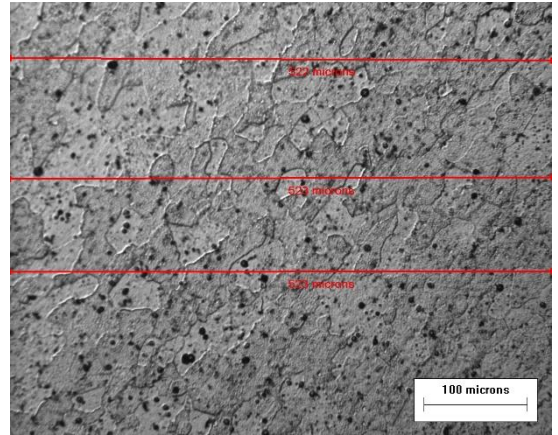
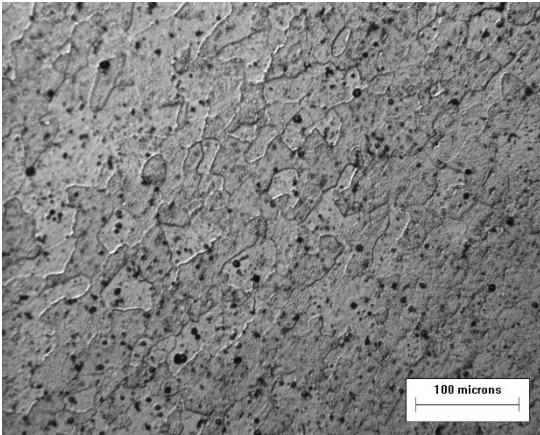
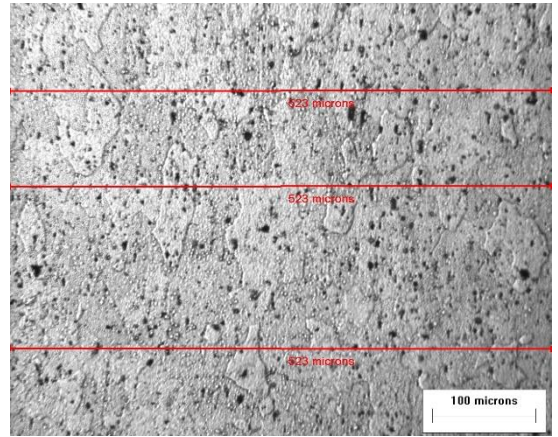
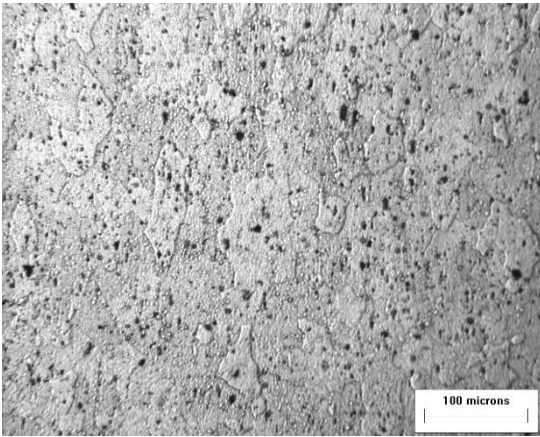
SC - 5 - 3



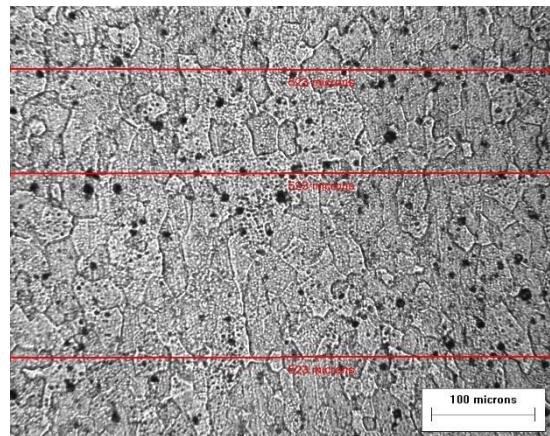
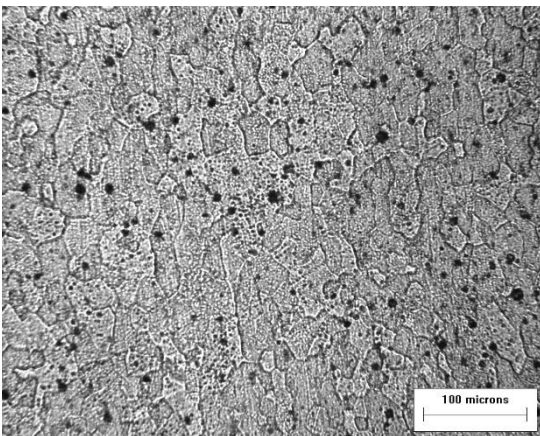
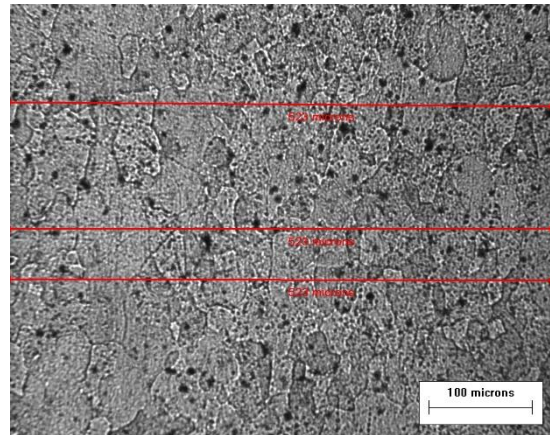
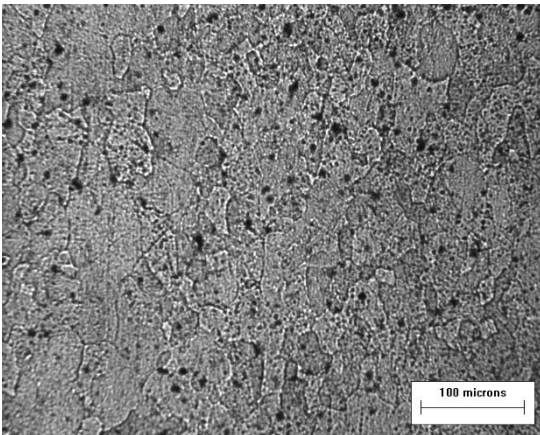
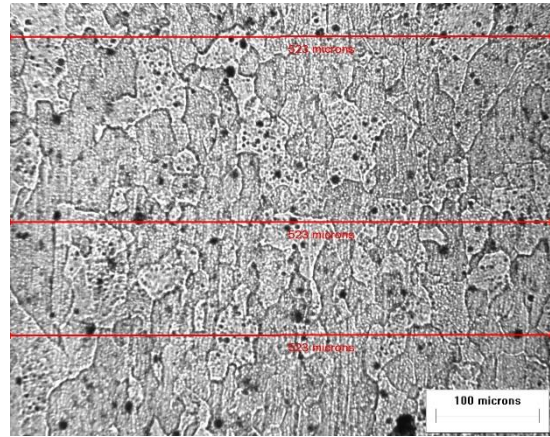
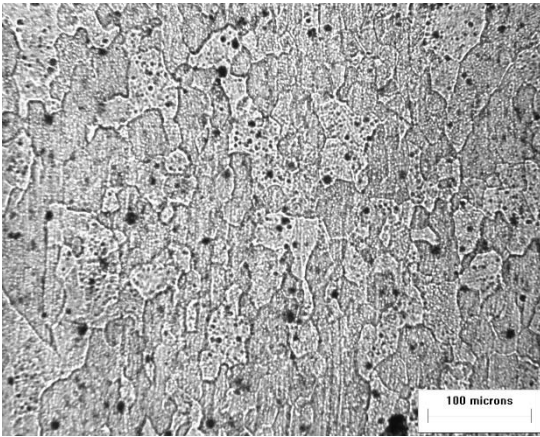
SC - 10 - 1



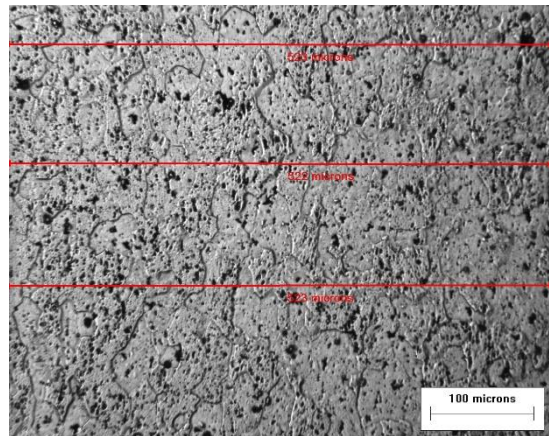
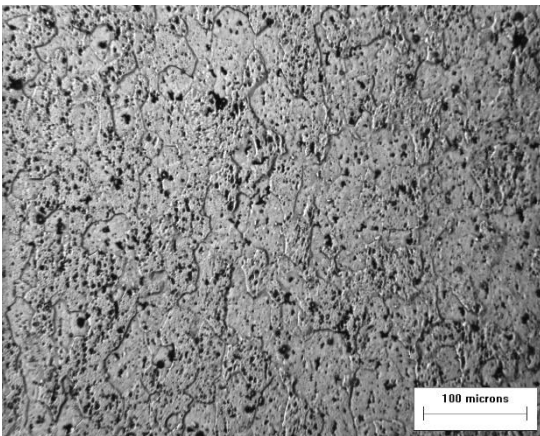
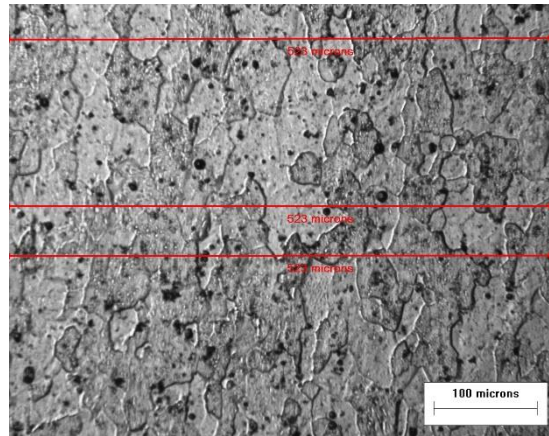
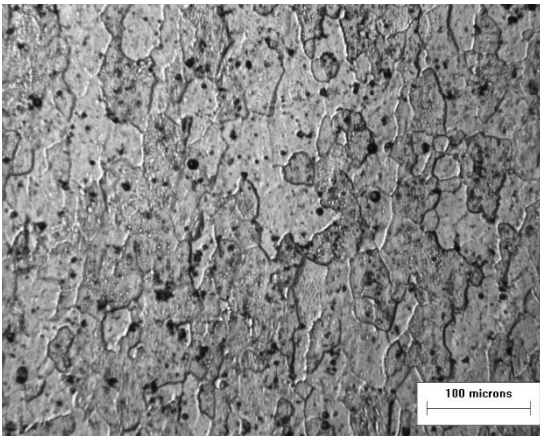
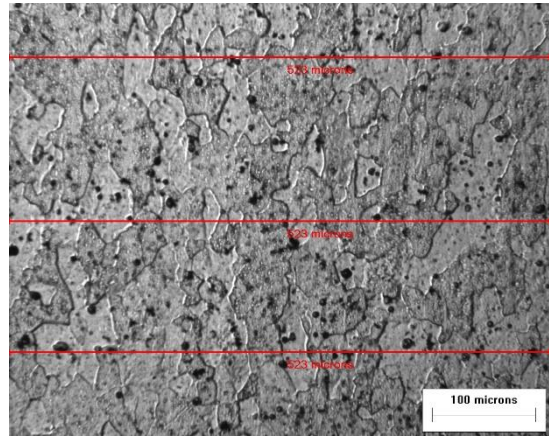
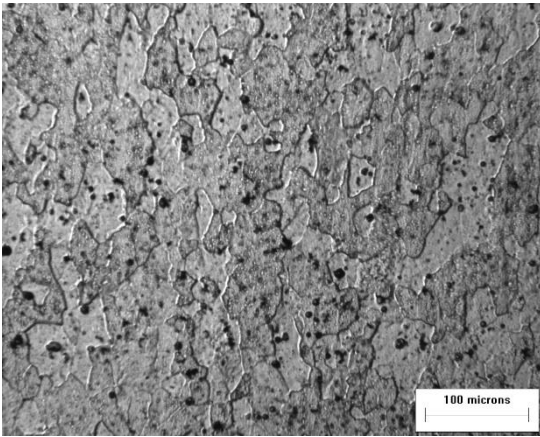
SC - 10 - 2



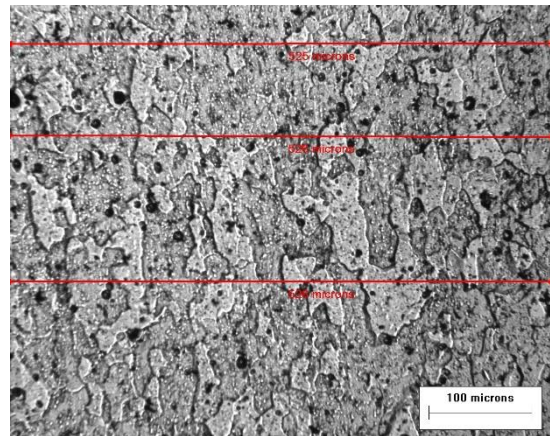
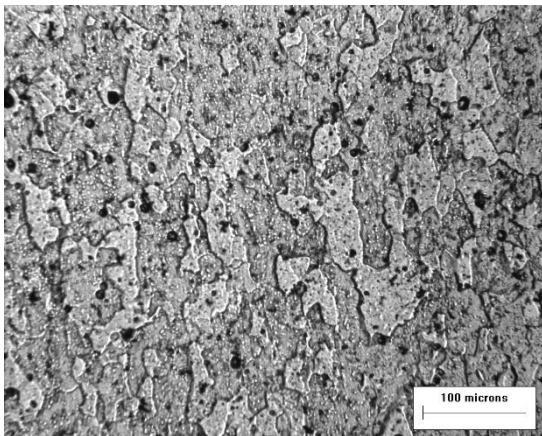
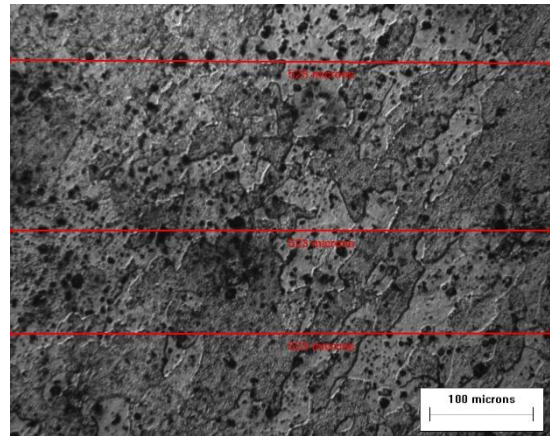
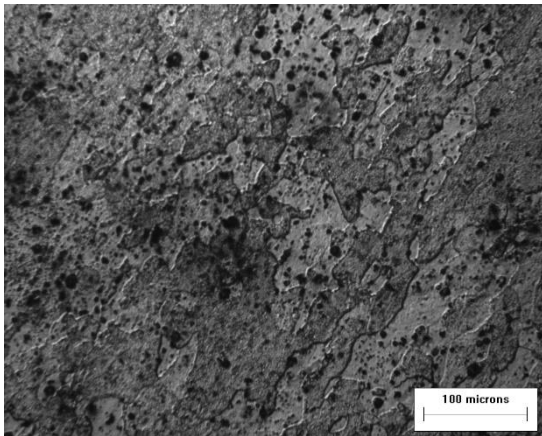
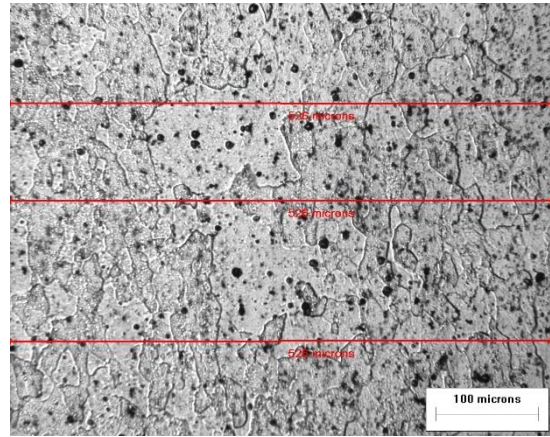
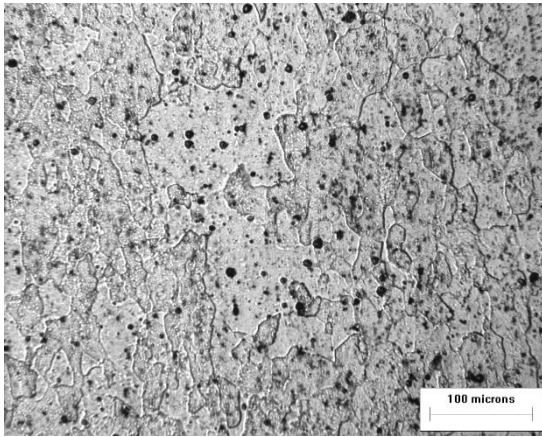
SC – 10 – 3



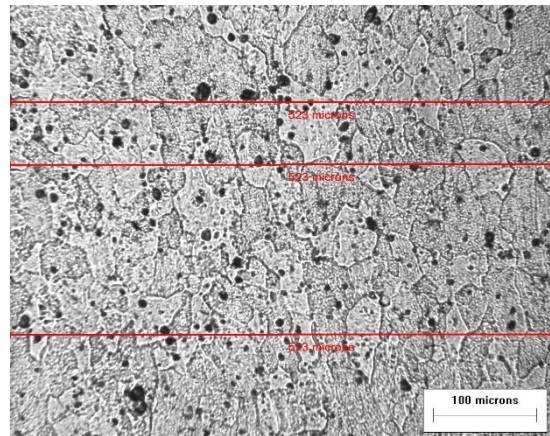
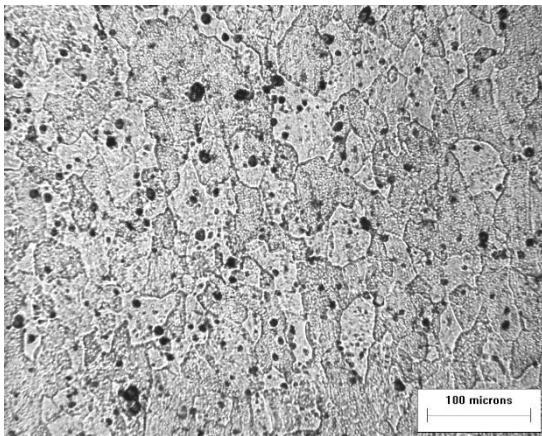
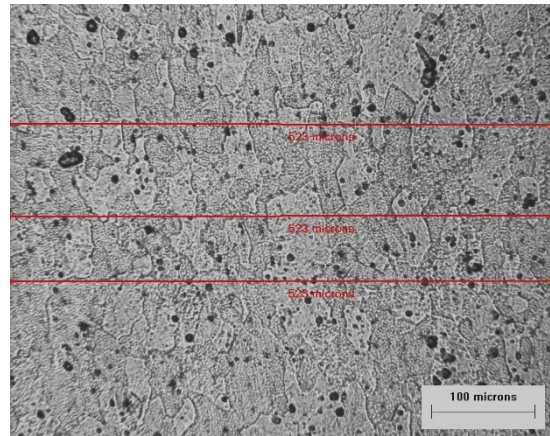
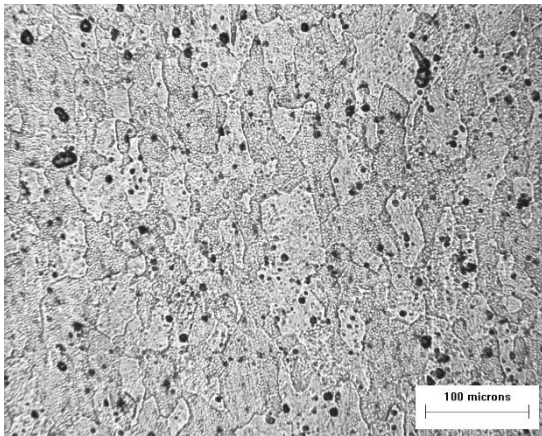
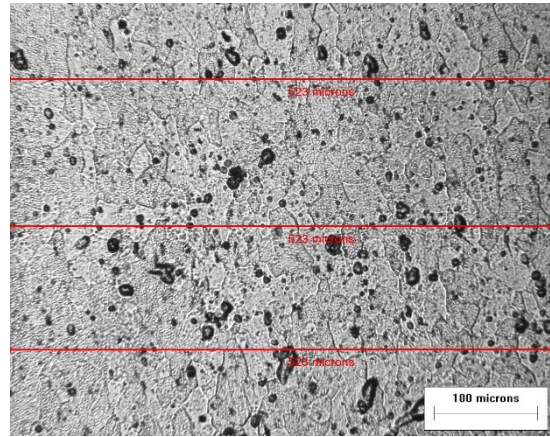
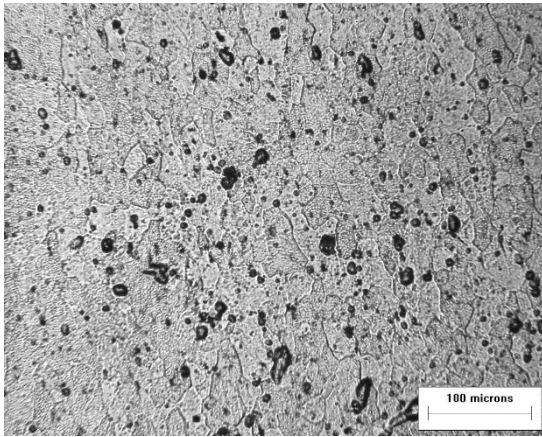
SC - 15 - 1



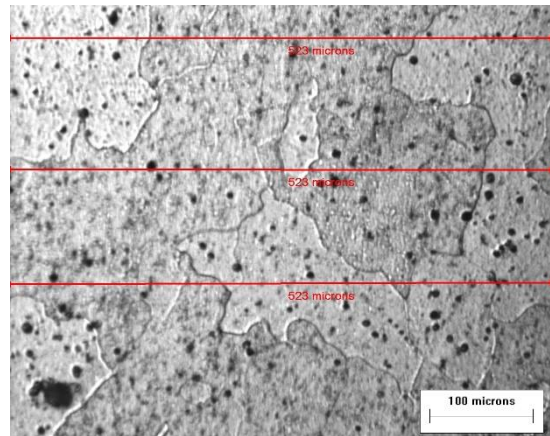
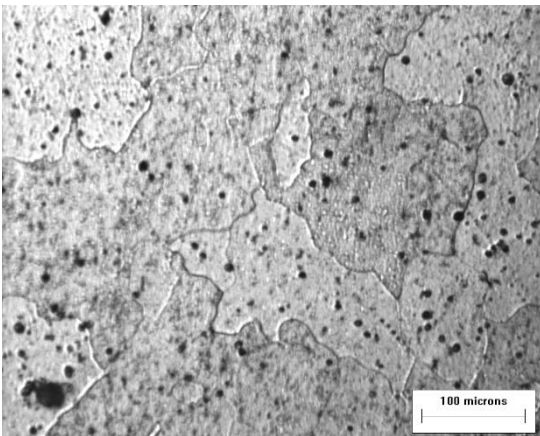
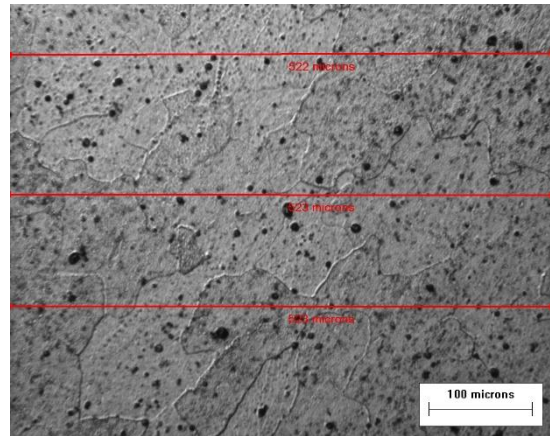
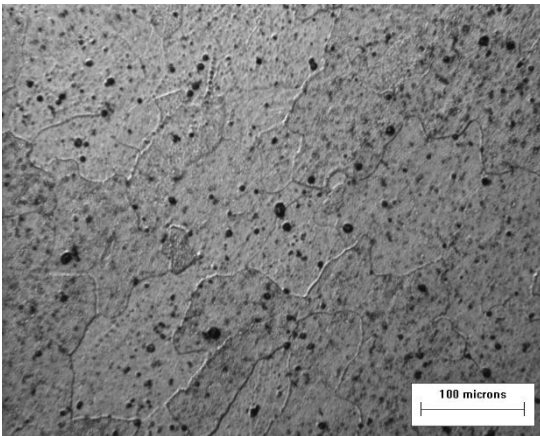
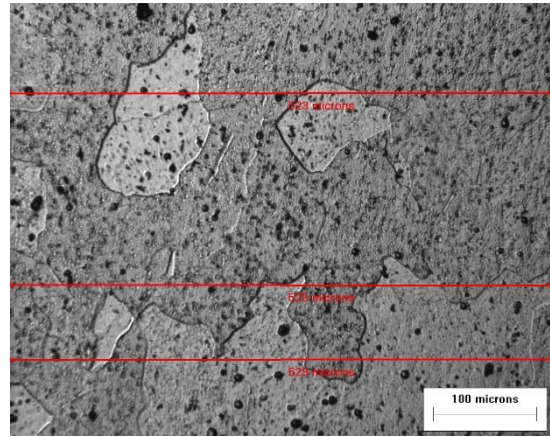
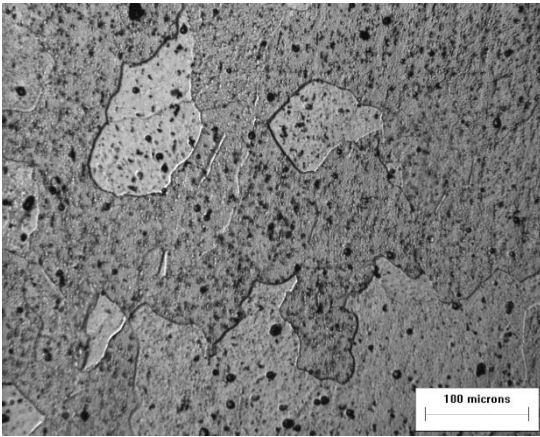
SC - 15 - 2



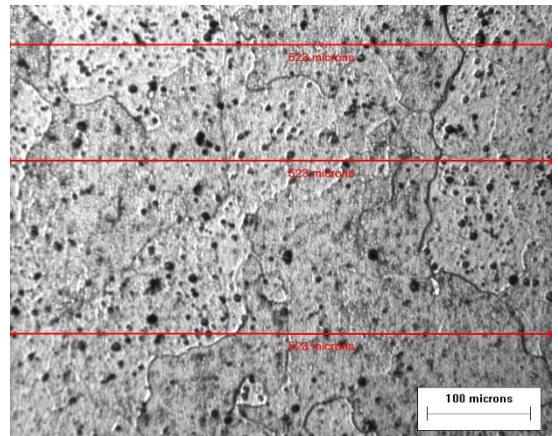
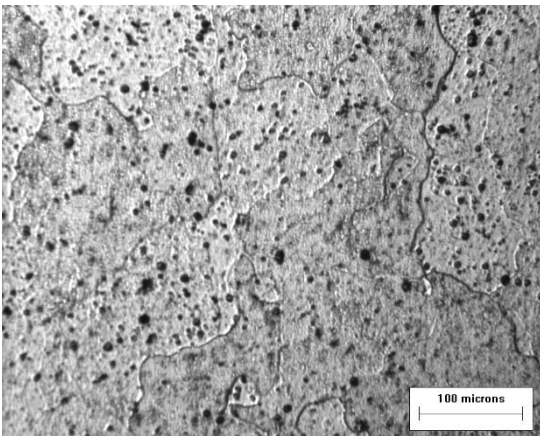
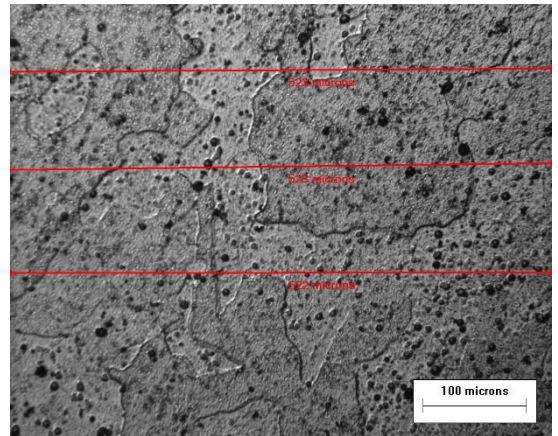
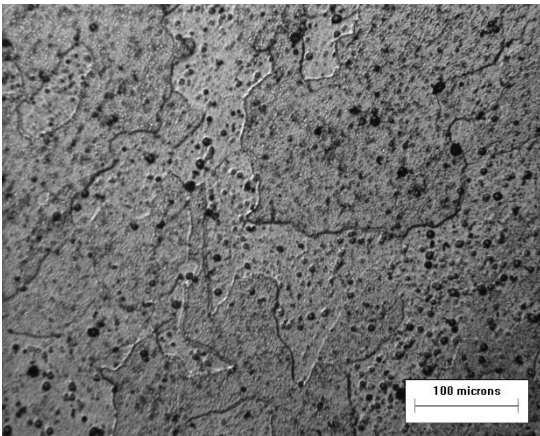
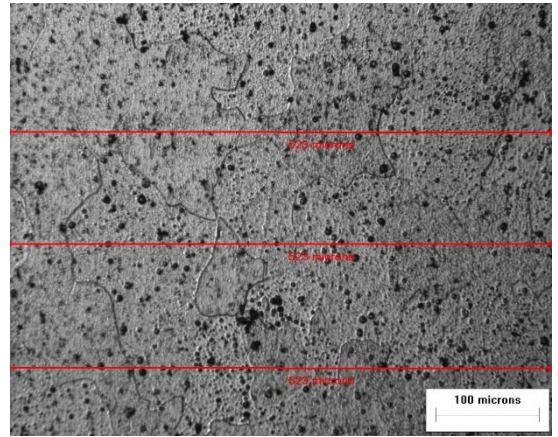
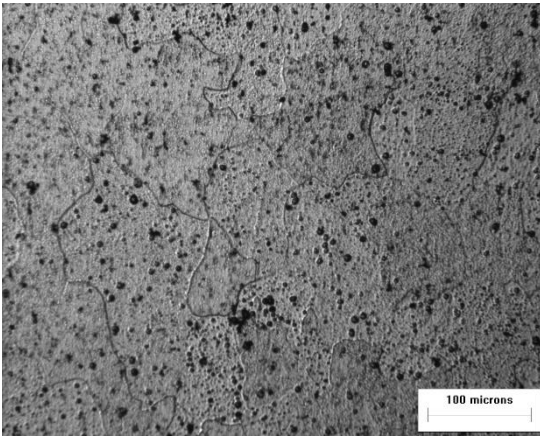
SC - 15 - 3



SC - 30 - 1



SC - 30 - 2



SC – 30 – 3

